TEXAS INSTRUMENTS
INCORPORATED

HEAT STERILIZABLE AND IMPACT RESISTANT
Ni-Cd BATTERY DEVELOPMENT

Jet Propulsion Laboratory
Contract No. 951972, Modification No. 14

Final Report, Volume I
July 1, 1967 to December 31, 1969

Project Manager: P. V. Popat

Principal Contributors: R. L. Crawford

P. V. Popat

TEXAS INSTRUMENTS INC.
Research & Development Laboratories
34 Forest Street
Attleboro, Massachusetts
02703

NOTICE

This report was prepared as an account of government-sponsored work. Neither the United States, nor the National Aeronautics and Space Administration (NASA), nor any person acting on behalf of NASA:

(a) makes warranty of representation, expressed or implied with respect to the accuracy, completeness, or usefulness of the information contained in this report, or that the use of any information, apparatus, method, or process disclosed in this report may not infringe privately owned rights;

(b) assumes any liabilities with respect to the use of, or for damages resulting from the use of any information, apparatus, method or process disclosed in this report.

As used above, "person acting on behalf of NASA" includes any employees or contractor of NASA, or employee of such contractor to the extent that such contractor prepares, disseminates, or provides access to any information pursuant to his employment with such contractor.

Requests for copies of this report should be referred to:

National Aeronautics and Space Administration
Office of Scientific and Technical Information
Attention: AFSS-A

metallurgical
materials division

HEAT STERILIZABLE AND IMPACT. RESISTANT·
Ni-Cd BATTERY DEVELOPMENT

VOLUME I

metallurgical
materials division

VOLUME I

TABLE OF CONTENTS

metallurgical
materials division

VOLUME I, SECTION I

ELECTROCHEMISTRY OF HEAT-STERILIZABLE SEALED CELLS

LIST OF TABLES

- Cont!d. -

LIST OF TABLES -- Cont"d.

metallurgical
materials division

LIST OF TABLES -- Cont'd.

VOLUME I, SECTION I

ELECTROCHEMISTRY OF HEAT-STERILIZABLE SEALED CELLS

LIST OF FIGURES

LIST OF FIGURES -- Cont'd.

LIST OF FIGURES -- Cont'd.

metallurgical
materials division

VOLUME I

SECTION i

ABSTRACT, CONCLUSIONS AND RECOMMENDATIONS

Major Objectives of This Effort

The major objectives of this program were: Research, development, engineering design, fabrication, testing and delivery of heat-sterilizable, nickel-cadmium space cells, capable of 400 post-sterilization cycles at 50% depth-of-discharge.

In addition, it was required to develop heat-sterilizable, nickel-cadmium cells and components with an impact-resistance capability of up to 4000 g.

New Techniques Required to Achieve These Goals

The achievement of these goals required three technologies which were beyond the present state-of-the-art; namely,

1. Heat-sterilization technology, particularly for the separator;

2. Hermetic seal technology (heat-sterilizable and capable of withstanding space vacuum for extended period under various environments);

3. Impact resistance technology (cases, seals, active components and sealed cells).

Additionally, higher energy density, greater than 16 watt-hours per pound, was needed for the weight savings in space missions.

Major Accomplishments and Findings:

1. Product-Oriented Accomplishments:

    (a) Investigated heat-sterilizable, chemically and electrochemically stable separator capable of long cycle life after heat-sterilization. From all the separators evaluated, polypropylene Brand FT2140, manufactured by Pellon Corporation, has been found to be the best in overall performance. Sealed Ni-Cd cells made with a single layer of this separator have undergone 248 post-sterilization deep discharge (100% depth-of-discharge) cycles without significant performance deterioration. Another promising separator is the Pellon brand polypropylene 14019 which gives slightly better capacity and reproducibility. However, during post-sterilization cycling the cells made with this separator tend to fail by shorting through the separator during early cycle life. This separator appears superior for non-sterilizable, nickel-cadmium cells compared to the nylon separators used in most commercial cells.

    (b) Developed inexpensive, heat-sterilizable, hermetic metal-to-nonmetal seal capable of long cycle life after sterilization. A glass-to-metal seal (made by TI) coated and heat-cured successively by several layers of polymer KEL-F-300 by Durafilm Company showed

metallurgical
materials division

the best performance. Metal-to-ceramic seals (Ceramaseal) were also successfully used on approximately 70 cells of 25 AH capacity. These cells have been successfully cycled after sterilization for two months. The cycling was terminated due to contractual modification.

(3) Constructed 60 test stations for automatic charge-discharge cycling of 4 AH cells. The stations are equipped with automatic cut-off at 0.8 ± .05 V during discharge and above 100 psi under any condition. The current capability is 3A with .03% ± 5 ma accuracy. Similarly constructed 24 high current stations for 25 AH cells. They have current capability of 30 amps with accuracy of .03% ± 5 ma. The stations are equipped with an overcharge protection that can be adjusted to any voltage from 3.5 to 1.2V ± .05V. Similarly, overdischarge voltage can be adjusted to any value between 3.5 to 0.7V ± .05V. The stations are protected against excessive pressure or temperature by automatic cut-off devices.

(4) Established technical and engineering capability of making sealed Ni-Cd cells capable of continued post-sterilization cycling without significant changes in performance. Thus 4 AH prismatic cells have undergone 248 deep charge-discharge cycles at $^C/2.5$ rate of discharge to 1.0 V cut-off. Similarly, 25 AH cylindrical engineering prototype cells have undergone sixty-five post-sterilization cycles at $^C/2$ rate of discharge to 1.0 V cut-off without any drop in capacity. 25 AH prismatic cells exhibit approximately 10% loss in capacity after sterilization. No further loss of capacity occurs during post-sterilization cycling. Life-testing of 25 AH, prismatic and cylindrical production cells at 70 and 80% depths-of-

metallurgical
materials division

discharge at $30°$, $50°$, and $70°F$ respectively was terminated after 30 cycles in accordance with JPL instructions. There was essentially no change in performance during these cycles.

(5) In order to increase the energy density of heat-sterilizable cells, a series of heavily loaded positive and negative plates were manufactured and tested under flooded cell conditions. Positive plates with 0.045" thickness delivered approximately 11 AH per cubic inch under these conditions. The negative plates with .049" thickness had a theoretical loading of 13 AH per cubic inch but delivered only 6.7 AH per cubic inch in flooded cells. This indicates the need for an improved negative plate before the energy density of sealed cells can be improved.

(6) Designed and developed high impact testing facility for shock testing Ni-Cd cells and components. It has a capability of accelerating a 50 lb. carriage mass to an impact velocity of 125 feet per second. The sliding carriage has a payload accommodation for various size cells up to five pounds. Subsequent impact is controlled to produce a shock environment of over 4000 g uniform deceleration for 0.001 second square pulse.

(7) Extensive impact testing of existing Ni-Cd cells (~4 AH sizes) was carried out to identify prime failure modes. The inherent strength of sintered nickel electrodes exceeded impact induced loading. However, electrical shorting and terminal connection

metallurgical
materials division

failures were observed. Several large, 25 AH heat-
sterilizable (non-impact resistant) cylindrical and
prismatic cells were impact tested to obtain criti-
cal design data.

2. <u>Knowledge Oriented Findings</u>

(a) We have not encountered any fundamental problem that
would make heat sterilization of sealed Ni-Cd cells
impractical. We also do not see any fundamental
problem that would make heat-sterilizable, impact
resistant cells impractical.

(b) Heat-sterilization changes the porosity and pore size
distribution of the positive plate which may unfavor-
ably affect the electrolyte distribution in the steri-
lized, starved cells. Also, the oxygen-free capacity
(charge acceptance of the positive plate without any
oxygen evolution) of the sterilized positive is de-
creased.

(c) Sterilized cells exhibit approximately 60 millivolts
higher end-of-charge voltage than unsterilized cells.
This is due to increased polarization at the positive
(nickel) electrode and may be related to the changes
in the pore structure, surface area and/or oxygen
overvoltage characteristics of the positive plate.
This higher end-of-charge voltage, since it is not

metallurgical
materials division

associated with the negative (cadmium) electrode is
not indicative of hydrogen evolution in sterilized
cells.

(d)   On continued cycling of sterilized cells, some of
the parameters (e.g. pore size distribution, and end-
of-charge voltage) tend to return to pre-sterilized
values indicating some reversibility of these changes.

(e)   Heat-sterilization oxidizes some of the free cadmium
metal (charge adjust) which can result in negative
limited cells on discharge. This parameter has not
been fully optimized and may be the cause of lack of
desired reproducibility in the performance of 4 AH
cells.

(f)   Addition of cobalt to the positive plate and of indium
or thallium to the negative plate did not show any
improvement in the cell performance in flooded cell
experiments. These additives are not considered es-
sential in sterilized, sealed cells.

(g)   The optimum electrolyte amount (volume) is approxi-
mately 75% of the free pore volume of the cell for
optimum performance. This is the most critical
parameter having major effect on the cell performance.

(h)   Wetting and KOH absorption characteristics of the

metallurgical
materials division

separator, the positive and the negative plates change
during sterilization and cycling. These in turn
affect the kinetics.of oxygen,evolution and recom-
bination. Pre-treatments of the separator with (a)
chromic acid, (b) surfactants or (c) RAI proprietary
process show no permanent beneficial effect on the
cell performance during post-sterilized cycling.

(i) Studies concerning the effect of core-compression
show that the prismatic 4 AH cells with 18 plates
(higher compression) have better reproducibility
than 17 plate cells. The discharge behavior of the
18 plate configuration is more uniform from cell to
cell and cycle to cycle than the 17 plate cells.

(j) Further physico-chemical characterization of the
active components of the cell before and after
sterilization was performed using x-ray diffraction,
differential thermal analysis, thermo-gravimatic
analysis, electron microscope and gas chromatographic
techniques. The x-ray diffraction of plates did not
indicate the formation of any new phases due to
sterilization. The nickel hydroxide crystals in the
positive became more orderly and of larger size due
to the sterilization. However, the particle size of
the positive nearly returned to its initial (pre-
sterilization) state during post-sterilization cycling.

metallurgical
materials division

The crystallite sizes of cadmium plates were too
large to permit detection of any change. Electron-
microscopic studies showed that the cadmium active
material crystals become larger during sterilization,
thus, resulting in reduced surface area. No defi-
nite conclusions could be made from TGA and DTA data.
Gas chromatographic studies showed that there is
essentially no change in the hydrogen over-voltage
characteristics of the negative plate due to sterili-
zation.

(k)   High temperature stable plastic-to-metal seals,
        (Ziegler type) incorporating a KEL-F-300 insulator,
        a stainless steel outer sleeve and a nickel conductor
        (feed-through) were designed, built and tested prior
        to and after heat sterilization. Prior to steriliza-
        tion, the leak rate of these seals was less than
        1×10^{-10} cc He/sec/atm indicating an excellent seal
        for nonsterilizable cells. However, during heat
        sterilization, the plastic material flowed and caused
        seal leakage. Several successive design modifica-
        tions did not stop leakage after sterilization.
        Seals made with polypropylene material also failed
        after sterilization.

(l)   For a rational design of impact resistant Ni-Cd cells,
        the important mechanical properties (yield strength,

i-8

tensile strength, bearing strength, Poisson's ratio, modulus of elasticity, elongation and buckling information) of the prime structural elements in the cell, namely sintered positive and negative plates were measured under static and dynamic loading rates and were compared with the results of theoretical analysis. When sufficient lateral restraint is employed to prevent buckling, ultimate compression stresses from 3000-6000 psi are exhibited. Dry electrodes over 6 inches long will experience no apparent damage after 4000g impact loading. Employing the design criteria developed during this study, a 25 AH heat-sterilizable cell can be built to withstand a 4000 g impact environment without auxiliary strengthening of the sintered electrodes and without damage to the cell.

Recommendations:

On the basis of the results obtained to date under this contract, the following recommendations can be made for further development of heat-sterilizable, sealed nickel-cadmium cells for space missions:

1. Carry out a long-range, comprehensive testing program to characterize the heat-sterilized, cylindrical and prismatic sealed cells at various charge and discharge rates, charge inputs, depths-of-discharge and temperatures and

metallurgical
materials division

after storage. Determine and correct causes of any per-formance degradation.

2. Using the data generated under 1., perform regression analysis and develop mathematical model to predict cell performance characteristics for a given set of operating conditions.

3. Optimize charge parameters and develop more suitable charge control circuits for specific missions.

4. Carry out a program to develop heat-sterilizable plastic-to-metal seal using creep-resistant, thermally stable, newer plastics (such as polyphenylene oxide) that will not leak after sterilization and that will withstand 4000 g impact.

5. In order to increase the energy density and life, further optimize the following cell design parameters for heat-sterilizable cells:

    A: Ratio of positive to negative plate active material;

    B: Charge adjust (free cadmium metal in the negative plate);

    C: Plate thickness and higher loading of active materials.

6. Using the impact cell design data generated during this study for sintered nickel cadmium cells, build and test heat-sterilizable, impact resistant cells.

metallurgical
materials division

7. Perform flight qualification testing of optimized, final design cells for specific space mission requirements.

8. Utilize the more rugged crip KEL-F (polymeric) and other seals and the improved heat-sterilizable separator developed in this program for other sealed Ni-Cd cell production for other government needs as spin-off technology.

metallurgical
materials division

VOLUME I

SECTION ii

INTRODUCTION

This is the final report on the heat-sterilizable, as well as heat-sterilizable and impact-resistant Ni-Cd battery research and development under Jet Propulsion Laboratory Contract No. 951972, Modification No. 14. The program is sponsored under NASA Contract NAS-7-100, Task Order No. RD-26. The object of this contract is to perform research, development and engineering work leading to the design, development, engineering, manufacture and testing of hermetically sealed, rechargeable nickel-cadmium cells capable of satisfactory performance after heat sterilization as well as after heat sterilization and impact landing for space missions. The specific goal is to develop sealed nickel-cadmium cells capable of 400 post-sterilization cycles at 50% depth-of-discharge.

The purpose of heat sterilization of certain spacecrafts is to prevent contamination of planets while searching for extra terrestrial life. The heat-sterilization requirement has created the problem that some components are unable to function satisfactorily after undergoing heat sterilization. This appears to be especially true of rechargeable batteries which must function satisfactorily over hundreds of charge-discharge cycles after being subjected to the rigors of heat steriliza-

metallurgical
materials division

tion. Since no such storage battery was currently available, the Jet Propulsion Laboratory (JPL) undertook a systematic program to develop such batteries. The general objectives of the JPL program as outlined in the "Spacecraft Sterilization Technology"[1] are: (1) to obtain basic and new information regarding batteries and battery components subjected to heat-sterilization procedures; (2) to develop technology to assist in the proper designing and fabrication of heat-sterilizable batteries; (3) to test and to evaluate components and units of heat-sterilizable batteries; (4) to produce a battery which will satisfactorily meet flight program requirements. The heat-sterilization requirements include testing at $135^{\circ}C$ for type approval, and at $125^{\circ}C$ testing for flight acceptance. At the $135^{\circ}C$ sterilization temperature, the heating rate is $19^{\circ}C/hour$. The chamber is held at this temperature for sixty-four hours and then cooled to room temperature at the same rate at which it was heated. Two such cycles are required. For preliminary testing one 120-hour cycle is acceptable..

The hard-landing requirement includes the ability to withstand a uniform 4000 g deceleration from an impact velocity of 120 ft/sec. A square shock pulse is applied with a duration of 0.001 second. The battery should perform as required

---

(1) R. Lutwack, Spacecraft Sterilization Technology Proceedings, NASA SP 108; 11/16-18/65, pp. 361-370.

metallurgical
materials division

thereafter. Commercially produced nickel-cadmium cells are
not designed to withstand the rigors of the heat steriliza-
tion process or 4000 g impact and the factors responsible for
the deterioration in the performance of nickel-cadmium cells
needed to be investigated and understood before a reliable,
hermetically sealed, rechargeable cell with long cycle life
and satisfactory performance characteristics could be devel-
oped. The specific tasks under this contract incorporating
the latest modifications are given in Appendix I. These
tasks may be grouped under the following three broad sections
and are reported under these sections for convenience:

1. <u>Electrochemistry</u> of heat-sterilizable cells. This
   includes basic research and development work on the
   positive and negative plates and separator as well as
   design, assembly and testing of complete cells lead-
   ing to the batteries capable of satisfactory opera-
   tion after undergoing heat sterilization.

2. <u>Battery Engineering</u>: This includes full-size cell
   design, development, optimization, production and test-
   ing of heat-sterilizable as well as heat-sterilizable
   and impact-resistant cells. Investigate both the cy-
   lindrical as well as the rectangular cell designs and
   select one design for further development and optimi-
   zation. Hermetic seal design, assembly and testing
   to withstand the heat-sterilization as well as impact
   testing form part of the battery engineering program.

metallurgical
materials division

3. Impact Testing of Cells and Components: Both static
    and dynamic testing of seals, cases, plates, and
    complete cells are to be performed for hard impact
    landing missions.

The technical supervision from the Jet Propulsion Laboratory
for this contract was provided by Dr. Ralph Lutwack whose input
in terms of JPL requirements, suggestions and technical direc-
tion were very valuable and this contribution is gratefully
acknowledged.

metallurgical
materials division

VOLUME I

SECTION I

ELECTROCHEMISTRY OF HEAT-STERILIZABLE SEALED CELLS

A. <u>Screening, Selection and Optimization of Separators</u>:

<u>Separator Requirements</u>:

One of the most critical components in the heat-sterilizable, sealed nickel-cadmium cells is the separator. It must satisfy the following requirements:

1. It should be capable of surviving an exposure to 135°C in approximately 30 weight percent of potassium hydroxide solution for 128 hours without physical or chemical degradation. The conventional polyamide (Nylon) separator completely disintegrates under these severe conditions.

2. It should remain inert under the highly oxidizing and reducing conditions existing at the positive and the negative plates respectively during the battery charging conditions and charged stand.

3. Its wetting characteristics should be such that it exhibits minimum electrolytic resistance when in contact (holding) a given amount of potassium hydroxide solution.

4. Its mechanical properties should be such that a single layer of relatively thin (.007") non-woven separator between the positive and the negative plates

in a tightly packed assembly (core) should provide an effective barrier to migration of any solid particles and thus prevent any electrical shorting of the plates.

5. Its gas permeability should be such that it provides minimum impedance to the diffusion of oxygen from the positive to the negative plate during any overcharge.

In summary, the separator must remain thermally, chemically and mechanically stable during the severe thermal sterilization environments and also during all operating conditions including electrochemical charge, overcharge, shock and vibration.

Literature Review for Heat-Sterilizable Separator Selection: A literature review of the heat-sterilizable separator technology for alkaline cells was made to screen and select promising materials for preliminary evaluation. The review included government sponsored contract reports, proceedings of the "Power Sources Conferences," technical data bulletins published by the separator manufacturers, and other available literature on heat-sterilizable separator for nickel cadmium cells.

It was noted that on the subject of heat-sterilizable separator for Ni-Cd cells, there was only one report available viz.: ("Investigations of Sterilization of Secondary Batteries" First Quarterly Report from Gulton Industries to Langley Research Center, NASA CR-66105). It was found in later studies that heat-sterilizable "separator" or barriers to silver and zinc penetrations developed under NASA sponsorship for silver-zinc cells were not suitable for nickel-cadmium cells. Based upon this literature review as well as discussions with separator manufacturers and upon the experimental data for the stability of various separator materials in 30% KOH at 145°C for 128 hours (Technical Report, First Quarter, 1967, this contract, Table I, page 7) the following materials, often used in Ni-Cd cells or other alkaline cells as separators, were found to be

metallurgical
materials division

<u>unsatisfactory</u> for heat-sterilizable Ni-Cd cells since they either dissolved completely, or disintegrated or showed significant loss of weight and/or mechanical strength:

Nylon (Polyamides), asbestos papers, alumina papers, Dynel (Modacrylic polymer), Dacron, polyester, porous Teflon and cotton.

The above materials were therefore eliminated from further consideration for this program.

The above work revealed that the following separator brands are stable in 30% KOH at 145°C for 128 hours:

Pellon polypropylene Brands 14019 and 14020, 25/242, FT 2140 (earlier known as 25/249) and Kendall Brand EM 476 polypropylene.

Other polypropylene brands, although stable in 30% KOH at 145°C, were eliminated from further evaluation for other reasons. Thus Pellon Brand 25/242 was an experimental sample made by the Pellon Company in Germany and was not available in production quantities for further testing. Pellon Brand 14020 was eliminated due to poor electrochemical performance (First Quarterly Report, Table II, page 8, this contract). It was also noted that Pellon 25/249 was commercially known as FT 2140 which designation is used in this report.

Three polypropylene-type, non-woven (felted) separators were selected for further studies and optimization. These were Pellon FT 2140 and 14019 and Kendall EM 476.

metallurgical
materials division

Further characterization included a study of the wetting prop-
erties and electrolyte distribution of the separators described
next.

Wetting Properties of Polypropylene Separators:

Characteristically pure polyalkanes (e.g. polypropylene) have
relatively poor wetting properties (i.e. contact angle $\sim 90^{\circ}$)
in concentrated alkaline solutions. Often these separators
are treated with wetting agents or surfactants during the
manufacturing process. Past experience in our laboratories
has shown that some of these additives or their constituents
may be detrimental to battery performance due to their oxidiz-
ing or reducing characteristics in the cell environment. The
selected separators, mentioned previously, were therefore,
analyzed for trace "impurities" using emission spectrograph.
Results of these analyses are shown in Table I-1. From the
past experience it is believed that none of these ions in the
quantities present are harmful.

TABLE I-1

SPECTROSCOPIC ANALYSES OF SEPARATOR MATERIALS

Separator	Ash %	Major Constituent of Ash	Cations Present (ppm)						
			Si	Al	Mg	Zn	Fe	Cu	Na
Kendall EM476	0.2	---	200	20	10	10	10	100	1
Pellon 14019	1.3	Zn	1000	200	20	--	20	300	500
Pellon FT2140	11.1	Mg	100	1	--	10	20	200	1000

metallurgical
materials division

An attempt was made to enhance the wetting properties of the polypropylene separators by replacing and/or adding a known surface active agent. Three surfactants based on the wetting characteristics, thermal stability and compatibility with potassium hydroxide solutions, as described by the manufacturers, were selected for evaluation. These were FC 98 and FC 95 made by the 3M Company and Triton X-100 made by Rohm and Hass. To determine the effectiveness of these surfactants in enhancing the wetting characteristics of the separators, samples of the various felts as received were impregnated with the surfactant solutions. In another set of experiments, the separator samples were washed free of any surfactants incorporated by the manufacturer and were then treated with the surface active agents to determine their effectiveness on electrolyte wetting, absorption and retention characteristics of the separators. Effectiveness of the surfactants was measured in terms of grams of 31 weight percent KOH solution absorbed per gram of dry separator. Untreated separators were used as control samples. These data are shown in Table I-2 for surfactants Triton X-100, FC-95, and FC-98 with water or methanol as solvents. Nylon (2505K) which is used as separator in our standard product was used for comparison. These data show that the attempts to date to enhance the wetting and absorption properties of these polypropylene separators by the leaching and/or addition of surfactants have been unsuccessful.

metallurgical
materials division

TABLE I-2

ABSORPTION OF KOH BY VARIOUS SEPARATORS

(gm of 31% KOH/gm of dry separator)

Separator Treatment and Surfactant Used	Separator Material		
	Kendall EM476	Pellon 25/249	Pellon 14019
Material Untreated (control sample)	3.2	2.2	10.9
Material Unwashed FC-95 in H_2O 1:1000	2.5	2.2	9.9
Material Unwashed Triton X-100 in H_2O 1:1000	2.5	2.7	10.1
Material Washed FC-98 in Ch_3OH 7.5% Soln.	1.8	1.2	2.8
Material Unwashed FC-98 in CH_3OH 7.5% Soln.	3.5	1.5	2.7
Material Washed Triton X-100 in H_2O 1:1	3.0	3.0	4.7
Material Unwashed Triton X-100 in H_2O 1:1	2.5	2.0	4.6
Material Unwashed FC-98 in CH_3OH 1:100	2.2	2.2	3.1
Material Unwashed Triton X-100 in H_2O 1:100	3.2	2.1	7.7
Unwashed Samples FC-98 in 30% KOH 500 ppm	2.0	2.6	10.1

Further optimization of the separator was based upon the electrochemical performance data on pre- and post-sterilization cycling in hermetically sealed cells.

B. Development of Heat-Sterilizable Cell Case and Cover:

Our past experience in the packaging of Ni-Cd cells has shown that both nickel and stainless 304 are satisfactory materials for the case and the cover of sealed, heat-sterilizable Ni-Cd cells. Since stainless steel cases and covers were readily available from our previous programs, it was decided to use 304 stainless steel cases (.030" thickness) for experimental purposes. The size selected was our standard, prismatic (rectangular) 4 AH cell shown schematically (actual size) in Figure I-1. These cases and covers have successfully passed two sterilization cycles in 30% KOH at 145°C for over 128 hours and have been used successfully for hundreds of charge-discharge cycles for this program. Larger size (25 AH) prismatic and cylindrical cell cases and covers were also made from stainless steel 304 and have worked well as described in Section II.

Development of Heat-Sterilizable Seal

The hermetic seal for the cell is another very critical component of a sealed, heat-sterilizable cell. It should maintain its hermeticity during and after thermal sterilization and should not degrade in the KOH and in the oxidizing or reducing environments.

metallurgical
materials division

FIGURE I-1

NICKEL LID

VALVE

TERMINAL POST

GLASS-TO-METAL
SEAL

NICKEL TABS
WELDED TO POST

PLATES

STAINLESS
STEEL CAN
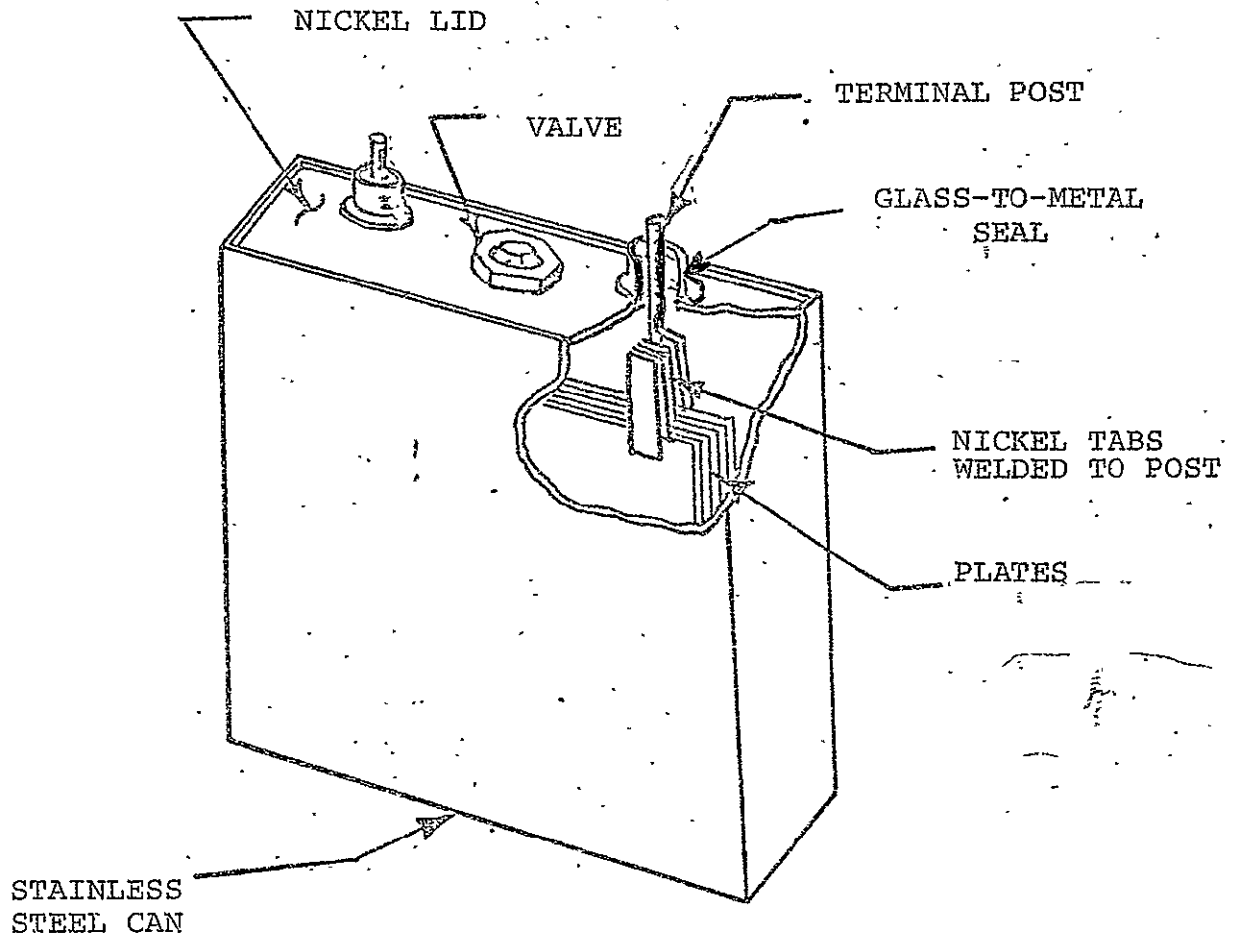
HEAT STERILIZABLE NICKEL-CADMIUM CELL

Since a literature search revealed no previous work
on such a seal, a significant portion of the initial develop-
ment work was devoted to this task. After considering various
approaches, it was decided to use thermally and chemically
stable polymeric materials as firmly adherent coatings on con-
ventional hermetic, glass-to-metal seals.

The seals used for the initial development were of the glass-
to-metal type whose construction in shown in Figure I-2. Mass-
produced, hermetically sealed glass-to-metal seals of this
type are used extensively in the electronics industry for
diodes, transistors, etc., and for electrical feed-throughs.
We have had considerable experience in the fabrication and
testing of these seals for electronic devices. Since glass
is not resistant to KOH at sterilization temperatures, it
must be protected from chemical attack. Work performed prior
to this contract with epoxy coated glass seals has shown no
leakage over a one-year period at room temperature and sev-
eral weeks at $145^{\circ}F$. After a review of the literature and
discussions with several vendors, KEL-F, Durafilm K (an
epoxy) and Stycast (an epoxy) were selected for further eval-
uation as protective coatings.

These materials were applied to several case tops and hermetic
seals by the Durafilm Company which specializes in protective
coating technology. The coating is applied in four or five
steps, each step involving spraying and baking of the thin

metallurgical
materials division

FIGURE I-2

LID (Ni)

Ni PLATED
Cold Rolled Steel

GLASS

SEALANT

52 ALLOY

Cu

TERMINAL
POST

-7/32"

-1/4"

3/8"

TYPE I

LID (Ni)

Ni PLATED
Cold Rolled Steel

RESIN

TERMINAL
POST

Ni

0.112"

TYPE II
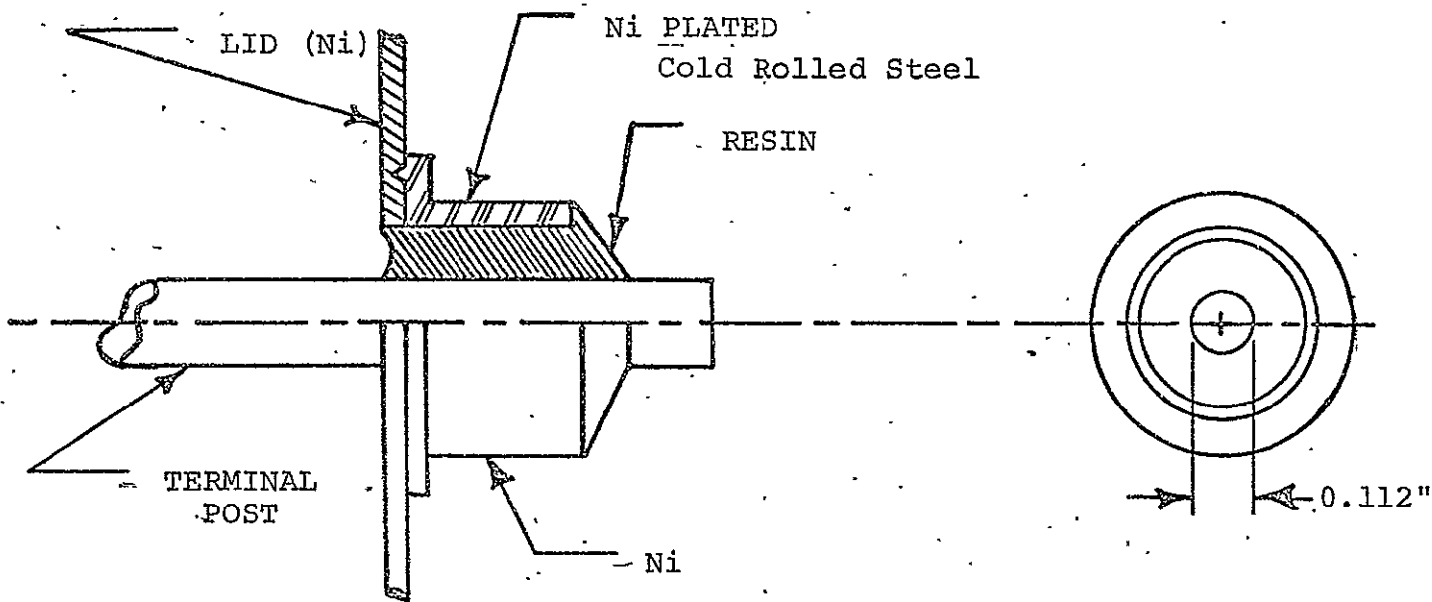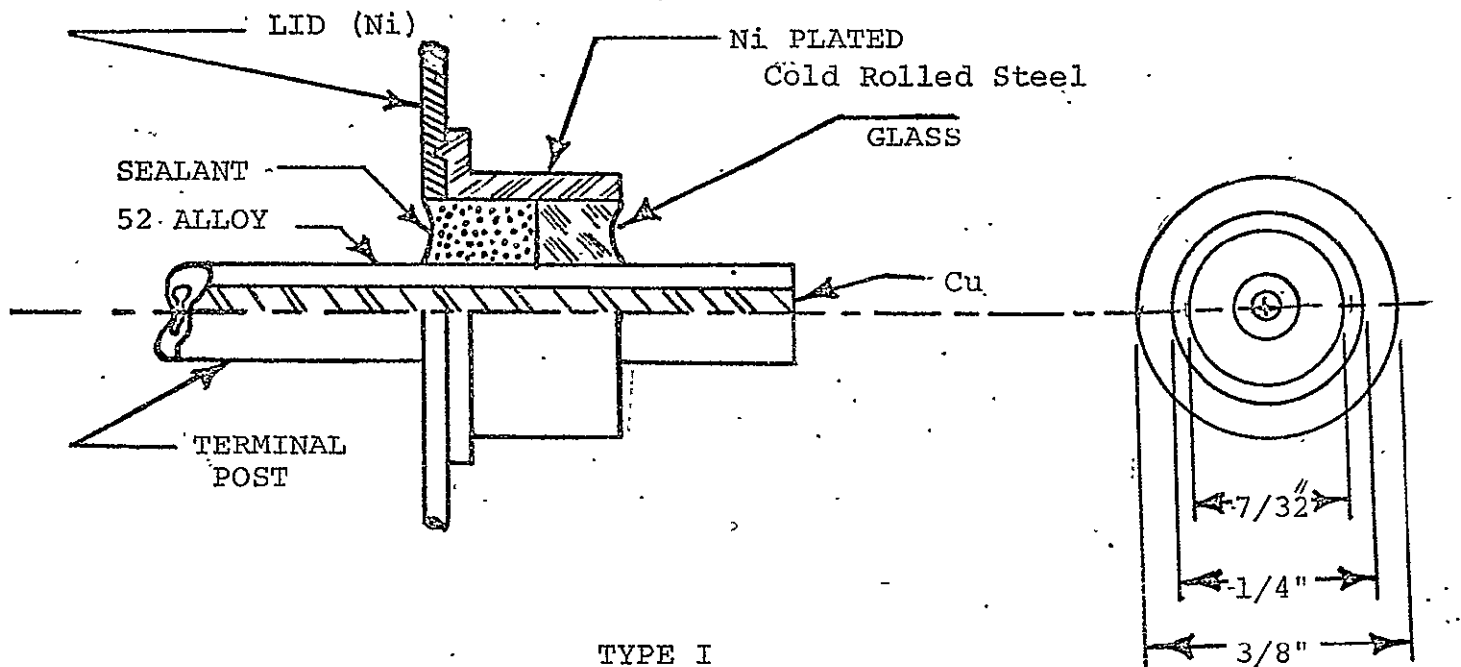
HEAT STERILIZABLE HERMETIC SEAL

coating prior to applying the next coating.

The evaluation of these coatings was done in experimental, 4 AH, prismatic cells. The details of the cell construction are described in Subsection C. An examination of the glass-to-metal seals coated with KOH resistant Durafilm K as well as KEL-F polymeric materials and other polymers mentioned above, after two heat-sterilization cycles, has indicated that the adherence of KEL-F polymer coating was somewhat better than all other coatings. Therefore, the KEL-F coating was selected for the final design of the cells. Other in-house sealants (coatings) such as silicone rubbers, epoxies, etc., were also tried in initial experiments in sealed cells but were discarded in favor of superior KEL-F.

C. Experimental Prismatic Cell Construction:

The details of the design and construction of the stainless steel cases and tops as well as glass-to-metal seals coated with KOH resistant polymeric materials for the rectangular, 4 ampere-hour cells are given in Figures I-1 and I-2. The details of the cell design parameters are given below.

The electrode sizes are as follows:

Positive plates: 2.25" x 1.812"; .025" nominal thickness
Negative plates: 2.25" x 1.812"; .025" nominal thickness

The number of plates used initially was 9 positive plates and 10 negative plates. However, 18-plate construction with 8 positive

metallurgical
materials division

and 10 negative plates was found best in later studies. Some cells were prepared with 8 positives and 9 negatives. The 18-plate construction, which is the preliminary standard for most rectangular prototype cells gave optimum performance and were relatively easy to assembly. This observation is based upon data reported in Tables I-19 and I-21.

Cell Fabrication Procedure

Each cell assembly for the production of rectangular 4 AH cells used in this program involved the following procedure:

1. Preparation of top cover assembly described in the first quarter Progress Report and shown in Figure I-1;

2. Preparation of two terminal subassemblies (glass-to-metal seals) also described in the first quarter Progress Report;

3. Leak check each terminal for any pinholes by the dye penetration test;

4. Welding the terminal subassemblies to the top cover;

5. Leak checking the top assembly for weld integrity using helium leak test;

6. Coating the glass-to-metal seals with thermally stable, KOH-resistant polymer coating by an outside vendor (Durafilm Company);

7. Cutting the positive and negative plates to size, quality control checks for burrs, loose wire, etc.;

8. Welding nickel tabs to positive and negative plates;

9. Separator assembly (wrapping the separator around each positive and negative plate);

metallurgical
materials division

10. Core compression under controlled condition (~400 psia);

11. Trimming the package and checking for and eliminating any possible electrical shorts;

12. Welding the positive and negative tabs to the cover terminals;

13. Checking for electrical shorts in the cell package by electrical continuity test;

14. Inserting the cell package into the steel case;

15. Checking for any possible short circuits in the cell package by electrical continuity test;

16. Welding the top cover to the case;

17. Checking for any possible short circuits during welding by electrical continuity test;

18. Checking for weld integrity by helium leak test;

19. Electrolyte addition (predetermined fill level);

20. Cell resistance measurement by A.C. bridge;

21. Attaching pressure relief vent or pressure gage as needed;

22. Cells ready for conditioning and tests.

Construction of Test Facilities

A test panel, complete with control stations, was built for electrochemical characterization of cells and plates prior to and following heat sterilization. The test stations were connected to our automatic data acquisition system which records all pertinent electrochemical characteristics of the cells. The data which are recorded on punchcards are then processed by an IBM 360-30 computer according to programs available in the system's library. A schematic diagram of the data acquisition

metallurgical
materials division

system is given in Figure I-3. A typical computer printout is shown in Table I-3 with an explanation of symbols given in Table I-4. This facility was used routinely for all the electrochemical characterization under this contract.

metallurgical
materials division

ENERGY BRANCH BATTERY DATA ACQUISITION SYSTEM

```
┌──────────┐          ┌────────────────────────────┐
│ PRESS    │─────────▶│ TEST STATION PANEL (20     │
│ GAUGES   │          │ STATIONS PER PANEL)        │
└──────────┘          └────────────────────────────┘
     │                    ▲                │
     │           ┌────────────────┬────────────────────────┐
     │           │ PANEL          │  SWITCHING AND          │
     │           │ CONTROL        │  DATA TRANSFER          │
     │           │ UNIT           │  CIRCUITRY              │
     │           ├────────────────┼────────────────────────┤
     │           │ PANEL          │  INDIVIDUAL             │
     │           │ POWER          │  STATION                │
     ▼           │ SUPPLY         │  TIMERS                 │
                 └────────────────┴────────────────────────┘

     ┌───────────────────────────────────────┐
     │ 300 CHANNEL, GUARDED                   │
     │ CROSS-BAR SCANNER                      │      "DYMEC"
     ├───────────────────────────────────────┤      SYSTEM
     │ SCANNER CONTROL UNIT                   │      INTERFACE
┌────────────────┐  ├────────────────────────┤      UNIT
│ NON-VOLTAGE    │  │ INTEGRATING DIGITAL     │
│ TYPE DATA      │  │ VOLTMETER               │
└────────────────┘  ├────────────────────────┤
     │              │ CARDPUNCH COUPLER       │
     │              └─────────────────────────┘
     │                        │
     │              ┌──────────────┐
     │─MANUAL PUNCH─▶│ IBM 526     │      ┌───────────────────────────────┐
                    │ CARD        │──────│ INTERCHANGEABLE "CARD          │
                    │ PUNCH       │      │ FORMAT" CIRCUIT BOARD          │
                    └──────────────┘      └───────────────────────────────┘
                           │
                    ┌──────────────┐      ┌───────────────────────────────┐
                    │ IBM "360"   │◀─────│ PROGRAMS STORED ON             │
                    │ MODEL 30    │─────▶│ DISC FILE                      │
                    └──────────────┘      └───────────────────────────────┘
                           │
                    ┌────────────────────────────┐
                    │ PRINTED OUTPUT ACCORDING    │
                    │ TO CHOSEN PROGRAM           │
                    └────────────────────────────┘
```

FIGURE I-3

metallurgical
materials division

Table I-3

JPL SEPARATOR EVALUATION =1

NI-CD, SUB-C, SINTERED PLATE, HERMETICALLY SEALED CELLS.

CELLS 1-9 SEPARATOR KENDALL EM476
CELLS 10-16 SEPARATOR PELLON 25/249
CELLS 17-23 SEPARATOR PELLON 14019

TEST NO. 0   CYCLE NO. 1   DATE. 8/18/1967   TEMP. DEGREES C. 22

	CURRENT	TIME		RATE	LEVEL
	AMPS	HR(S)	MIN(S)		(P/C)
CHARGE.	0.060	24 .	0 .	C/ 0.0	
DISCHARGE.	1.500, TO 1 VOLT CUT-OFF.			C/ 0.0	

OPEN CIRCUIT STAND TIME. 0 HR(S)., 0 MIN(S).

CELL VOLTAGE AT VARIOUS DISCHARGE LEVELS

CELL NUMBER	ECV (V)	ECN-R (V)	OCV. (V)	DCN-R (V)	25 PER CENT T-V (V)	25 PER CENT N-R (V)	50 PER CENT T-V (V)	50 PER CENT N-R (V)	75 PER CENT T-V (V)	75 PER CENT N-R (V)	ECR MILLI OHMS	EDR MILLI OHMS	ECP PSIA	EDP PSIA	ECC AMP-HRS	EFF
1	1.420	0.0	1.391	0.0	0.0	0.0	1.174	0.0	0.0	0.0	38.64	22.82	0.0	0.0	0.475	0.0
2	1.423	0.0	1.391	0.0	0.0	0.0	1.195	0.0	0.0	0.0	22.41	17.04	0.0	0.0	0.564	0.0
3	1.419	0.0	1.388	0.0	0.0	0.0	1.193	0.0	0.0	0.0	26.50	17.19	0.0	0.0	0.513	0.0
4	1.420	0.0	1.387	0.0	0.0	0.0	1.170	0.0	0.0	0.0	35.77	21.93	0.0	0.0	0.489	0.0
5	1.422	0.0	1.394	0.0	0.0	0.0	1.198	0.0	0.0	0.0	27.12	19.01	0.0	0.0	0.613	0.0
6	1.407	0.0	1.381	0.0	0.0	0.0	1.159	0.0	0.0	0.0	29.70	22.53	0.0	0.0	0.424	0.0
7	1.418	0.0	1.389	0.0	0.0	0.0	1.188	0.0	0.0	0.0	29.35	18.57	0.0	0.0	0.525	0.0
8	1.411	0.0	1.392	0.0	0.0	0.0	1.155	0.0	0.0	0.0	36.84	21.35	0.0	0.0	0.400	0.0
9	1.408	0.0	1.383	0.0	0.0	0.0	1.158	0.0	0.0	0.0	34.66	21.32	0.0	0.0	0.414	0.0
10	1.420	0.0	1.389	0.0	0.0	0.0	1.147	0.0	0.0	0.0	39.98	29.14	0.0	0.0	0.339	0.0
11	1.424	0.0	1.392	0.0	0.0	0.0	1.150	0.0	0.0	0.0	42.97	30.21	0.0	0.0	0.450	0.0
12	1.422	0.0	1.387	0.0	0.0	0.0	1.141	0.0	0.0	0.0	41.32	32.11	0.0	0.0	0.463	0.0
13	1.424	0.0	1.389	0.0	0.0	0.0	1.154	0.0	0.0	0.0	44.26	30.97	0.0	0.0	0.463	0.0
14	1.427	0.0	1.393	0.0	0.0	0.0	1.170	0.0	0.0	0.0	36.86	28.81	0.0	0.0	0.499	0.0
15	1.433	0.0	1.395	0.0	0.0	0.0	1.162	0.0	0.0	0.0	45.25	31.45	0.0	0.0	0.513	0.0
16	1.421	0.0	1.374	0.0	0.0	0.0	1.148	0.0	0.0	0.0	40.48	37.01	0.0	0.0	0.533	0.0
17	1.412	0.0	1.375	0.0	0.0	0.0	1.216	0.0	0.0	0.0	14.76	14.38	0.0	0.0	0.625	0.0
18	1.410	0.0	1.377	0.0	0.0	0.0	1.217	0.0	0.0	0.0	14.35	14.50	0.0	0.0	0.613	0.0
19	1.412	0.0	1.375	0.0	0.0	0.0	1.210	0.0	0.0	0.0	16.10	16.18	0.0	0.0	0.639	0.0
20	1.412	0.0	1.376	0.0	0.0	0.0	1.212	0.0	0.0	0.0	15.44	15.18	0.0	0.0	0.613	0.0
21	1.410	0.0	1.376	0.0	0.0	0.0	1.21	0.0	0.0	0.0	14.30	14.67	0.0	0.0	0.600	0.0
22	1.410	0.0	1.374	0.0	0.0	0.0	1.2	0.0	0.0	0.0	15.01		0.0	0.0	0.613	0.0
23	1.420	0.0	1.379	0.0	0.0	0.0	1.219	0.0	0.0	0.0	13.91	13.39	0.0	0.0	0.675	0.0
MEAN	1.418	0.0	1.385	0.0	0.0	0.0	1.181	0.0	0.0	0.0	29.37	21.95	0.0	0.0	0.525	0.0
STAND. DEV.	0.007	0.0	0.010	0.0	0.0	0.0	0.027	0.0	0.0	0.0	11.16	6.93	0.0	0.0	0.087	0.0

TABLE I-4

KEY OF SYMBOLS FOR COMPUTER DATA

ECV   END-OF-CHARGE CELL VOLTAGE

ECN-R   END-OF-CHARGE NEG VS. REF VOLTAGE

OCV   OPEN CIRCUIT CELL VOLTAGE

OCN-R   OPEN CIRCUIT NEG VS. REF VOLTAGE

T-V   CELL VOLTAGE   ⎫ AT SPECIFIED
                                    ⎬   DISCHARGE
N-R   NEG VS. REF VOLTAGE   ⎭   LEVELS

ECR   END-OF-CHARGE RESISTANCE

EDR   END-OF-DISCHARGE RESISTANCE

ECP   END-OF-CHARGE PRESSURE

EDP   END-OF-DISCHARGE PRESSURE

ECC   ELECTROCHEMICAL CAPACITY (AMPERE-HOUR)

EFF   EFFICIENCY

LEVEL

RATE CHARGE

    DISCHARGE

D. Preliminary Electrochemical Investigations With Heat-Sterilizable Sealed Cells

Further evaluation of the three best non-woven polypropylene separators was continued together with polymer-coated glass seal evaluation in experimental 4 AH prismatic cells described earlier. The electrochemical parameters described in Table I-3 were measured. The primary object was to select the best separator for the factorial program and also to screen and select the most promising seal(s). Table I-5 gives the averaged performance data for cells made with 14019, FT2140 and EM476 separators before and after sterilization. A comparison of the delivered capacities and end-of-charge resistance values before and after sterilization show the 14019 brand of poly-propylene to be superior. The next best separator is FT2140. No further evaluation of EM476 was performed since it contributed to high cell resistance on cycling and shorting after steriliza-tion.

It will be noted that both the end-of-charge resistance and end-of-charge voltage increase after sterilization. The higher end-of-charge voltage is primarily due to increased overvoltage although there is some contribution by increased IR drop.

The cell characterization following the second sterilization cycle indicated a greater failure frequency for the cells con-taining 14019 and EM476 separators compared to cells containing FT2140 separator. The shorting mode of failure, after second

metallurgical
materials division

TABLE I-5

POLYPROPYLENE SEPARATOR EVALUATION

Type 14019

Condition	No. Cells	Cycle Number	Capacity AH	ECV Volts	ECR mΩ
Presterilized	6	5	4.009±.032	1.459±.006	5.64±1.63
1st Steriliz.	5	5	3.187±.604	1.688±.315	12.31±1.83
2nd Steriliz.	4	All 4 failed			

Type FT2140

Condition	No. Cells	Cycle Number	Capacity AH	ECV Volts	ECR mΩ
Presterilized	6	5	3.520±.255	1.507±.028	8.23±1.64
1st Steriliz.	5	5	3.226±.274	1.588±.072	27.25±21.70
2nd Steriliz.*	2	4	2.842±.076	1.555±.005	12.54± 1.62

*2 failed of original 4

Type EM476

Condition	No. Cells	Cycle Number	Capacity AH	ECV Volts	ECR mΩ
Presterilized	5	5	3.431±.371	1.559±.064	11.23±2.22
1st Steriliz.	2	5	2.876±.058	1.579±.010	19.70±5.28
2nd Steriliz.	2	4	1.717±.017	1.615±.004	34.74±0.37

Charge rate 2 amps, 3 hours discharge; at 2 amp to 1.0V cut-off

I-19

sterilization, is much lower with cells containing FT2140. This is consistent with better physical and mechanical properties observed with FT2140.

It is interesting to note that the cells containing FT2140 after second sterilization did not show as much capacity loss as did the cells with 14019 or EM476 separators. Among the various polymeric coatings used for the seals, KEL-F was again found to be the best.

E. Planning and Selection of Factors for the Design of Statistical Experiments

One of the tasks in the development of a satisfactory heat-sterilizable, sealed Ni-Cd battery is to perform planned statistical studies to determine the effects of the following variables on the cell performance.

1) Concentration of KOH (2 levels) -- two factors;

2) Addition of Li^+, Na^+ and Bi^{+++} ions and surfactants (2 types) to the electrolyte -- five factors;

3) Addition of Tl^+ and In^{+++} ions to the negative plate -- two factors;

4) Addition of Co^{++} ions to the positive plate -- one factor at one conc.;

5) Various separators (2 levels) -- two factors for FT2140 and 14019.

Assuming only two levels of electrolyte concentration and two types of separator material, a two level of factorial

metallurgical
materials division

experiment with only two cells of each kind (one control, one for sterilization) with the twelve factors listed above would require over 4,000 cells. This does not include the important design factors such as the amount of electrolyte (% pore fill), the charge adjustment on the negative $\left[Cd:Cd(OH)_2 \right.$ ratio $\left. \right]$ or the ratio of the total cadmium to nickel hydroxide and cell geometry factors. It is therefore necessary to screen the effects of some of these variables in preliminary screening experiments, so that the variables showing very significant and reproducible effects can be incorporated in the final factorial experiments.

Preliminary screening tests described below eliminated several of the above factors from the factorial design experiment.

1) <u>Bismuth Ion Addition to the Electrolyte</u>

Appreciable solubility of the bismuth hydroxide in the potassium hydroxide electrolyte is a prerequisite for studying the effect of bismuth ion on the performance of sealed Ni-Cd cells.

Solubility data for bismuth hydroxide in KOH solutions reported by Seidell in "Solubilities of Inorganic and Metal Organic Compounds," Volume 1, page 437 are given below. The concentration of KOH in terms of grams of KOH per liter reported by Seidell is converted to molarity for easy comparison with Ni-Cd battery electrolyte.

metallurgical
materials division

Molarity of KOH	0.5	1.0	2.0	3.0	4.0	5.0	6.0	8.0	10.0
Sol. g/l (20°C)	0	trace	0.037	0.074	0.100	0.124	0.137	0.137	0.174
Sol. g/l (100°C)	0.188	0.249	0.373	---	0.622	0.622	---	1.494	2.054

These data show that at room temperature in 6 to 8 molar KOH, the solubility is only about (0.137)(100)/(1000)(1.37) g/cc or 0.01 percent. This maximum amount of bismuth ion that can be incorporated in the electrolyte appears to be too low to have any permanent beneficial effect on the performance of Ni-Cd cells.

2) Effect of Cobalt Additive to the Positive Plate

Positive plates containing various amounts of cobalt hydroxide were prepared for use in the initial screening experiments. Several solutions containing various concentrations of cobalt nitrate and nickel nitrate were prepared. Porous sintered nickel plaques were vacuum impregnated in these solutions and then cathodically converted in 30% KOH to the corresponding insoluble hydroxides in the porous plaque structure. All the nitrate was completely reduced to ammonia, and the resulting plates were washed and dried. The total capacity of the plates with 7.5% and 15% cobalt was 0.203 and 0.232 AH respectively. The electrode size was 4 in^2. These plates were tested for electrochemical performance before and after heat sterilization in flooded, plastic cells using Hg/HgO

metallurgical
materials division

reference electrodes. Negative plates with approximately 10 times the capacity of the test electrodes were used as counter electrodes to avoid complication by any possible H_2 evolution at the counter electrodes during charge. Oxygen evolved during the charge cycle was collected and measured at known ambient temperature and pressure to obtain the equivalent coulombs used in the gas evolution. "Oxygen-free capacity" was obtained by noting the total coulombs passed before any bubbles of oxygen appeared as indicated by an electronic instrument specially designed to indicate the initiation of gas evolution. Delivered capacity was determined from time potential plot with Hg/HgO reference electrode. Electrochemical data for positive plates with and without cobalt addition, both prior to and after heat sterilization are given in Table I-6. The ratio "O_2-free cap./delivered cap." is a measure of charge acceptance efficiency. Coulombic efficiency reported in the last column of Table 6 is an empirical quantity and is obtained by adding delivered capacity and AH equivalent to total gas evolved and dividing this quantity by the total charge input.

It will be noted that addition of cobalt improves the charge acceptance of the positive plate as indicated by relatively high ratio of oxygen-free capacity to delivered capacity before and after sterilization. However, after

metallurgical
materials division

TABLE I-6

EFFECT OF COBALT ADDITION ON THE PERFORMANCE OF POSITIVE PLATE IN FLOODED PLASTIC CELL
Hg/HgO Reference; Positive Limited Cell, 75°F

PRE-STERILIZATION PERFORMANCE DATA

Plate No.	Cycle No.	Plate Add. %	Charge Rate ma	Charge Time Hrs	AH Input	O_2-Free Capacity AH	O_2 Evolved cc	O_2 Evolved AH	Discharge Rate ma	Delivered Capacity AH	O_2-Free AH / Del. AH %	Coulombic Balance %
S	2	Control	260	7.5	1.95	0.317	122.4	0.546	650	1.30	24.3	94.8
S	3	Control	260	7.5	1.95	0.273	127.9	0.568	650	1.20	22.8	90.8
1	3	7.5	200	2.0	0.400	0.201	15.8	0.147	116	0.234	85.8	95.3
	4	7.5	50	6.0	0.300	0.195	1.8	0.017	116	0.261	74.7	92.7
2	3	15.0	200	2.0	0.400	0.201	18.4	0.081	116	0.237	84.8	79.5
	4	15.0	50	6.0	0.300	0.195	4.4	0.019	116	0.267	73.0	95.5

POST-STERILIZATION PERFORMANCE DATA

Plate No.	Cycle No.	Plate Add. %	Charge Rate ma	Charge Time Hrs	AH Input	O_2-Free Capacity AH	O_2 Evolved cc	O_2 Evolved AH	Discharge Rate ma	Delivered Capacity AH	O_2-Free AH / Del. AH %	Coulombic Balance %
S	1	Control	260	7.1	1.85	0.104	107.4	0.476	650	0.725	14.3	65.0
	2	Control	260	7.0	1.82	0.182	157.8	0.697	650	0.865	21.0	86.0
1	1	7.5	46	7.0	0.322	0.046	19.0	0.084	116	0.077	59.7	50.0
	2	7.5	46	6.8	0.313	0.067	29.5	0.131	116	0.083	80.7	68.4
	3	7.5	46	6.8	0.313	0.071	25.6	0.111	116	0.106	67.0	70.0
	4	7.5	46	6.0	0.276	0.100	16.8	0.074	116	0.095	105.0	61.2
	5	7.5	46	5.8	0.267	0.104	..	--	116	0.112	92.9	--
2	1	15.0	46	7.0	0.322	0.020	28.8	0.128	116	0.054	37.0	56.5
	2	15.0	46	6.8	0.313	0.051	34.0	0.150	116	0.058	87.9	67.2
	3	15.0	46	6.8	0.313	0.058	31.4	0.136	116	0.079	73.4	69.0
	4	15.0	46	6.0	0.276	0.079	24.4	0.108	116	0.066	120.0	63.0
	5	15.0	46	6.8	0.267	0.063	30.2	0.125	116	0.083	75.9	78.3

sterilization the absolute values of oxygen-free capacity and delivered capacity are drastically reduced for the plates containing cobalt. This reduction of oxygen-free capacity is accompanied by an increased polarization of the sterilized positive plate. Physico-chemical characterization of the unsterilized and sterilized positive plates with and without cobalt additives is reported later. From these preliminary data it appears that cobalt addition does not have any permanent beneficial effect on sterilized nickel electrode. Cobalt is a standard additive to the positive plate of sealed and vented Ni-Cd cells manufactured by several companies. However, its exact function or role is not well understood. Further work is required to clarify its beneficial effect, if any, on the performance of sterilized nickel-cadmium cells.

3) <u>Thallium and Indium Ion Addition to the Negative Plate</u>

It was originally planned to incorporate thallium hydroxide in the negative plate to improve its performance characteristics. The idea of using thallium ion addition was a logical follow-up of the indium ion addition which has been described by other workers as having a beneficial effect on the negative plate properties and since thallium (At. No. 81) is the next element in the family of similar elements Ga, In, Tl. However, the primary requirement in the addition of foreign ions to the positive

or negative plates is that the hydroxide of the foreign metal ion be highly insoluble. Any appreciable solubility of the metal hydroxide in the negative plate could result in shorting by the plating of dissolved metal ions during the charging sequence. A literature search of the solubility of the thallium hydroxide was therefore undertaken. "A Comprehensive Treatise on Inorganic and Theoretical Chemistry" by Mellor, Vol. 5, page 431, gives the following data for the solubility of thallium hydroxide in water as a function of temperature:

<u>Solubility (grams/liter)</u>
of <u>Thallium Hydroxide in Water</u>

Temp ($^{\circ}$C)	0	18.50	29.00	32.10	40.0	54.30	78.5	99.5
S (g/l)	25.44	34.44	39.85	41.14	49.5	64.97	103.3	148.3

The aqueous solution of thallium hydroxide is strongly alkaline. Because of the relatively high solubility of the thallium hydroxide its addition to the negative plate is not expected to have any permanent beneficial effect since as soon as it is oxidized during the discharge cycle, it will dissolve out in the battery electrolyte.

The following results describe the effect of various concentrations of these ions on the negative plate.

Standard cadmium nitrate solutions containing definite amounts of indium nitrate or thallium nitrate were used

metallurgical
materials division

for this purpose. Vacuum impregnation of the porous sintered plaque by these salts followed by cathodic conversion in KOH to form the respective hydroxides was carried out using the standard procedure used for control negative plates. The following solutions were used for these plates:

Solutions	AH Capacity of the Plate
(a) 4.45 molar $Cd(NO_3)_2$ + 0.05 molar $TlNO_3$	0.56
(b) 4.45 molar $Cd(NO_3)_2$ + 0.05 molar $TlNO_3$	0.57
(c) 4.45 molar $Cd(NO_3)_2$ + 0.05 molar $In(NO_3)_2$	0.192
(d) 4.45 Molar Cd $(NO_3)_2$ + 0.005 molar $In(NO_3)_2$	0.18

The capacity values are based upon analytical determination of Cd plus $Cd(OH)_2$ and do not include any contribution by indium or thallium salts. The effect of these ions, if involved in the cell reactions, will be to increase the actual capacities above the values listed above.

The electrochemical behavior was determined in flooded plastic cells similar to those used for positive plates containing cobalt. The results are given in Tables I-7 and I-8.

The addition of indium to the negative plate does not appear to have any beneficial effect on the performance of the plate before or after sterilization as shown by the data in Table I-7. Addition of indium generally reduces the hydrogen-free capacity. The delivered capacity

metallurgical
materials division

TABLE I-7

EFFECT OF THALLIUM ADDITION ON THE PERFORMANCE OF NEGATIVE PLATE IN FLOODED PLASTIC CELL

Hg/HgO Reference; Negative Limited Cell, 75°F

PRE-STERILIZATION PERFORMANCE DATA

Plate No.	Cycle No.	Plate Additive TlNO₃	Charge Rate ma	Charge Time Hrs	AH Input	H₂-Free Capacity AH	H₂ Evolved		Discharge Rate ma	Delivered Capacity AH	H₂-Free, AH Del., AH %	Coulombic Balance %
							cc	AH				
2	1	Control	260	7.2	1.86	1.11	329.6	0.695	650	0.856	130.0	83.5
2	2	Control	260	7.5	1.95	0.84	456.8	0.960	650	0.870	97.9	94.0
2	3	Control	260	7.5	1.95	0.78	486.2	1.020	650	0.791	99.0	93.8
1	1	0.005M	115	7.5	0.862	0.604	82.5	0.184	288	0.586	103.0	89.4
1	2	0.005M	115	7.0	0.805	0.605	89.2	0.198	288	0.480	126.0	84.2
2	1	0.05M	115	7.5	0.862	0.575	99.5	0.222	288	0.523	110.0	86.3
2	2	0.05M	115	7.0	0.805	0.611	88.6	0.196	288	0.485	127.0	84.5

POST-STERILIZATION PERFORMANCE DATA

Plate No.	Cycle No.	Plate Additive TlNO₃	Charge Rate ma	Charge Time Hrs	AH Input	H₂-Free Capacity AH	H₂ Evolved cc	H₂ Evolved AH	Discharge Rate ma	Delivered Capacity AH	H₂-Free, AH Del., AH %	Coulombic Balance %
2	1	Control	260	7.1	1.85	0.910	326.4	0.685	650	0.890	102.0	85.7
2	2	Control	260	7.0	1.85	0.905	377.6	0.834	650	0.865	105.0	93.3
1	1	0.005M	115	6.8	0.782	0.316	146.0	0.324	288	0.269	118.0	76.5
1	2	0.005M	115	6.5	0.748	0.251	104.6	0.232	288	0.259	97	65.5
2	1	0.05M	115	6.8	0.782	0.358	134.0	0.298	288	0.374	96	86.8
2	2	0.05M	115	6.5	0.748	0.340	131.6	0.292	288	0.369	92	88.2

TABLE I-8

EFFECT OF INDIUM ADDITION ON THE PERFORMANCE OF NEGATIVE PLATE IN FLOODED PLASTIC CELL
Hg/HgO Reference; Negative Limited Cell, 75°F

PRE-STERILIZATION PERFORMANCE DATA

Plate No.	Cycle No.	Plate Add. In(NO$_3$)$_3$	Charge Rate ma	Charge Time Hrs	AH Input	H$_2$-Free Capacity AH	H$_2$ Evolved cc	H$_2$ Evolved AH	Discharge Rate ma	Delivered Capacity AH	H$_2$-Free, AH Del / AH %	Coulombic Balance %
2	1	Control	260	7.2	1.86	1.11	329.6	0.615	650	0.856	130	83.5
2	2	Control	260	7.5	1.95	0.840	456.8	0.852	650	0.870	96.6	88.3
2	3	Control	260	7.5	1.95	0.780	486.2	0.907	650	0.791	98.6	59.0
1	1	0.005M	36	7.5	0.270	0.117	35.0	0.077	90	0.158	74.1	87.0
1	2	0.005M	36	7.5	0.225	0.126	23.6	0.052	90	0.158	79.7	93.3
2	1	0.05M	36	7.5	0.270	0.054	60.6	0.133	90	0.083	65.1	80.0
2	2	0.05M	36	7.5	0.225	0.027	53.6	0.119	90	0.060	50.0	79.5

POST-STERILIZATION PERFORMANCE DATA

Plate No.	Cycle No.	Plate Add. In(NO$_3$)$_3$	Charge Rate ma	Charge Time Hrs	AH Input	H$_2$-Free Capacity AH	H$_2$ Evolved cc	H$_2$ Evolved AH	Discharge Rate ma	Delivered Capacity AH	H$_2$-Free, AH Del / AH %	Coulombic Balance %
2	1	Control	260	7.1	1.846	0.910	326.4	0.685	650	0.890	102.2	85.7
2	2	Control	260	7.0	1.846	0.905	377.6	0.834	650	0.865	104.6	93.3
1	1	0.005M	36	7.0	0.252	0.081	46.5	0.102	90	0.083	97.6	73.4
1	2	0.005M	36	7.0	0.252	0.089	29.8	0.071	90	0.091	97.8	63.8
2	1	0.05M	36	7.0	0.252	0.019	71.0	0.155	90	0.030	63.3	73.4
2	2	0.05M	36	7.0	0.252	0.025	66.6	0.160	90	0.045	55.6	81.3

following heat sterilization is also significantly reduced. On the basis of these facts no further work with indium additive was planned or contemplated.

Addition of thallium hydroxide apparently increases the hydrogen-free capacity prior to sterilization, although the control plate, without any thallium, also gave relatively high hydrogen-free capacity on first cycle. This hydrogen-free capacity for control cells dropped on second and third cycle while for the plates containing thallium, hydrogen-free capacity increased on second cycle.

More definitive work with thallium ion effect on the cell performance is needed.

In general, however, the above results support the views stated by P. C. Milner and U. B. Thomas* that these additives are really adjuncts to the basic Ni-Cd system, which it seems reasonable to believe, is fundamentally capable of satisfactory performance without them. This same view appears to be true with heat-sterilizable Ni-Cd cells.

---

* P. C. Milner and U. B. Thomas, ADVANCES IN ELECTROCHEMISTRY AND ELECTROCHEMICAL ENGINEERING, Vol. 5, Editors Delahey and Tobias; Interscience 1967, page 81.

F. Factorial Design Experiments for Cell Optimization

Sealed Control Cell Development:

As a part of the factorial design experiments for the development of hermetically-sealed, heat-sterilizable nickel-cadmium cells, it was necessary to develop a standard, reproducible control cell against which cells containing different design variables can be compared. Rectangular developmental cells containing heat-sterilizable polypropylene separator types Pellon 14019 and Pellon FT2140 and with varying amounts (60, 70, 80 and 90% of free pore volume) of 30% KOH were fabricated according to the procedure described earlier and put on automatic charge-discharge cycling tests to determine the performance on continued cycling prior to sterilization. One additional purpose of this continued cycling of control cells was to determine what if any degradation in capacity or other changes occur during cycling. A summary of cycle data for cells containing Pellon FT2140 and 14019 separators for various rates of charge and discharge are given in Tables I-9 and I-10. The efficiency data given in Tables I-9 and I-10 are not based upon so-called "rated capacity" which is a variable quantity but are based upon theoretical capacity of the plates as determined by chemical analysis of the positive plates. This theoretical capacity for cells of Tables I-9 and I-10 is 5.58 AH.

An examination of the data of Tables I-9 and I-10 leads to

metallurgical
materials division

Table I-9

Performance Data for Heat-Sterilizable, Sealed Rectangular,
Ni-Cd Control Cells (Unsterilized) with Polypropylene
14019 Separator on Continuous Cycling at 22°C. Charge
Routines are as follows:

(1) 0.250 A for 24 hrs (6 AH); Discharge @ 2.0A to 1.0V cut-off
(2) .400A for 16 hrs (6.4 AH); Discharge @ 2.0A to 1.0V cut-off
(3) 1.0A for 5 hrs (5 AH); Discharge at 2.0A to 1.0V cut-off

Nominal Capacity of the Positive Plate 4.0AH, Theoretical
5.6AH.

Cell No.	% Pore Fill	Cycle No.	Charge Routine	ECP PSIA	Delivered Capacity 1V Cut-off	
					AH	% Eff.
1	60	1	1	26.7	2.6	46.6
1	60	1	1	24.7	2.75	48.7
1	60	2	1	36.7	2.7	48.4
1	60	2	1	36.7	2.7	48.4
2	60	2	1	29.2	2.8	50.2
1	60	3	1	39.7	2.1	37.8
2	60	3	1	26.7	2.2	38.9
1	60	10	2	57.7	2.55	45.2
2	60	10	2	59.7	2.75	48.7
1	60	21	3	37.7	3.78	67.0
2	60	21	3	46.2	4.13	73.2
2	60	33	3	49.7	4.2	74.7
2	60	47	1	42.7	3.4	59.3
2	60	59	3	---	4.1	72.0
3	70	1	1	29.7	3.2	57.0
4	70	1	1	32.7	2.8	49.3
3	70	2	1	42.7	3.2	55.8
4	70	2	1	41.7	2.9	51.9
3	70	3	1	53.7	2.5	44.0
4	70	3	1	50.7	2.3	41.3
3	70	10	2	75.7	3.8	67.3
4	70	10	2	63.2	3.6	62.9
3	70	21	3	33.2	4.3	75.8
4	70	21	3	38.7	4.3	75.5
3	70	33	3	37.7	4.4	77.6
4	70	33	3	39.7	4.4	77.3
3	70	47	1	44.7	3.9	69.3
4	70	47	1	50.7	3.85	68.2
3	70	59	3	---	4.5	79.6
4	70	59	3	---	4.6	81.7
5	80	1	1	59.7	3.2	56.4
6	80	1	1	36.2	3.3	58.7
5	80	2	1	70.7	3.3	59.0
6	80	2	1	57.7	3.3	58.4
5	80	3	1	74.7	2.9	50.7
6	80	3	1	66.7	2.7	46.9
5	80	10	2	76.2	4.0	69.9

metallurgical
materials division

Table I-9 (Cont'd.)

Cell No.	% Pore Fill	Cycle No.	Charge Routine	ECP PSIA	Delivered Capacity 1.0 Cut-off	
					AH	% Eff.
6	80	10	2	87.7	3.2	56.6
5	80	21	3	40.7	4.2	74.7
6	80	21	3	39.7	4.3	76.7
5	80	33	3	44.7	4.3	76.7
6	80	33	3	42.2	4.4	77.6
5	80	47	1	31.7	4.3	76.1
6	80	47	1	64.7	4.1	73.2
5	80	59	3	---	4.4	78.5
6	80	59	3	---	4.6	82.0
7	90	1	1	79.7	3.3	58.1
8	90	1	1	67.7	3.32	58.7
7	90	21	3	45.7	4.2	74.7
8	90	21	3	43.2	4.3	76.7
7	90	33	3	39.7	4.32	76.4
8	90	33	3	52.7	3.9	69.3
7	90	47	1	60.7	4.1	72.9
8	90	47	1	69.7	4.82	86.0
7	90	59	3	---	4.7	83.2
8	90	59	3	---	4.5	79.0

I-33

TABLE I-10

Summary of Performance Data for Sealed, Rectangular Control Cells (Unsterilized) on Continued Cycling at 22°C

Separator: Pellon Polypropylene FT2140

Charge Routine:
(1) .250A for 24 hrs (6AH); Discharge @ 2.0A to 1.0V cut-off
(2) .400A for 16 hrs (6.4AH); Discharge at 2.0A to 1.0V cut-off
(3) 1.0A for 5 hrs (5AH); Discharge at 2.0A to 1.0V cut-off

Cell No.	% Pore Fill	Cycle No.	Charge Routine	ECP PSIA	Delivered Capacity 1.0V Cut-off AH	% Eff.
1	60	1	1	16.7	2.07	36.6
2	60	1	1	10.7	1.97	34.8
1	60	2	1	15.7	1.65	29.2
2	60	2	1	14.7	1.57	27.7
1	60	3	1	15.7	1.53	27.2
2	60	3	1	15.7	1.48	26.3
1	60	10	2	14.7	1.70	30.1
2	60	10	2	23.7	1.43	25.4
1	60	16	3	15.7	3.10	54.3
2	60	16	3	48.7	2.12	37.0
1	60	20	2	15.7	2.05	36.1
2	60	20	2	28.2	1.45	25.5
1	60	30	2	15.7	1.27	22.4
2	60	30	2	27.2	1.22	21.5
1	60	40	2	15.7	1.08	19.0
2	60	40	2	25.7	1.10	19.4
1	60	50	2	15.7	1.15	20.2
2	60	50	2	24.7	1.30	22.9
3	70	1	1	14.7	2.75	48.7
4	70	1	1	17.7	2.48	44.0
3	70	2	1	89.7	2.20	38.9
4	70	2	1	24.7	2.02	25.7
3	70	3	1	26.7	2.05	36.3
4	70	3	1	29.7	1.934	34.2
3	70	10	2	57.7	2.33	41.3
4	70	10	2	54.7	2.22	39.3
3	70	16	3	63.2	3.72	76.2
4	70	16	3	59.2	3.77	66.0
3	70	20	2	60.7	2.98	52.6
4	70	20	2	56.7	3.00	52.8
3	70	30	2	67.7	2.65	46.6
4	70	30	2	61.7	2.85	50.2
3	70	40	2	67.7	2.52	44.2
4	70	40	---	---	---	---
3	70	50	2	65.7	2.22	39.1
4	70	50	---	---	---	---
5	80	1	1	21.7	2.48	49.6
6	80	1	1	38.7	2.80	45.7

- Cont'd. -

I-34

TABLE I-10 (Cont'd.)

Cell No.	% Pore Fill	Cycle No.	Charge Routine	ECP PSIA	Delivered Capacity 1.0V Cut-off AH	% Eff.
5	80	2	1	32.7	2.23	39.5
6	80	2	1	61.7	2.07	36.6
5	80	3	1	40.7	2.15	38.1
6	80	3	1	65.7	2.08	36.9
5	80	10	2	104.7	2.60	46.0
6	80	10	2	72.7	2.98	52.8
5	80	16	3	62.7	4.15	72.9
6	80	16	3	61.7	4.10	71.0
5	80	20	2	77.7	3.50	61.6
6	80	20	2	57.7	3.48	61.3
5	80	30	2	73.7	3.63	62.9
6	80	30	2	51.7	3.35	59.0
5	80	40	2	74.7	3.38	59.7
6	80	40	2	57.2	3.35	59.0
5	80	50	2	69.7	3.03	53.2
6	80	50	2	71.7	3.07	54.1
7	90	1	1	57.7	3.20	56.6
8	90	1	1	50.7	3.03	53.7
7	90	2	1	77.2	2.47	43.6
8	90	2	1	74.7	2.33	41.3
7	90	3	1	75.7	2.09	41.6
8	90	3	1	64.7	2.33	38.3
7	90	10	2	46.2	3.58	63.4
8	90	10	2	51.7	2.78	49.3
7	90	20	2	52.7	3.87	68.1
8	90	20	2	50.7	3.72	65.2
7	90	30	2	48.7	3.58	63.1
8	90	30	2	41.2	3.70	65.1
7	90	40	2	44.7	3.58	63.0
8	90	40	2	31.7	3.73	65.6
7	90	50	2	41.7	3.22	56.7
8	90	50	2	24.7	3.75	66.0

metallurgical
materials division

the following general observations and conclusions:

1) The rate of charge has a significant effect on the charge
    acceptance and on the delivered capacity for a given rate
    of discharge, in this case, 2 ampere discharge rate to
    1.0V cut-off.   The charge acceptance varies
    directly with the rate of charge.   Thus, for
    instance, with the cells containing type 14019 separator
    and 80% pore fill, the efficiency values are approximately
    55%, 68% and 78% for charge rates of 250 ma, 400 ma and
    1.0A respectively. For the cells containing FT2140
    separator and 80% pore fill, the corresponding efficiency
    values are approximately 35%, 50% and 70% respectively.
    It is well established that the charge acceptance (or
    oxygen-free capacity) at the positive plate increases
    with the charge rate. This is related to the fact that
    the oxygen overvoltage increases more rapidly with
    increase in current density than does the overvoltage for
    the oxidation of the positive active material.

2) The optimum amount of the electrolyte with both types of
    separator is between 70 and 80% of the free volume.
    Cells with 60% pore fill exhibited high resistances, par-
    ticularly with FT2140 separator. Cells with 90% pore
    fill exhibited excessive end-of-charge pressures and
    relatively slow rates of oxygen recombination as expected.
    Since previous experience has shown that the rate of

metallurgical
materials division

oxygen diffusion from the positive to the negative plate
and its recombination is a function of the electrolyte
amount, (pressure build up in general increasing exponen-
tially with increase in the electrolyte fill level), pore
fills of 90% and above are generally not desirable. Fur-
ther work on the electrolyte optimization was therefore
limited to the range of 70 to 80% pore fill.

3) There is a significant variation in the end-of-charge
pressure data and more careful measurements of the
pressure rise on charge are required to determine the
effect of charge rate on pressure rise. Preliminary
analysis shows little difference in the rates of oxygen
recombination with 70% and 80% pore fills in the cells
containing 14019 and FT2140 separators.

4) There is no significant difference in the end-of-charge
voltages between the two types of separators with 70%
and 80% pore fills.

5) While from these results 14019 separator appears to be
superior to FT2140, the tendency of cells with 14019 to
develop short circuits after second heat sterilization
requires the inclusion of both separator materials in
further factorial experiments.

6) It should be noted that there is a gradual decrease in
the delivered capacity as a function of cycle number.

metallurgical
materials division

This is one of the critical problems.

7) Another problem that must be solved before undertaking an extensive statistical design experiment is to control the uniformity of cells. However, because of the effectiveness of factorial or fractional factorial design experiments in the optimization of the cell design parameters work is continuing in a parallel effort on the factorial design experiments.

metallurgical
materials division

G. __Preliminary 2^n Factorial Experiment With Sealed Ni-Cd Cells__

The purpose of the 2^n factorial experiment was to elucidate the effects of various factors on the electrochemical behavior of the heat-sterilizable, hermetically-sealed, rechargeable Ni-Cd cell. An additional purpose was to cycle selected cells to 100% depth-of-discharge after heat sterilization to determine their electrochemical characteristics to see if they meet the post-sterilization mission requirements.

Originally, a four factor experiment was planned and initiated. The factors chosen, their letter designations and the two levels are shown in Table I-11.

TABLE I-11

Ni-Cd Rectangular, 17 Plate Cells (8 Positive - 9 Negative)

Theoretical Capacity of the Positive Plate (limiting) 4.96 AH

Factors		Factor Levels	
Designation	Description	Low (0)	High (1)
A	Type of Polypropylene Separator	#14019	#FT2140
B	Concentration of KOH Electrolyte	30 w/o	34 w/o
C	Percentage Pore Fill With KOH Electrolyte	70	80
D	Heat Treatment	Unsterilized	Sterilized

In this particular experiment, because of the choice of the

metallurgical
materials division

fourth factor, viz, heat treatment, only eight (2^3) cells are required per factorial set, each member containing the appropriate combination of the first three factors, A, B and C. They are first tested prior to sterilization, factor D at the low (0) level. Following sterilization, factor D at the high (1) level, testing is continued. In this manner, one obtains the necessary 16 (2^4) sets of data required for the complete calculation of primary and interaction effects. Four replicates of each of the eight cells were constructed. Of the four groups only the first were fitted with pressure gauges. In the tests performed to date, two charging routines have been employed. In all cases, the cells were discharged at the C/2.5 rate, i.e. with a current of 2.0 A for a theoretical loading of 4.96 AH, based upon the positive plate formation capacity. The first charge routine R1 was a charge at 0.4A for 17 hours, i.e. C/12.5 rate to 137% charge level. The second routine, R2, was a charge at 1.0A for 5 hours, i.e. C/5 rate to 100% charge level. Typical results for the pre-sterilization cycling tests have been presented in the Fourth Quarterly Report, April 1 - June 30, 1968, and are summarized in Table I-12. After pre-sterilization characterization, the cells were heat sterilized as per JPL requirements and put on automatic cycling.

The history of the post-sterilization cycling up to 90 cycles is summarized in Figure I-4. Only half of the original 32

cells devoted to the factorial experiment are represented in Fig. I-4 since only these cells were cycled. Of the cells not being cycled one group of eight (cells Numbered 4, 8, 12, 16, 20, 24, 28, 32) were cycled twenty-four times, sterilized, and set aside. The other groups of eight (cells numbered 2, 6, 10, 14, 18, 22, 26, 30) were cycled thirty-seven times and set aside without having been sterilized.

It is immediately apparent from Figure I-4 that of the eight cells m a d e with Separator 14019, (Factor A, low level (0)), only one cell, #13, in Group I remains active. Three of the cells (Numbers 3, 5, and 7) were opened and examined for the cause of failure. In cells #3 and #5, a short occurred between the negative electrode and the can, apparently because the outer layer of the separator had slipped upward slightly when the pack was inserted during cell assembly. There was indication of a short in the middle of the pack in cell #7. It is clear that sterilization weakens the 14019 separator in such a way that shorting becomes highly probable.

metallurgical
materials division

FIGURE I-4

Ni-Cd RECTANGULAR 17-PLATE CELLS, THEORETICAL CAPACITY (FORMATION) 4.96 AH

FACTORIAL EXPERIMENT. POST-STERILIZATION CYCLING HISTORY TO 12/31/68
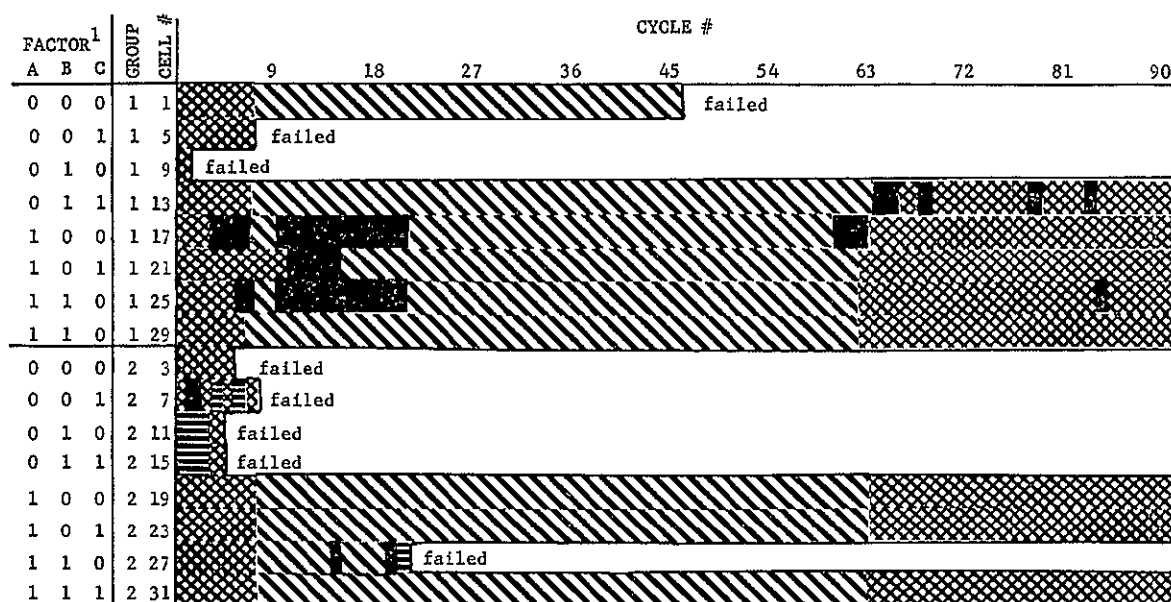
Factor Code

Factor		Level	
		Low(0)	High(1)
A	Separator	14019	FT2140
B	Conc. KOH	30%	34%
C	% Pore Fill	70%	80%

Group 1 - Cells with pressure gauges
(until Cycle 75)

Group 2 - Cells without pressure gauges

BAR-GRAPH KEY

Charge at C/12.5 for 17 hrs to 137% level.
Discharge at C/2.5 to 1 V cut-off.

Charge at C/5 for 5 hrs to 100% level.
Discharge at C/2.5 to 1 V cut-off.

Not fully charged due to pressure cut-off.

Not fully charged due to shorting or other unknown cause.

I-42

TABLE I-12

Ni-Cd Rectangular Cells; Factorial Design Experiment
ELECTROCHEMICAL PERFORMANCE DATA
FOR FACTOR DESCRIPTION AND LEVELS   SEE TABLE I-11

Cell No.	Factors				Cycle No.	Charge Data						Discharge Data; 1.0V Cut Off				
	A	B	C	D		Amp.	Hrs.	AH Input	ECV Volts	ECP PSIA	ECR mΩ	Amp	AH Output	EDP PSIA	EDR mΩ	Eff. %
1	0	0	0	0	2	.400	17.0	6.8	1.413	72.7	6.23	2.0	3.618	37.7	6.03	72.9
2	0	0	0	0	2	.400	17.0	6.8	1.412	----		2.0	2.618	----		52.8
3	0	0	0	0	2	.400	17.0	6.8	1.419	----	6.52	2.0	2.984	----	7.13	60.2
4	0	0	0	0.	2	.400	17.0	6.8	1.424	----	6.73	2.0	3.284	----	7.32	66.2
5	0	0	1	0	2	.400	17.0	6.8	1.414	84.7	6.88	2.0	3.666	52.7	6.90	73.9
6	0	0	1	0	2	.400	17.0	6.8	1.409	----		2.0	2.966	----		59.8
7	0	0	1	0	2	.400	17.0	6.8	1.429	----	6.66	2.0	3.366	----	7.34	67.9
8	0	0	1	0	2	.400	17.0	6.8	1.429	----	7.11	2.0	3.534	----	7.70	71.2
9	0	1	0	0	2	.400	17.0	6.8	1.430	64.7	8.16	2.0	3.718	37.7	7.72	75.0
10	0	1	0	0	2	.400	17.0	6.8	Not Charged							
11	0	1	0	0	2	.400	17.0	6.8	1.427	----	6.40	2.0	3.600	----	7.03	72.6
12	0	1	0	0	2	.400	17.0	6.8	1.425	----	6.42	2.0	3.700	----	7.06	74.6
13	0	1	1	0	2	.400	17.0	6.8	1.346	64.7	6.46	2.0	3.418	49.7	3.99	68.9
14	0	1	1	0	2	.400	17.0	6.8	1.399	----	8.30	2.0	2.336	----	7.65	47.1
15	0	1	1	0.	2	.400	17.0	6.8	1.427	----	7.19	2.0	3.700	----	7.84	74.6
16	0	1	1	0	2	.400	17.0	6.8	1.429	----	6.41	2.0	3.852	----	7.09	77.7

TABLE I-12 (Cont'd.)

Ni-Cd Rectangular Cells; Factorial Design Experiment
ELECTROCHEMICAL PERFORMANCE DATA
FOR FACTOR DESCRIPTION AND LEVELS SEE TABLE I-11

Cell No.	Factors				Cycle No.	Charge Data						Discharge Data; 1.0V Cut Off				
	A	B	C	D		Amp.	Hrs.	AH Input	ECV Volts	ECP PSIA	ECR mΩ	Amp	AH Output	EDP PSIA	EDR mΩ	Eff. %
17	1	0	0	0	2	.400	17.0	6.8	1.379	39.7	8.75	2.0	2.984	18.7	8.16	60.2
18	1	0	0	0	2	.400	17.0	6.8	1.418	----		2.0	2.352	----		47.4
19	1	0	0	0	2	.400	17.0	6.8	1.426	----	7.53	2.0	3.084	----	7.97	62.2
20	1	0	0	0	2	.400	17.0	6.8	1.428	----	4.88	2.0	2.966	----	5.28	59.8
21	1	0	1	0	2	.400	17.0	6.8	1.427	22.7	7.86	2.0	4.284	0.7	6.99	86.4
22	1	0	1	0	2	.400	17.0	6.8	Not Charged							
23	1	0	1	0	2	.400	17.0	6.8	1.426	----	7.70	2.0	2.752	----	8.49	55.5
24	1	0	1	0	2	.400	17.0	6.8	1.437	----	7.07	2.0	3.266	----	7.78	65.8
25	1	1	0	0	2	.400	17.0	6.8	1.406	24.7	8.14	2.0	3.084	24.7	8.55	66.2
26	1	1	0	0	2	.400	17.0	6.8	1.399	----	9.46	2.0	2.534	----	8.58	51.1
27	1	1	0	0	2	.400	17.0	6.8	1.421	----	6.93	2.0	2.884	----	7.71	58.1
28	1	1	0	0	2	.400	17.0	6.8	1.421	----	8.24	2.0	3.134	----	9.05	63.2
29	1	1	1	0	2	.400	17.0	6.8	1.413	29.7	7.52	2.0	2.734	46.7	7.81	55.1
30	1	1	1	0	2	.400	17.0	6.8	1.401	----	8.27	2.0	3.052	----	7.74	61.5
31	1	1	1	0	2	.400	17.0	6.8	1.421	----	6.17	2.0	2.918	----	6.83	58.8
32	1	1	1	0	2	.400	17.0	6.8	1.424	----	7.12	2.0	3.000	----	7.89	60.5

TABLE I-12 (Cont'd.)

Ni-Cd Rectangular Cells; Factorial Design Experiment

ELECTROCHEMICAL PERFORMANCE DATA

FOR FACTOR DESCRIPTION AND LEVELS SEE TABLE I-11

Cell No.	Factors				Cycle No.	Charge Data						Discharge Data; 1.0V Cut Off				
	A	B	C	D		Amp.	Hrs.	AH Input	ECV Volts	ECP PSIA	ECR mΩ	Amp	AH Output	EDP PSIA	EDR mΩ	Eff. %
1	0	0	0	0	3	.400	17.0	6.8	1.425	68.2	6.12	2.0	3.500	34.7	5.74	70.6
2	0	0	0	0	3	.400	17.0	6.8	1.422	----			2.234	----		45.0
3	0	0	0	0	3	.400	17.0	6.8	No Charge							
4	0	0	0	0	3	.400	17.0	6.8	1.419	----	7.12	2.0	3.118	----	7.00	62.9
5	0	0	1	0	3	.400	17.0	6.8	1.421	81.7	6.63	2.0	3.266	44.7	6.54	65.8
6	0	0	1	0	3	.400	17.0	6.8	1.415	----		2.0	2.752	----		55.5
7	0	0	1	0	3	.400	17.0	6.8	1.425	----	7.00	2.0	3.284	----	6.98	66.2
8	0	0	1	0	3	.400	17.0	6.8	1.423	----	7.45	2.0	3.352	----	7.36	67.6
9	0	1	0	0	3	.400	17.0	6.8	1.424	68.7	7.88	2.0	3.634	35.7	7.42	73.3
10	0	1	0	0	3	.400	17.0	6.8	1.404	----		2.0	3.518	----		70.9
11	0	1	0	0	3	.400	17.0	6.8	1.423	----	6.68	2.0	3.500	----	6.72	70.6
12	0	1	0	0	3	.400	17.0	6.8	1.421	----	6.79	2.0	3.518	----	6.74	70.9
13	0	1	1	0	3	.400	17.0	6.8	1.343	61.2	6.45	2.0	2.734	48.7	62.1	55.1
14	0	1	1	0	3	.400	17.0	6.8	1.406	----		2.0	3.118	----		62.9
15	0	1	1	0	3	.400	17.0	6.8	1.426		7.56	2.0	3.652		7.49	73.6
16	0	1	1	0	3	.400	17.0	6.8	No Charge							

TABLE I-12 (Cont'd.)

Ni-Cd Rectangular Cells; Factorial Design Experiment
ELECTROCHEMICAL PERFORMANCE DATA
FOR FACTOR DESCRIPTION AND LEVELS SEE TABLE I-11

Cell No.	Factors				Cycle No.	Charge Data						Discharge Data; 1.0V Cut Off				
	A	B	C	D		Amp.	Hrs.	AH Input	ECV Volts	ECP PSIA	ECR mΩ	Amp	AH Output	EDP PSIA	EDR mΩ	Eff. %
17	1	0	0	0	3	.400	17.0	6.8	1.378	47.7	8.83	2.0	2.534	18.7	7.59	51.1
18	1	0	0	0	3	.400	17.0	6.8	1.135	----		2.0	1.934	----		40.0
19	1	0	0	0	3	.400	17.0	6.8	1.420	----	8.11	2.0	2.566	----	7.98	51.7
20	1	0	0	0	3	.400	17.0	6.8	1.420	----	5.11	2.0	2.666	----	5.16	53.7
21	1	0	1	0	3	.400	17.0	6.8	1.427	65.7	7.77	2.0	3.766	-0.3	6.68	75.9
22	1	0	1	0	3	.400	17.0	6.8	1.427	----		2.0	3.018	----		60.8
23	1	0	1	0	3	.400	17.0	6.8	1.422	----	8.16	2.0	2.766	----	7.96	55.8
24	1	0	1	0	3	.400	17.0	6.8	1.437	----	7.57	2.0	3.418	----	7.34	68.9
25	1	1	0	0	3	.400	17.0	6.8	1.408	63.7	8.84	2.0	2.168	24.7	8.02	52.8
26	1	1	0	0	3	.400	17.0	6.8	1.405	----	9.30	2.0	2.234	----	9.18	45.0
27	1	1	0	0	3	.400	17.0	6.8	1.415	----	7.40	2.0	2.784	----	7.34	56.1
28	1	1	0	0	3	.400	17.0	6.8	1.414	----	8.93	2.0	2.766	----	8.69	55.8
29	1	1	1	0	3	.400	17.0	6.8	1.330	38.7	7.20	2.0	1.984	48.7	7.07	40.0
30	1	1	1	0	3	.400	17.0	6.8	1.410	----	8.17	2.0	2.818	----	8.31	56.8
31	1	1	1	0	3	.400	17.0	6.8	1.413	----	6.55	2.0	2.666	----	6.41	53.7
32	1	1	1	0	3	.400	17.0	6.8	1.419	----	7.50	2.0	2.900	----	7.42	58.5

TABLE I-12 (Cont'd.)

Ni-Cd Rectangular Cells; Factorial Design Experiment
ELECTROCHEMICAL PERFORMANCE DATA
FOR FACTOR DESCRIPTION AND LEVELS   SEE TABLE I-11

Cell No.	Factors				Cycle No.	Charge Data						Discharge Data; 1.0V Cut Off				
	A	B	C	D		Amp.	Hrs.	AH Input	ECV Volts	ECP PSIA	ECR mΩ	Amp	AH Output	EDP PSIA	EDR mΩ	Eff. %
1	0	0	0	0	7	.400	17.0	6.8	1.432	70.7	6.03	2.0	4.100	31.2	6.41	82.7
2	0	0	0	0	7	.400	17.0	6.8	1.409	-----	8.01	2.0	2.600	-----	8.14	52.4
3	0	0	0	0	7	.400	17.0	6.8	1.412	-----	6.76	2.0	3.184	-----	7.41	64.2
4	0	0	0	0	7	.400	17.0	6.8	1.415	-----	7.20	2.0	3.152	-----	7.37	63.5
5	0	0	1	0	7	.400	17.0	6.8	1.367	49.7	6.00	2.0	2.934	38.7	6.40	59.2
6	0	0	1	0	7	.400	17.0	6.8	1.423	-----	7.10	2.0	3.400	-----	7.00	68.5
7	0	0	1	0	7	.400	17.0	6.8	1.423	-----	6.90	2.0	3.500	-----	7.24	70.6
8	0	0	1	0	7	.400	17.0	6.8	1.421	-----	7.36	2.0	3.452	-----	7.74	69.6
9	0	1	0	0	7	.400	17.0	6.8	1.425	73.7	7.53	2.0	4.000	34.7	7.85	80.6
10	0	1	0	0	7	.400	17.0	6.8	1.414	-----	7.92	2.0	3.234	-----	7.72	65.2
11	0	1	0	0	7	.400	17.0	6.8	1.422	-----	6.64	2.0	3.666	-----	7.15	73.9
12	0	1	0	0	7	.400	17.0	6.8	1.418	-----	6.80	2.0	3.666	-----	7.13	73.9
13	0	1	1	0	7	.400	17.0	6.8	1.374	65.7	6.27	2.0	2.934	53.2	6.83	59.2
14	0	1	1	0	7	.400	17.0	6.8	1.421	-----	7.73	2.0	3.552	-----	7.62	71.6
15	0	1	1	0	7	.400	17.0	6.8	1.410	-----	7.43	2.0	3.100	-----	7.79	62.5
16	0	1	1	0	7	.400	17.0	6.8	1.423	-----	6.67	2.0	3.700	-----	7.26	74.6

TABLE I-12 (Cont'd.)

Ni-Cd Rectangular Cells; Factorial Design Experiment
ELECTROCHEMICAL PERFORMANCE DATA
FOR FACTOR DESCRIPTION AND LEVELS SEE TABLE I-11

Cell No.	Factors				Cycle No.	Charge Data						Discharge Data; 1.0V Cut Off				
	A	B	C	D		Amp.	Hrs.	AH Input	ECV Volts	ECP PSIA	ECR mΩ	Amp	AH Output	EDP PSIA	EDR mΩ	Eff. %
17	1	0	0	0	7	.400	17.0	6.8	1.378	60.7	8.48	2.0	2.534	23.7	8.38	51.1
18	1	0	0	0	7	.400	17.0	6.8	1.416	-----	9.78	2.0	2.266	-----	9.64	45.7
19	1	0	0	0	7	.400	17.0	6.8	1.416	-----	7.89	2.0	3.084	-----	8.14	62.2
20	1	0	0	0	7	.400	17.0	6.8	1.417	-----	4.82	2.0	3.118	-----	5.06	62.9
21	1	0	1	0	7	.400	17.0	6.8	1.378	50.7	7.03	2.0	3.152	23.7	7.38	63.5
22	1	0	1	0	7	.400	17.0	6.8	1.417	-----	8.95	2.0	3.024	-----	8.84	61.2
23	1	0	1	0	7	.400	17.0	6.8	1.423	-----	8.07	2.0	3.284	-----	8.39	66.2
24	1	0	1	0	7	.400	17.0	6.8	1.443	-----	7.41	2.0	3.700	-----	7.70	74.6
25	1	1	0	0	7	.400	17.0	6.8	1.409	84.7	8.03	2.0	2.700		8.69	54.4
26	1	1	0	0	7	.400	17.0	6.8	1.411	-----	8.91	2.0	2.418	-----	8.60	48.7
27	1	1	0	0	7	.400	17.0	6.8	1.418	-----	7.40	2.0	3.066	-----	7.73	61.8
28	1	1	0	0	7	.400	17.0	6.8	1.413	-----	10.06	2.0	2.852	-----	10.80	57.5
29	1	1	1	0	7	.400	17.0	6.8	1.366	44.7	7.08	2.0	1.984		7.71	40.0
30	1	1	1	0	7	.400	17.0	6.8	1.418	-----	8.05	2.0	3.134	-----	7.76	63.2
31	1	1	1	0	7	.400	17.0	6.8	1.412	-----	6.38	2.0	2.918	-----	6.68	58.8
32	1	1	1	0	7	.400	17.0	6.8	1.419	-----	7.33	2.0	3.052	-----	7.76	61.5

I-48

TABLE I-12 (Cont'd.)

Ni-Cd Rectangular Cells; Factorial Design Experiment
ELECTROCHEMICAL PERFORMANCE DATA
FOR FACTOR DESCRIPTION AND LEVELS SEE TABLE I-11

Cell No.	Factors				Cycle No.	Charge Data						Discharge Data; 1.0V Cut Off				
	A	B	C	D		Amp.	Hrs.	AH Input	ECV Volts	ECP PSIA	ECR mΩ	Amp	AH Output	EDP PSIA	EDR mΩ	Eff. %
1	0	0	0	0	15	.400	17.0	6.8	1.444	65.7	6.15	2.0	4.234	22.7	6.73	85.4
2	0	0	0	0		.400	17.0	6.8	1.421	-	8.18	2.0	2.966	-	8.86	59.8
3	0	0	0	0		.400	17.0	6.8	1.425	-	7.06	2.0	3.434	-	7.32	69.2
4	0	0	0	0		.400	17.0	6.8	1.421	-	7.61	2.0	3.584	-	7.69	72.3
5	0	0	1	0	15	.400	17.0	6.8	1.455	78.7	6.50	2.0	4.418	39.7	6.79	89.1
6	0	0	1	0		.400	17.0	6.8	1.427	-	7.09	2.0	4.084	-	7.96	82.3
7	0	0	1	0		.400	17.0	6.8	1.425	-	7.24	2.0	3.734	-	7.41	75.3
8	0	0	1	0		.400	17.0	6.8	1.425	-	7.57	2.0	3.700	-	7.83	74.6
9	0	1	0	0	15	.400	17.0	6.8	1.427	65.7	7.67	2.0	4.052	4.7	8.23	81.7
10	0	1	0	0		.400	17.0	6.8	1.419	-	7.90	2.0	3.500	-	8.76	70.6
11	0	1	0	0		.400	17.0	6.8	1.422	-	7.26	2.0	3.834	-	7.55	77.3
12	0	1	0	0		.400	17.0	6.8	1.416	-	7.29	2.0	3.552	-	7.44	71.6
13	0	1	1	0	15	.400	17.0	6.8	1.424	63.7	5.95	2.0	3.184	40.7	6.60	64.2
14	0	1	1	0		.400	17.0	6.8	1.423	-	7.79	2.0	4.016	-	8.56	81.0
15	0	1	1	0		.400	17.0	6.8	1.415	-	7.74	2.0	3.452	-	8.01	69.6
16	0	1	1	0		.400	17.0	6.8	1.427	-	7.16	2.0	4.000	-	7.42	80.6

I-49

TABLE I-12 (Cont'd.)

Ni-Cd Rectangular Cells; Factorial Design Experiment
ELECTROCHEMICAL PERFORMANCE DATA
FOR FACTOR DESCRIPTION AND LEVELS SEE TABLE I-11

Cell No.	Factors				Cycle No.	Charge Data						Discharge Data; 1.0V Cut Off				
	A	B	C	D		Amp.	Hrs.	AH Input	ECV Volts	ECP PSIA	ECR mΩ	Amp	AH Output	EDP PSIA	EDR mΩ	Eff. %
17	1	0	0	0	15	.400	17.0	6.8	1.408	63.7	8.59	2.0	2.634	19.7	9.18	53.1
18	1	0	0	0		.400	17.0	6.8	1.421	-	10.21	2.0	2.666	-	11.67	53.7
19	1	0	0	0		.400	17.0	6.8	1.416	-	8.30	2.0	2.666	-	8.55	53.7
20	1	0	0	0		.400	17.0	6.8	1.417	-	5.26	2.0	2.652	-	5.32	53.5
21	1	0	1	0	15	.400	17.0	6.8	1.438	62.7	7.02	2.0	3.418	16.7	7.75	68.9
22	1	0	1	0		.400	17.0	6.8	1.424	-	11.11	2.0	3.534	-	10.99	71.2
23	1	0	1	0		.400	17.0	6.8	1.422	-	8.49	2.0	3.352	-	8.62	67.6
24	1	0	1	0		.400	17.0	6.8	1.439	-	7.80	2.0	3.618	-	7.95	72.9
25	1	1	0	0	15	.400	17.0	6.8	1.419	84.7	9.43	2.0	3.166	22.7	10.65	63.8
26	1	1	0	0		.400	17.0	6.8	1.415	-	8.97	2.0	2.852	-	10.13	57.5
27	1	1	0	0		.400	17.0	6.8	1.424	-	8.00	2.0	3.500	-	8.21	70.6
28	1	1	0	0		.400	17.0	6.8	1.415	-	11.40	2.0	2.700	-	11.97	54.4
29	1	1	1	0	15	.400	17.0	6.8	1.439	77.7	7.37	2.0	3.452	10.7	8.22	69.6
30	1	1	1	0		.400	17.0	6.8	1.422	-	7.93	2.0	3.518	-	8.90	70.9
31	1	1	1	0		.400	17.0	6.8	1.415	-	6.77	2.0	3.000	-	6.96	60.5
32	1	1	1	0		.400	17.0	6.8	1.417	-	7.73	2.0	3.134	-	8.03	63.2

TABLE I-12 (Cont'd.)

Ni-Cd Rectangular Cells; Factorial Design Experiment
ELECTROCHEMICAL PERFORMANCE DATA
FOR FACTOR DESCRIPTION AND LEVELS -- SEE TABLE I-11

Cell No.	Factors				Cycle No.	Charge Data						Discharge Data; 1.0V Cut Off				
	A	B	C	D		Amp.	Hrs.	AH Input	ECV Volts	ECP PSIA	ECR mΩ	Amp	AH Output	EDP PSIA	EDR mΩ	Eff. %
17	1	0	0	1	110	400	17	6.8	1.465	--	17.79	2.0	3.218	--	32.60	64.9
19	1	0	0	1	110	400	17	6.8	1.461	--	13.74	2.0	3.484	--	19.85	70.2
21	1	0	1	1	110	400	17	6.8	1.469	--	10.44	2.0	3.734	--	12.30	75.3
23	1	0	1	1	110	400	17	6.8	1.476	--	11.00	2.0	4.000	--	11.78	80.6
25	1	1	0	1	110	400	17	6.8	1.464	--	14.90	2.0	3.718	--	40.41	75.0
27	1	1	0	1	110											
29	1	1	1	1	110	400	17	6.8	1.461	--	9.36	2.0	3.884	--	11.61	78.3
31	1	1	1	1	110	400	17	6.8	1.478	--	34.59	2.0	4.084	--	32.58	82.3

* Cell 27 not charged

TABLE I-12 (Cont'd.)

Ni-Cd Rectangular Cells; Factorial Design Experiment
ELECTROCHEMICAL PERFORMANCE DATA
FOR FACTOR DESCRIPTION AND LEVELS -- SEE TABLE I-11

Cell No.	Factors				Cycle No.	Charge Data						Discharge Data; 1.0V Cut Off				
	A	B	C	D		Amp.	Hrs.	AH Input	ECV Volts	ECP PSIA	ECR mΩ	Amp	AH Output	EDP PSIA	EDR mΩ	Eff. %
17	1	0	0	1	129	.400	17	6.8	1.451	--	19.02	2.0	3.184	--	35.18	64.2
19	1	0	0	1	129	.400	17	6.8	1.443	--	15.93	2.0	3.100	--	35.87	62.5
21	1	0	1	1	129	.400	17	6.8	1.462	--	11.09	2.0	3.666	--	11.75	73.9
23	1	0	1	1	129	.400	17	6.8	1.486	--	11.44	2.0	4.252	--	16.02	85.7
25	1	1	0	1	129	.400	17	6.8	1.440	--	15.88	2.0	3.218	--	37.77	64.9
27	1	1	0	1	129											
29	1	1	1	1	129	.400	17	6.8	1.463	--	10.14	2.0	3.866	--	11.14	77.9
31	1	1	1	1	129	.400	17	6.8	1.471	--	20.14	2.0	4.352	--	31.30	87.7

TABLE I-12 (Cont'd.)

Ni-Cd Rectangular Cells; Factorial Design Experiment
ELECTROCHEMICAL PERFORMANCE DATA
FOR FACTOR DESCRIPTION AND LEVELS -- SEE TABLE I-11

Cell. No.	Factors				Cycle No.	Charge Data						Discharge Data; 10V Cut Off				
	A	B	C	D		Amp.	Hrs.	AH Input	ECV Volts	ECP PSIA	ECR mΩ	Amp	AH Output	EDP PSIA	EDR mΩ	Eff. %
17	1	0	0	1	146	400	17	6.8	1.473	----	19.42	2.0	3.084	----	36.09	62.2
19	1	0	0	1	146	400	17	6.8	1.452	----	18.90	2.0	3.118	----	41.45	62.9
21	1	0	1	1	146	400	17	6.8	1.473	----	11.13	2.0	3.700	----	11.24	74.6
23	1	0	1	1	146	400	17	6.8	1.488	----	11.94	2.0	4.166	----	14.94	84.0
25	1	1	0	1	146	400	17	6.8	1.474	----	16.08	2.0	3.266	----	42.10	65.8
27	1	1	0	1	146											
29	1	1	1	1	146	400	17	6.8	1.472	----	10.48	2.0	3.952	----	11.07	79.7
31	1	1	1	1	146	400	17	6.8	1.475	----	25.28	2.0	4.384	----	37.72	88.4

I-53

TABLE I-12

Ni-Cd Rectangular Cells; Factorial Design Experiment 17 Plate
ELECTROCHEMICAL PERFORMANCE DATA
FOR FACTOR DESCRIPTION AND LEVELS -- SEE TABLE I-11

Cell No.	Factors				Cycle No.	Charge Data						Discharge Data; 10V Cut Off				
	A	B	C	D		Amp.	Hrs.	AH Input	ECV Volts	ECP PSIA	ECR mΩ	Amp	AH Output	EDP PSIA	EDR mΩ	Eff. %
17	1	0	0	1	166	.400	17	6.8	1.458	----	18.06	2.0	3.118	-----	42.36	62.9
19	1	0	0	1	166	.400	17	6.8	1.443	----	18.48	2.0	3.134	-----	35.12	63.2
21	1	0	1	1	166	.400	17	6.8	1.464	----	11.21	2.0	3.634	-----	12.43	73.3
23	1	0	1	1	166	.400	17	6.8	1.478	----	11.91	2.0	4.252	-----	12.39	85.7
25	1	1	0	1	166	.400	17	6.8	1.470	----	15.35	2.0	3.266	-----	52.30	65.8
27	1	1	0	1	166											
29	1	1	1	1	166	.400	17	6.8	1.470	----	10.37	2.0	4.000	-----	12.24	80.6
31	1	1	1	1	166	.400	17	6.8	1.456	----	15.72	2.0	4.318	-----	22.13	87.1

TABLE I-12 (Cont'd.)

Ni-Cd Rectangular Cells; Factorial Design Experiment 17 Plate
ELECTROCHEMICAL PERFORMANCE DATA
FOR FACTOR DESCRIPTION AND LEVELS -- SEE TABLE I-11

Cell No.	Factors				Cycle No.	Charge Data						Discharge Data; 1.0V Cut Off				
	A	B	C	D		Amp.	Hrs.	AH Input	ECV Volts	ECP PSIA	ECR mΩ	Amp	AH Output	EDP PSIA	EDR mΩ	Eff. %
17	1	0	0	1	187	.400	17.0	6.8	1.473	--	17.33	2.0	3.184	--	34.09	64.2
19	1	0	0	1	187	.400	17.0	6.8	1.462	--	19.55	2.0	3.352	--	29.41	67.6
21	1	0	1	1	187	.400	17.0	6.8	1.467	--	11.09	2.0	3.834	--	10.59	77.3
23	1	0	1	1	187	.400	17.0	6.8	1.514	--	13.86	2.0	4.400	--	13.08	88.7
25	1	1	0	1	187	.400	17.0	6.8	1.471	--	15.01	2.0	3.234	--	40.87	65.2
27	1	1	0	1	187	.										
29	1	1	1	1	187	.400	17.0	6.8	1.448	--	10.45	2.0	4.166	--	10.34	84.0
31	1	1	1	1	187	.400	17.0	6.8	1.466	--	13.56	2.0	4.500	--	15.35	90.7

TABLE I-12 (Cont'd.)

Ni-Cd Rectangular Cells; Factorial Design Experiment 17 Plate
ELECTROCHEMICAL PERFORMANCE DATA
FOR FACTOR DESCRIPTION AND LEVELS -- SEE TABLE I-11

Cell No.	Factors				Cycle No.	Charge Data						Discharge Data; 1.0V Cut Off				
	A	B	C	D		Amp.	Hrs.	AH Input	ECV Volts	ECP PSIA	ECR mΩ	Amp	AH Output	EDP PSIA	EDR mΩ	Eff. %
17	1	0	0	1	207	400	17	6.8	1.471	---	19.28	2.0	2.984	-----	39.76	60.2
19	1	0	0	1	207	400	17	6.8	1.460	---	22.62	2.0	3.200	-----	37.65	64.5
21	1	0	1	1	207	400	17	6.8	1.471	---	11.88	2.0	3.718	-----	11.78	75.0
23	1	0	1	1	207	400	17	6.8	1.536	---	16.93	2.0	3.734	-----	23.56	75.3
25	1	0	0	1	207	400	17	6.8	1.476	---	16.67	2.0	3.000	-----	46.69	60.5
27	1	0	0	1	207	400	17.	6.8	1							
29	1	0	1	1	207	400	17	6.8	1.474	---	11.04	2.0	4.166	-----	11.90	84.0
31	1	0	1	1	207	400	17	6.8	1.470	---	14.04	2.0	4.418	-----	17.64	89.1

FIG. I-5

AH CAPACITY OF 17 PLATE FACTORIAL CELLS VS. CYCLE NUMBER
POST STERILIZATION
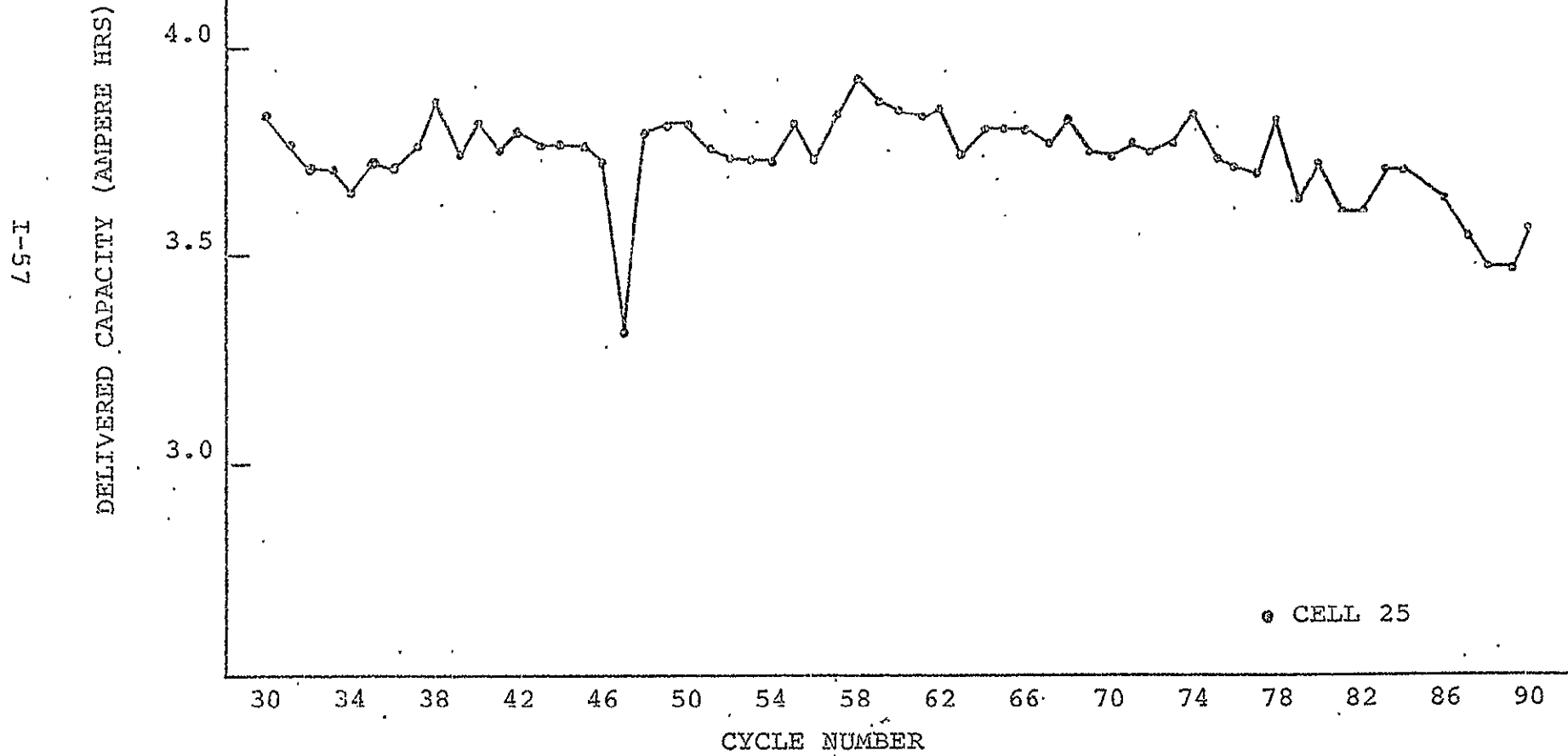CELL DESIGN: TYPE FT2140 SEPARATOR

34% KOH, 70% PORE FILL

FIG. I-6

END-OF-CHARGE VOLTAGE OF 17 PLATE FACTORIAL CELLS VS. CYCLE NUMBER

POST STERILIZATION

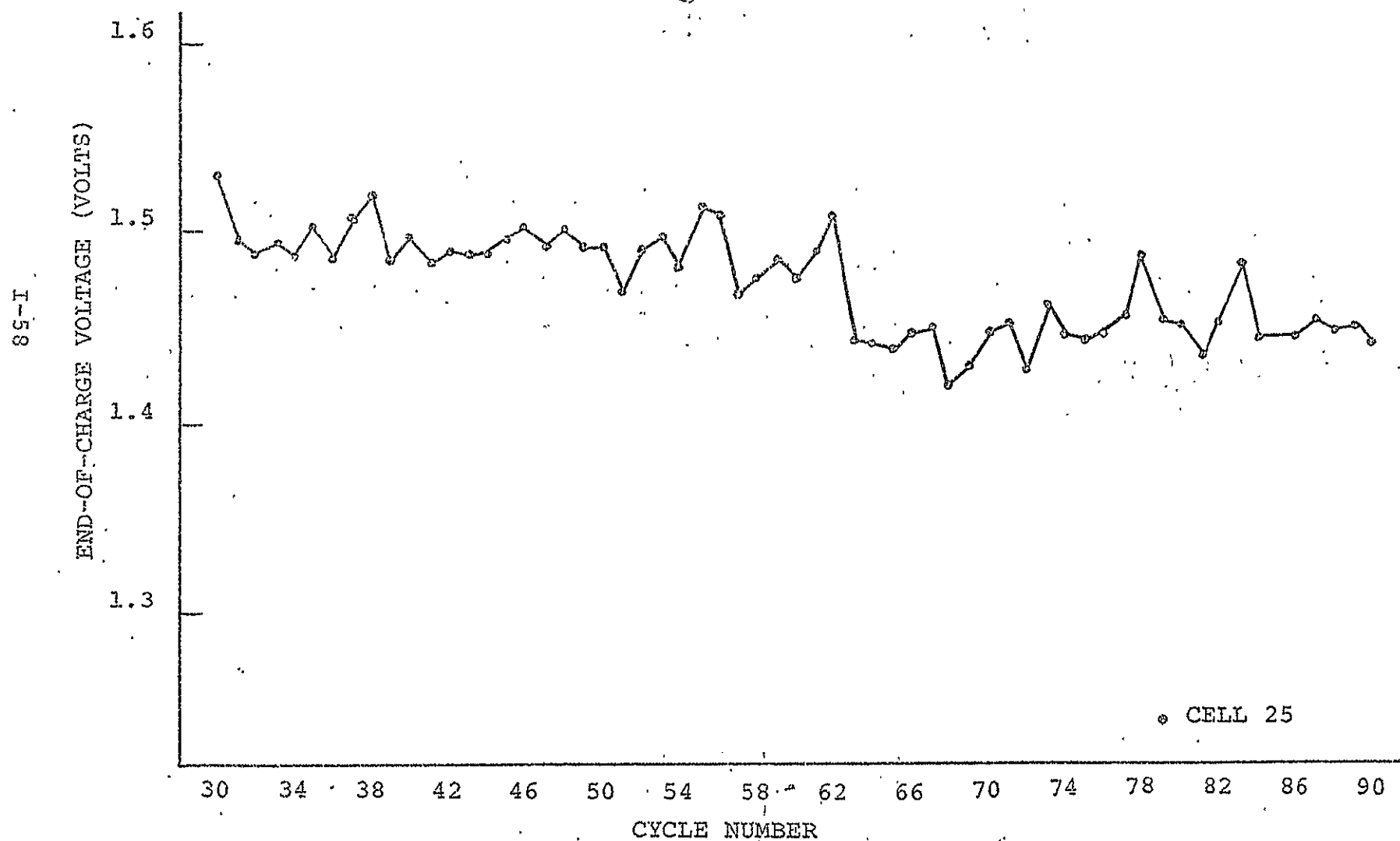CELL DESIGN: TYPE FT 2140 SEPARATOR

34% KOH; 70% PORE FILL

FIG. I-7 .

END-OF-CHARGE RESISTANCE OF 17 PLATE FACTORIAL CELL VS. CYCLE NUMBER

POST STERILIZATION
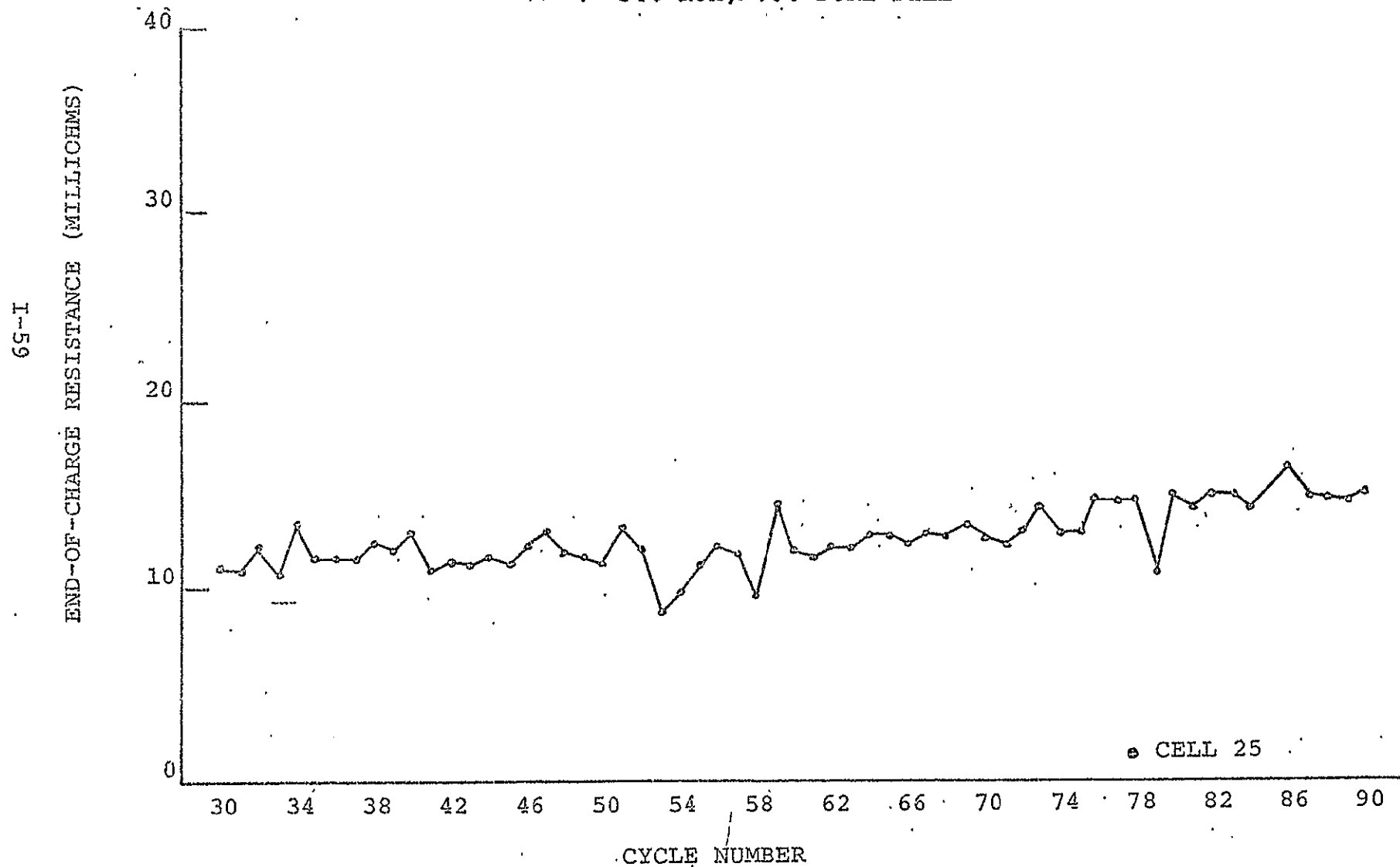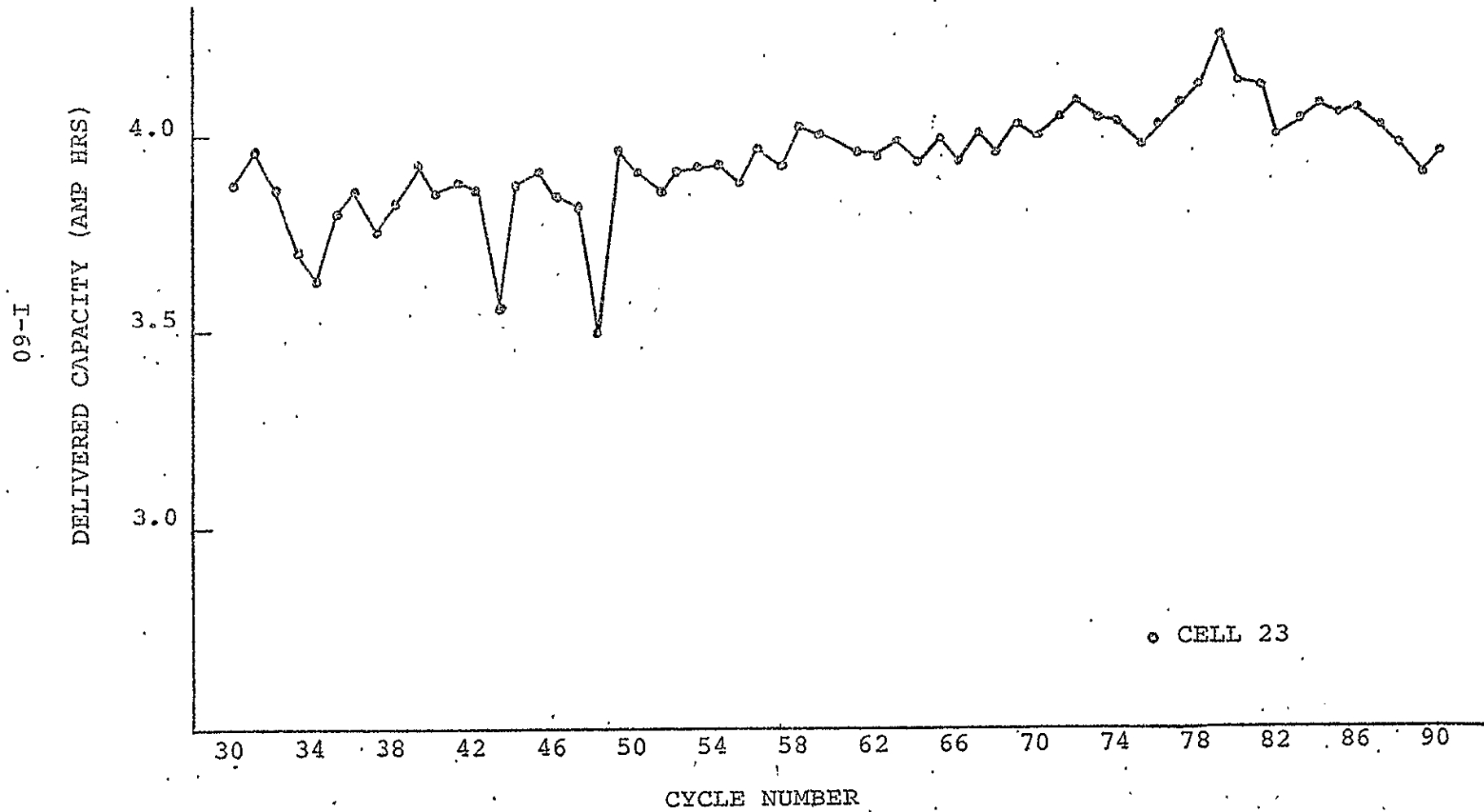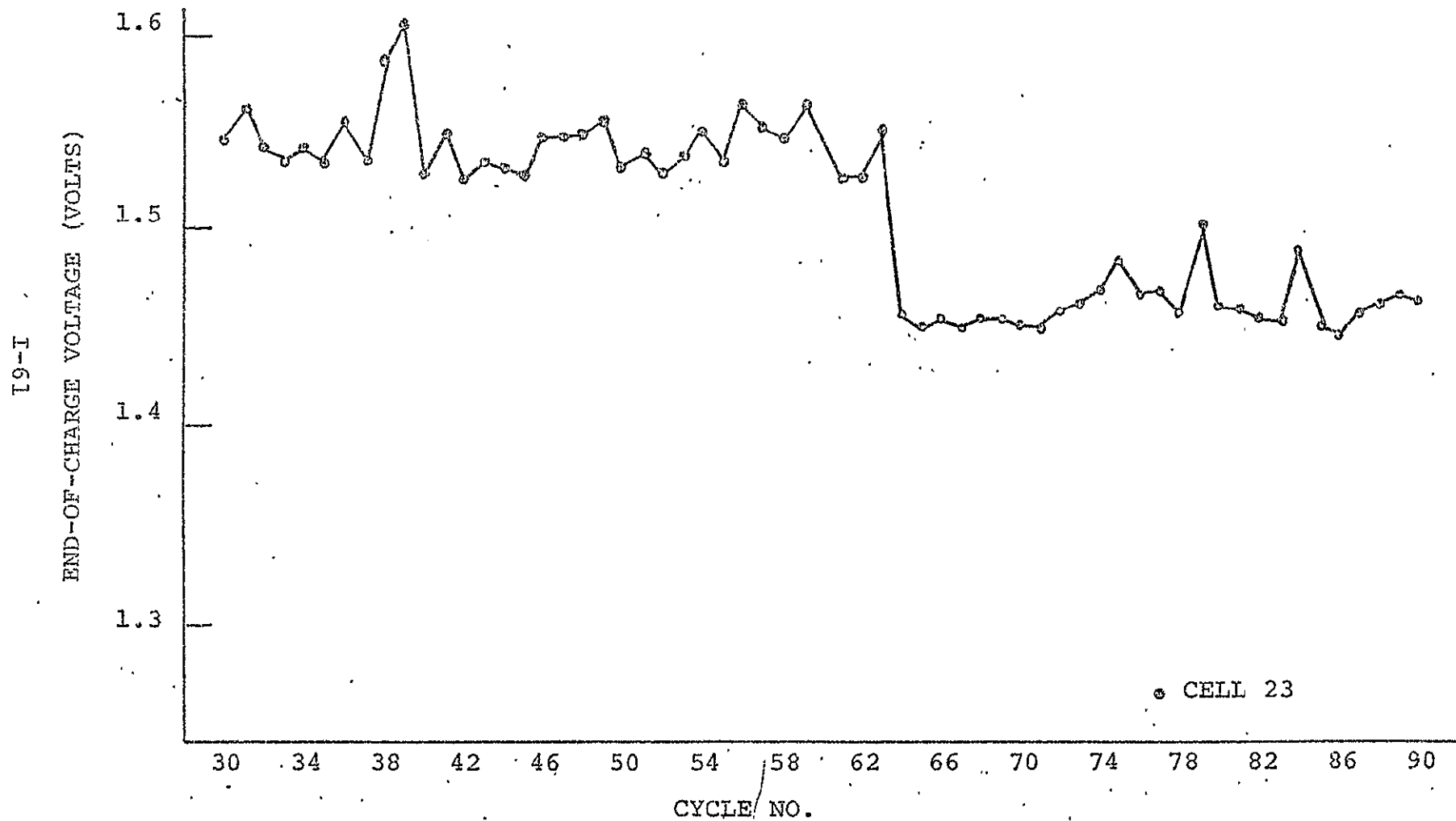CELL DESIGN: TYPE FT2140 SEPARATOR

34% KOH, 70% PORE FILL

FIG. I-8.
AH CAPACITY OF 17 PLATE FACTORIAL CELLS VS. CYCLE NUMBER
POST STERILIZATION
CELL DESIGN: TYPE FT2140 SEPARATOR

30% KOH, 80% PORE FILL

I-60

DELIVERED CAPACITY (AMP HRS)

4.0

3.5

3.0

○ CELL 23

30   34   38   42   46   50   54   58   62   66   70   74   78   82   86   90

CYCLE NUMBER

FIG. I-9

END-OF-CHARGE VOLTAGE OF 17 PLATE FACTORIAL CELLS VS. CYCLE NUMBER

POST STERILIZATION

CELL DESIGN: TYPE FT2140 SEPARATOR

30% KOH, 80% PORE FILL

FIG. I-10

END-OF-CHARGE RESISTANCE OF 17 PLATE FACTORIAL CELL VS. CYCLE NUMBER
POST STERILIZATION
CELL DESIGN: TYPE FT 2140 SEPARATOR
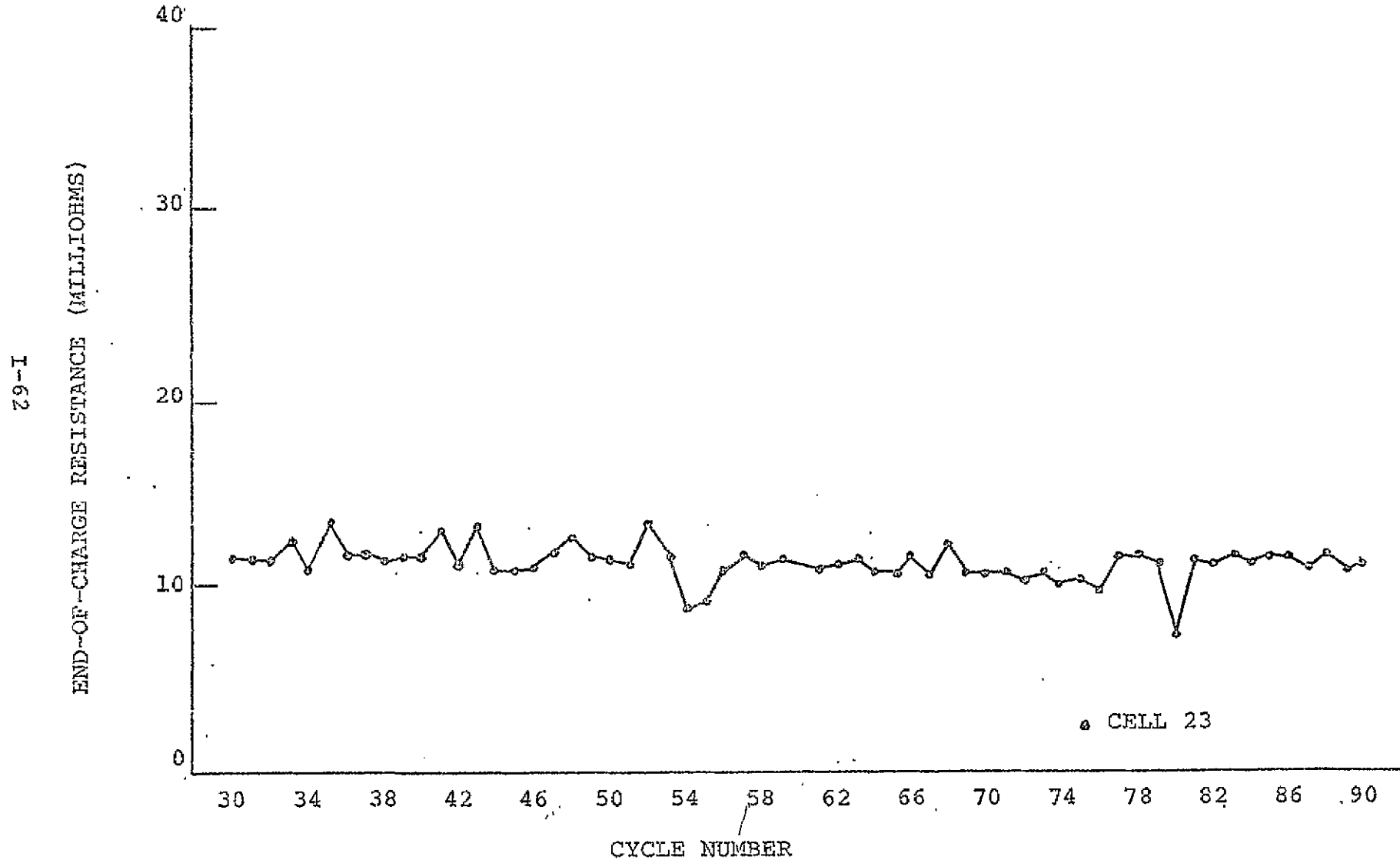
30% KOH, 80% PORE FILL

FIG. I-11

AH CAPACITY OF 17 PLATE FACTORIAL CELLS VS. CYCLE NUMBER

POST STERILIZATION

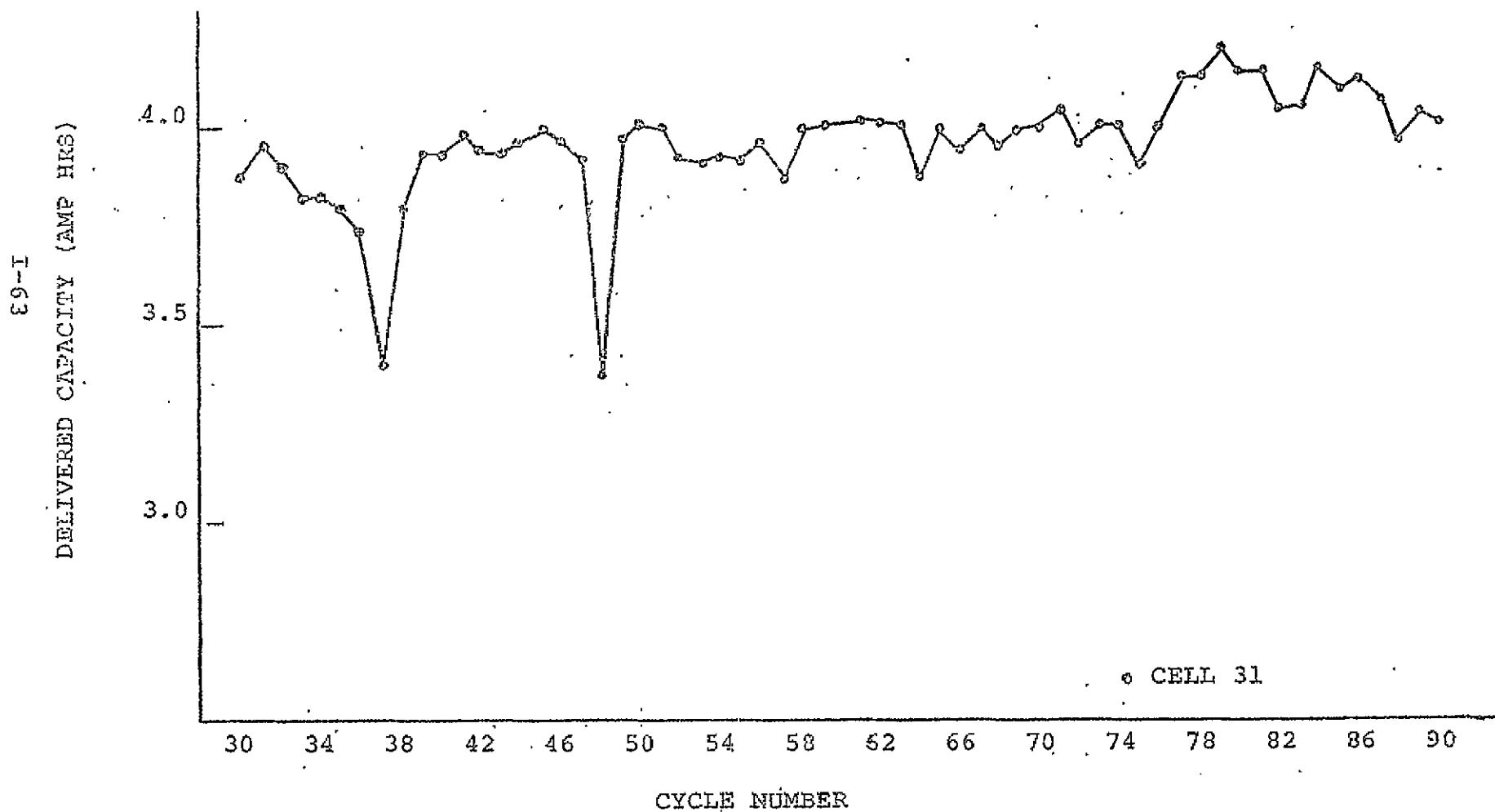CELL DESIGN: TYPE FT2140 SEPARATOR

.34% KOH, 80% PORE FILL

○ CELL 31

Fig. I-12

END-OF-CHARGE VOLTAGE OF 17 PLATE FACTORIAL CELLS VS. CYCLE NUMBER
POST STERILIZATION

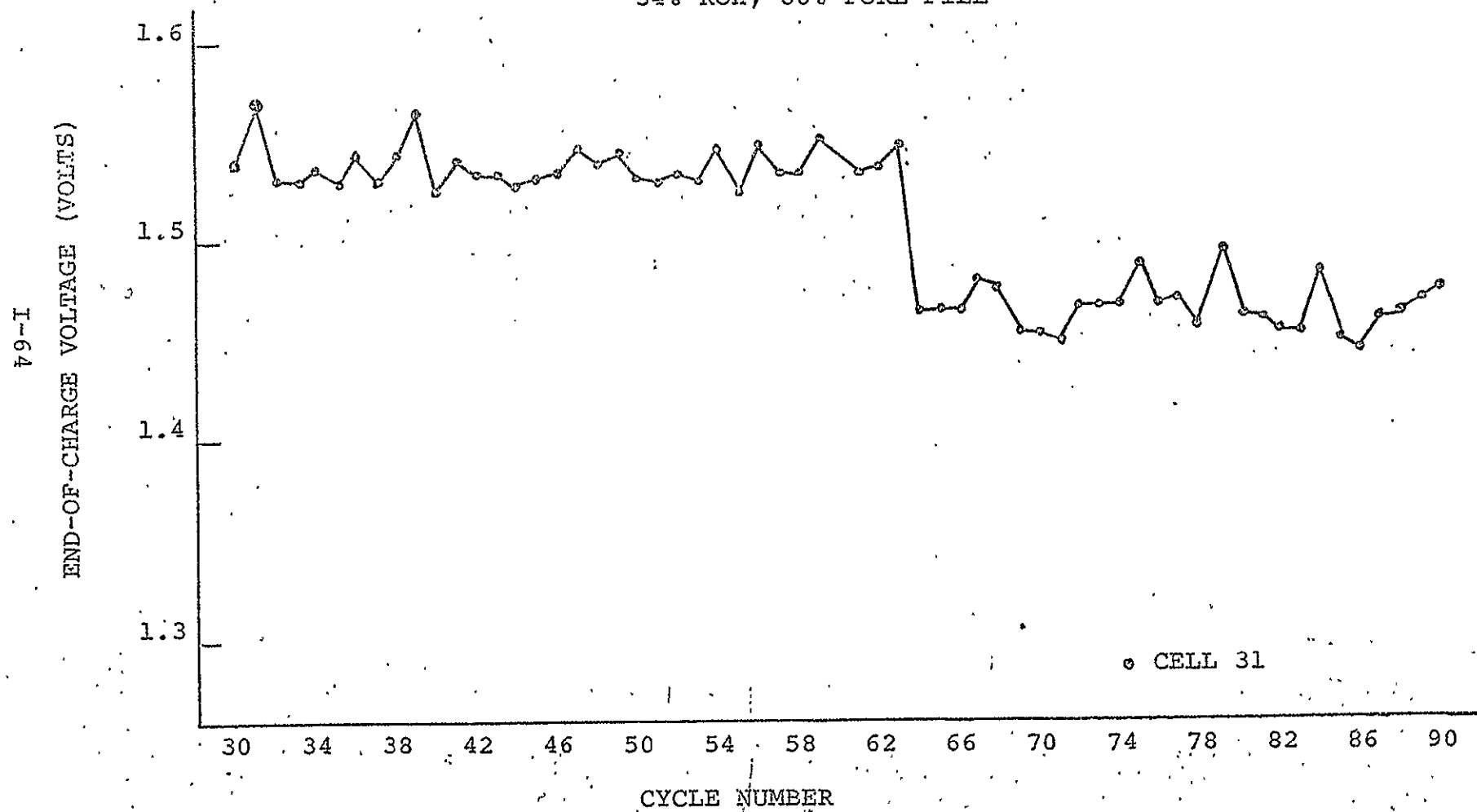CELL DESIGN: TYPE FT2140 SEPARATOR

34% KOH, 80% PORE FILL

FIG. I-13

END-OF-CHARGE RESISTANCE OF 17 PLATE FACTORIAL CELL VS. CYCLE NUMBER
POST STERILIZATION
CELL DESIGN: TYPE FT2140 SEPARATOR

34% KOH, 80% PORE FILL

CELL 31
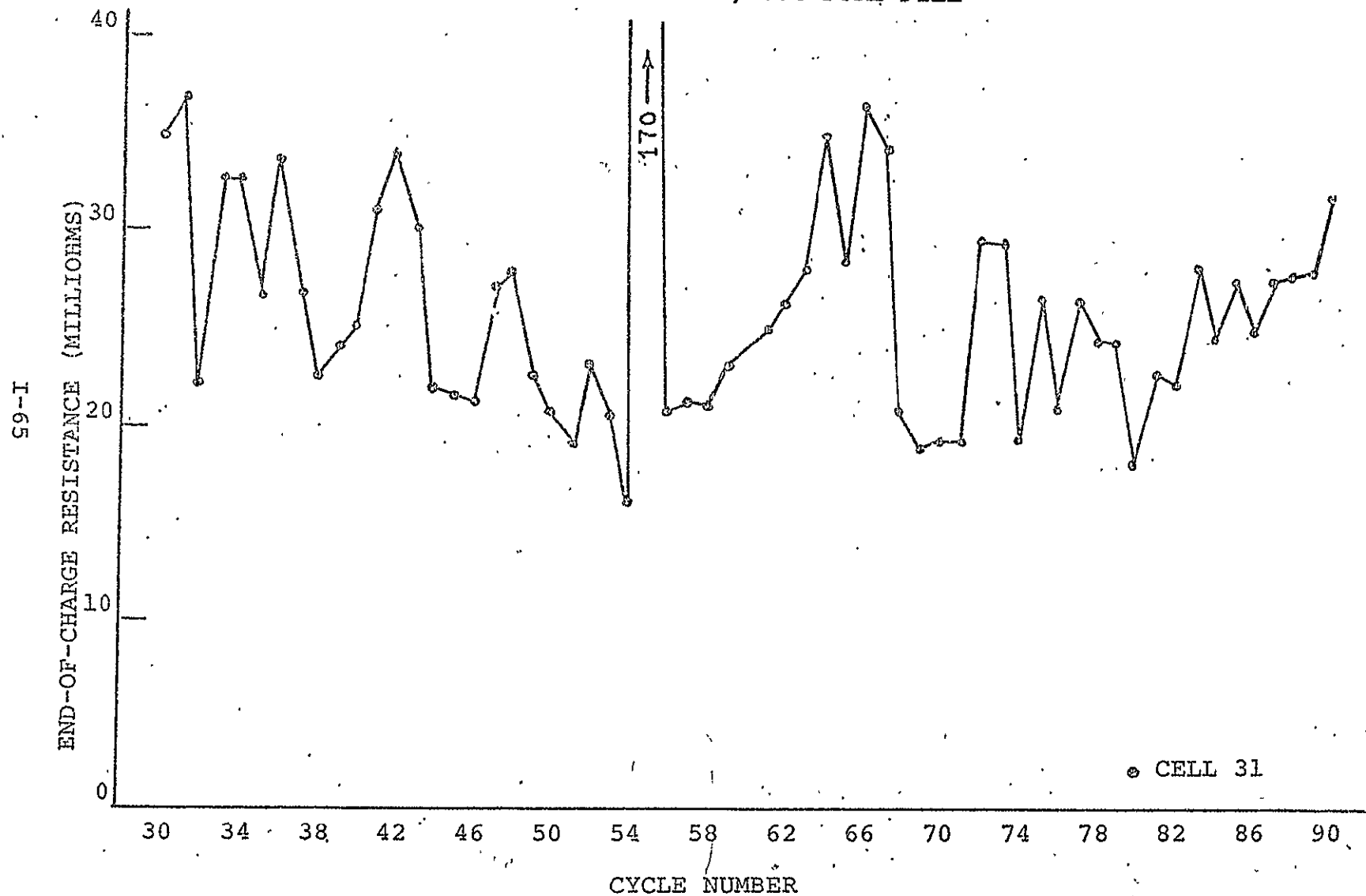
CYCLE NUMBER

END-OF-CHARGE RESISTANCE (MILLIOHMS)

I-65

Fig. I-14

AH CAPACITY OF 17 PLATE FACTORIAL CELLS VS. CYCLE NUMBER
POST STERILIZATION
CELL DESIGN: TYPE FT2140 SEPARATOR
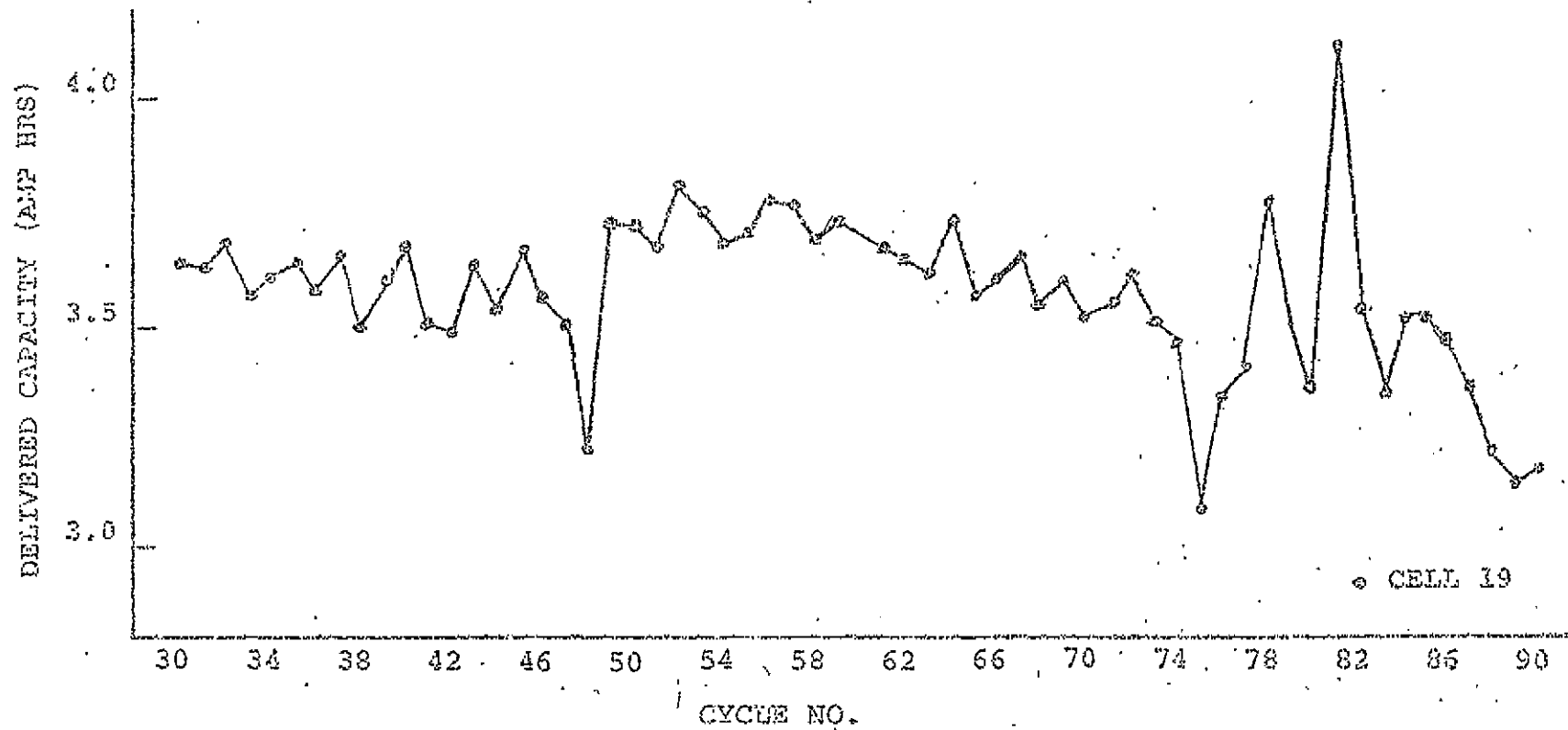30% KOH, 70% PORE FILL

○ CELL 19

FIG. I-15

END-OF-CHARGE VOLTAGE OF 17 PLATE FACTORIAL CELLS VS. CYCLE NUMBER

POST STERILIZATION

CELL DESIGN: TYPE FT2140 SEPARATOR
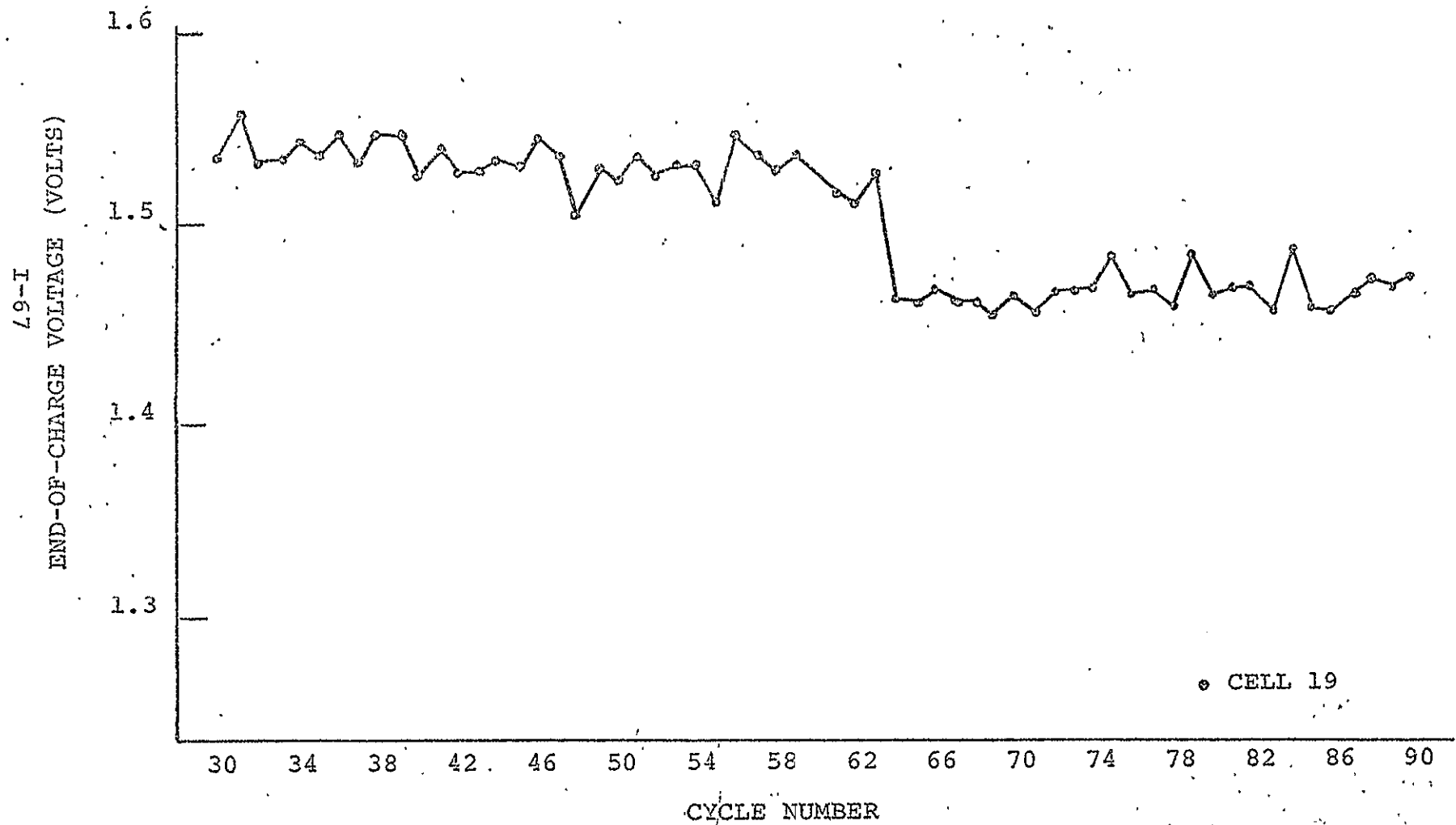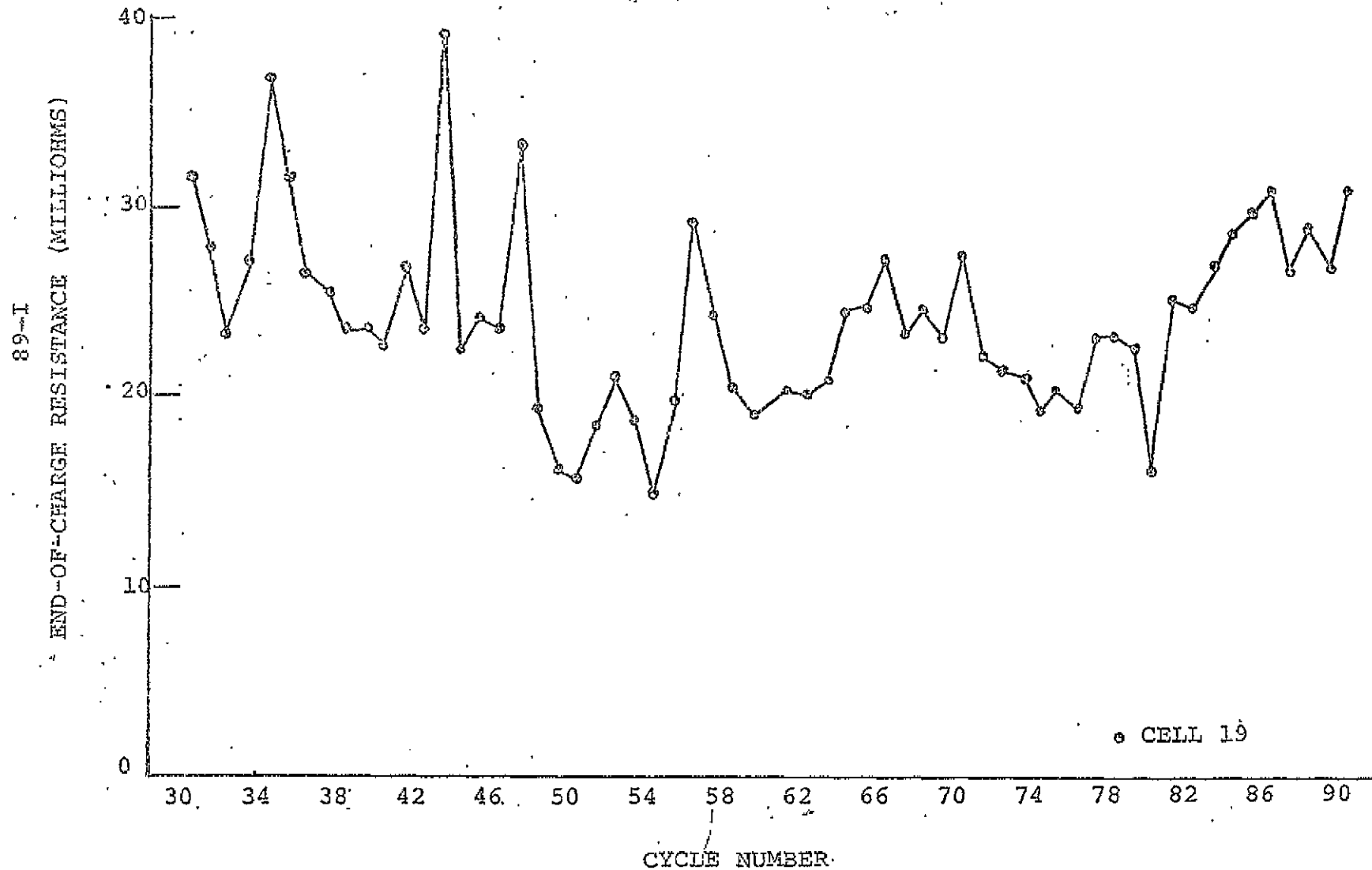
30% KOH, 70% PORE FILL

FIG. I-16

END-OF-CHARGE RESISTANCE OF 17 PLATE FACTORIAL CELL VS. CYCLE NUMBER

POST STERILIZATION
CELL DESIGN: TYPE FT2140 SEPARATOR
30% KOH, 70% PORE FILL

CELL 19

CYCLE NUMBER

89—I

Cycling Studies on Selected Cells From Factorial Design

Electrochemical data for selected cells containing FT2140 separator for up to 90 cycles following heat sterilization are summarized in graphical forms in Figures I-5 to I-16. Additional typical data for certain cycles up to 207 cycles are given in Table I-12. The capacity, ECV and ECR data for the following cells as a function of cycle number are given in Figs. I-5 to I-16.

Cell	KOH (w/o)	Pore Fill %	Pressure Gauge Attach.	Capacity Fig. #	ECV Fig.#	ECR Fig. #
19	30	70	no	I-14	I-15	I-16
23	30	80	no	I-8	I-9	I-10
25	34	70	yes	I-5	I-6	I-7
31	34	80	no	I-11	I-12	I-13

It is interesting to compare the data of Figures I-5 - I-16 with the cycling history shown in Figure I-4. For example, a dramatic decrease in the average value of the end-of-charge voltage is evident at Cycle 63 on all four cells. This corresponds to the change in charge routine noted in Figure I-4. Little change in the cell data occurred as a result of the removal of the pressure gauges from all cells but Cell I-13 at Cycle 75.

The high capacity reported earlier is maintained, and no decreasing trend is evident.

The decrease in end-of-charge voltage at Cycle 63 brings the average level of end-of-charge voltage from 1.53 V to about

metallurgical
materials division

1.46 V. In general, the end-of-charge voltage behavior can be summed up as follows:

1) The increase observed after sterilization is highly dependent upon charge rate, increasing by approximately 50 mv for a two-fold increase in charge rate (C/10 to C/5).

2) The high post-sterilization end-of-charge voltage remains constant with continued cycling, as does its dependency upon charge rate.

The end-of-charge resistances of Cells 19 and 31 continue to be erratic, while this parameter is much more steady in Cells 25 and 23. The amount of scatter in the data does not appear to correlate with any of the factors present in the experiment and is apparently due to some uncontrolled variable in the cell design.

Statistical Analysis of Data for Significant Effects

An attempt was made to analyze the cycle data to see if electrolyte concentration and/or pore fill had any significant effect upon cell performance. Some difficulty was encountered in selecting cells for a suitable factorial analysis. Two of the original factors -- type of separator and sterilization -- are no longer valid. All but one of the cells employing the 14019 separator have failed. Only 37 cycles were carried out prior to sterilization so there are no pre-sterilization cycles to compare with Cycles 37 through 91.

metallurgical
materials division

In order to employ as many cells as possible, a factorial
experiment was designed with a full compliment of cells from
Group 1 of Figure I-4, and nearly a full compliment from
Group 2. By "full compliment" it is meant a total of four
cells with all possible combinations of fill level and elec-
trolyte concentration. For Group 1, full compliment would be
Cells, 17, 21, 25 and 29. For Group 2, the corresponding
cells would be 19, 23, 27 and 31 except that Cell 27 is miss-
ing. Therefore, the data for the corresponding cell of Group
1 (Cell 25) was substituted in order to make the calculation
possible. Cells of Group 1 had pressure gauges attached until
Cycle 75. Cells of Group 2 did not. Thus, substitution of
Cell 25 for Cell 27 in this experiment would tend to reduce
the effects observed for presence or absence of pressure
gauges.

The factors included are shown in Table I-13, Factors D and E
were included so that data from several cycles could be ar-
ranged. These factors would be expected to have no effect
other than to improve the statistical reliability of the data.

Factor C is shown in Table I-13 as "pressure gauge treatment."
However, it should be noted that all data were chosen from
cycles after Cycle 75 when the pressure gauges were removed.
Thus, any significant effects observed for Factor C would ap-
pear to be either permanent effects caused by the presence of

a pressure gauge during early cycling, or some unknown differ-
ence in construction between the cells (i.e. "error").

TABLE I-13

Ni-Cd Rectangular 17-Plate Cell
Modified Factorial Experiment

Factor Designation	Description	LEVEL	
		Low (0)	High (1)
A	% Pore Fill	70%	80%
B	Conc. KOH	30%	34%
C	Pres. Gauge Attach.	yes	no
D	Successive Cycles	n	n + 1
E	Cycle Number	n = 86	n = 90

The original data used for the statistical computations are
given in Table I-14. The results of the analysis are summar-
ized in Tables I-15 and I-16. Very little significance could
be attributed to the cycle factors, and, therefore, these ef-
fects and their consequent interactions are not shown. There-
fore, the data given in the efficiency column of Table I-15
and the ECV column of Table I-16 are actually an average of the
values given for four different cycles in Table I-14. The
effects, variance ratios and significance values, however, are
based upon all of the results shown in Table I-14, and not
upon the average values.

The apparent results in Tables I-14, 15 and 16 can be summar-
ized as follows:

metallurgical
materials division

TABLE I-14

Factorial Design Experiment: Factor Effects on Performance

Ni-Cd, Rectangular, 17-Plate Cells, Theoretical Capacity: 4.96 AH

Cell/Cycle		A	B	C	D	E	Effc.	E.C.V.	Cell/Cycle		A	B	C	D	E	Effcy.	E.C.V.
17	86	0	0	0	0	0	.669	1.446	17	90	0	0	0	0	1	.672	1.442
21	86	1	0	0	0	0	.746	1.450	21	90	1	0	0	0	1	.739	1.448
25	86	0	1	0	0	0	.736	1.445	25	90	0	1	0	0	1	.723	1.442
29	86	1	1	0	0	0	.766	1.445	29	90	1	1	0	0	1	.759	1.442
19	86	0	0	1	0	0	.699	1.455	19	90	0	0	1	0	1	.638	1.472
23	86	1	0	1	0	0	.820	1.447	23	90	1	0	1	0	1	.800	1.467
25	86	0	1	1	0	0	.736	1.445	25	90	0	1	1	0	1	.723	1.442
31	86	1	1	1	0	0	.830	1.447	31	90	1	1	1	0	1	.810	1.477
17	87	0	0	0	1	0	.625	1.449	17	91	0	0	0	1	1	.658	1.443
21	87	1	0	0	1	0	.712	1.451	21	91	1	0	0	1	1	.750	1.447
25	87	0	1	0	1	0	.716	1.455	25	91	0	1	0	1	1	.719	1.441
29	87	1	1	0	1	0	.750	1.448	29	91	1	1	0	1	1	.763	1.440
19	87	0	0	1	1	0	.679	1.463	19	91	0	0	1	1	1	.709	1.451
23	87	1	0	1	1	0	.813	1.458	23	91	1	0	1	1	1	.840	1.458
25	87	0	1	1	1	0	.716	1.455	25	91	0	1	1	1	1	.719	1.441
31	87	1	1	1	1	0	.823	1.460	31	91	1	1	1	1	1	.844	1.459

TABLE I-15

Calculation and Significance Testing of Factor Effects

Ni-Cd, Rectangular, 17-Plate Cells. Theoretical Cap.: 4.96 AH

EFFICIENCY DATA

Cell	Factor Code A B C	Effcy.	Effect.	Variance Ratio	F-Test Significance	Significant Effects Primary	Interaction
17	0 0 0	.656					
21	1 0 0	.739	+.089	515.4	0.999999	A	
25	0 1 0	.723	.035	80.4	0.9999	B	
29	1 1 0	.759	-.020	24.9	0.997		AB
19	0 0 1	.681	.043	122.4	0.99997	C	
23	1 0 1	.818	.031	61.7	0.9998		AC
25	0 1 1	.723	-.010	6.3	0.9542		BC
31	1 1 1	.828	.003	0.0	0.0		ABC

TABLE I-16

Calculation and Significance Testing of Factor Effects

Ni-Cd, Rectangular, 17-Plate Cells. Theoretical Cap.: 4.96 AH

END OF CHARGE VOLTAGE DATA

Cell	Factor Code A B C	ECV (volts)	Effect.	Variance Ratio	F-Test Significance	Significant Effects Primary	Interaction
17	0 0 0	1.445					
21	1 0 0	1.449	0.0036	5.04	0.934	A	
25	0 1 0	1.446	-0.0039	6.15	0.952	B	
29	1 1 0	1.444	0.0029	3.42	0.886		AB
19	0 0 1	1.460	0.0102	41.2	0.9993	C	
23	1 0 1	1.457	0.0026	2.61	0.842		AC
25	0 1 1	1.446	-0.0017	1.13	0.671		BC
31	1 1 1	1.461	0.0059	14.00	0.990		ABC

1) Cell efficiencies:

   a) There is a highly significant increase of 8.9%
in the efficiency in going from 70 to 80% pore
fill;

   b) There is a significant increase of 3.5% in
the efficiency in going from 30 to 34% KOH;

   c) The increase in efficiency due to pore fill is
less marked at higher electrolyte concentration
than it is at the lower electrolyte concentra-
tion;

   d) Cells which did not have pressure gauges attached
showed significantly greater efficiencies than
cells that did have pressure gauges. This is
notable because the data was taken from cycles
after the gauges had been removed. This effect,
noted in previous reports while the gauges were
still attached has apparently persisted for 10
to 15 cycles beyond the removal of the gauges.

2) End-of-Charge Voltages:

   a) Little significance is seen for increases or de-
creases in voltages due to either pore fill or
electrolyte concentration;

   b) A significant increase in end-of-charge voltage
results from the absence of a pressure gauge.
That is, cells without pressure gauges have an

end-of-charge voltage that is on the average
10 mv higher than cells with gauges.

c) The apparent interaction for all three varia-
bles is not based upon enough data to be con-
sidered a reliable effect.

The conclusions arrived at above are based upon the assumption
that only the listed variables (% pore fill, KOH concentration,
and pressure gauge attachment) are affecting the results. How-
ever, other experiments have shown that some less controllable
variables such as pack compression and separator wettability
can also affect cell behavior. If a large number of cells are
used in factorial experiments of this nature, such uncontrolled
variables will show up as random error. The above conclusions
are based on only 7 cells, and therefore, must be accepted with
some caution since there is some likelihood that random errors,
especially large ones, will not cancel with so few cells.

metallurgical
materials division

H. Further Electrochemical Studies to Improve Cell Performance

The investigations conducted so far, including the factorial experiment, have established the technical feasibility of sealed, heat-sterilizable cells capable of long cycle life and stable performance after heat sterilization. However, these studies have also revealed certain technical problem areas with cells using polypropylene separator, especially with FT2140. It will be noted that FT2140 is mechanically more rugged and is capable of withstanding heat-sterilization treatment without degradation. The problem areas include:

1) A decrease in capacity, often observed during pre-sterilization cycling of the sealed cells, and an increase in capacity after sterilization;

2) Increase of approximately 60 mv in the end-of-charge voltage after sterilization;

3) The scatter in cell data, showing a decrease after sterilization, suggests that some parameters in the cell design remain uncontrolled.

Several approaches were taken to understand and, if possible, solve these problems. A very likely cause of the irreproducibility could be uneven electrolyte distribution or insufficient wetting throughout the separator. Possible factors that control the electrolyte distribution such as core compression and separator wettability have, therefore, been investigated.

metallurgical
materials division

Ni-Cd Cell and Component Compression Studies

Ni-Cd cells employing 19 plates, i.e. 10 negatives and 9 positives, yield an electrochemical capacity comparable with that obtained with 17 plate cells. However, there is a marked lack of reproducibility. This has been associated with the excessive core compression, which affects electrolyte distribution, resulting in a variable utilization of available active material. A study of core and core component compression was therefore initiated. The compression tests were performed on the Instron tensile machine.

Ni-Cd Cell Component Compressive Characteristics

Five 1 square inch samples of each of the cell components, separated by steel blocks, were tested together. Each compression test was repeated twice for each component. Three types of separator were examined, Pellon (nylon) as a control, and 14019 and FT2140 (polypropylene). The average values of the separator thickness for the fifteen samples, during and after compression, are shown in Table I-17A.

It is observed from Table I-17A, for example, that in the case of the Pellon (nylon) separator, an increase in pressure from 50 to 500 psi effects a 34% reduction in thickness but a further increase from 500 to 1000 psi only effects a further thickness reduction of 2.7%. When the thicknesses are measured after compression at 200 and 1000 psi, only a 3.8% permanent reduction in thickness results. As can be seen, of the

metallurgical
materials division

TABLE I-17A

SUMMARY OF RESULTS OF CELL COMPONENTS COMPRESSION STUDIES

Component	Type	Component Thicknesses (mils)							
		Under Compression at					After Compression at		
		50 psi	500 psi		1000 psi		200 psi	1000 psi	%Δt
		t	t	%Δt	t	%Δt	t	t	
Separator	Nylon -Pellon	5.6	3.7	34	3.6	2.7	8.0	7.7	3.8
Separator	Polypropylene-14019	5.0	3.8	24	3.6	5.3	8.3	7.8	6.0
Sepatator	Polypropylene-FT2140	6.6	4.9	25.8	4.6	6.1	7.6	7.4	2.6
Electrode	Positive	26.0	25.0	3.8	24.8	0.8		25.4	
Electrode	Negative	27.2	26.4	2.9	26.0	1.5		27.0	

TABLE I-17B

SEPARATOR-ELECTRODE PLATE INTERACTION UNDER 1000 PSI COMPRESSION

Electrode-Separator Combination	Thickness (ins.)		
	Calculated*	Measured	Difference
5 Positive - 4 'Pellon'	0.158	0.153	-0.005 (-3.2%)
5 Negative - 4 'Pellon'	0.166	0.159	-0.007 (-4.2%)
5 Positive - 4 '14019'	0.158	0.143	-0.014 (-8.9%)
5 Negative - 4 '14019'	0.166	0.155	-0.011 (-6.6%)
5 Positive - 4 'FT2140'	0.157	0.149	-0.008 (-5.1%)
5 Negative - 4 'FT2140'	0.164	0.158	-0.007 (-4.2%)

* Calculated from single component compression studies (see Table I-16)

three separators studied, the permanent reduction in thickness
is least (2.6%) for the FT2140 as against 6% for the 14019.

When electrodes and separators in contact are compressed, an
interaction is observed. In Table I-17B are summarized the
results from a series of compression studies on a simulated
cell electrode-separator assembly, consisting of 5 electrode
plates interspersed with 4 separator layers. The calculated pack
thicknesses of the individual components after compressing at 1000
psi are .158" to .164". These data indicate that to a large extent
both separator and electrodes behave elastically in the com-
pression range 50 - 1000 psi. Thus, under moderate pressure,
there is negligible permanent reduction in the total cell
core thickness. The lower electrode-separator interaction
shown by FT2140 points to this material as the more suitable
choice. Using the 1000 psi compression data, one may calcu-
late the total core thicknesses for 17, 18 and 19 plate cells,
as shown in Table I-18.

TABLE I-18

Component	Thick- ness (mils)	17 Plate		18 Plate		19 Plate	
		No.	Thick- ness (ins.)	No.	Thick- ness (ins.)	No.	Thick- ness (ins.)
Positive	25.4	8	0.203	8	0.203	9	0.229
Negative	27.0	9	0.243	10	0.270	10	0.270-
FT2140	7.0	18	0.133	19	0.141	20	0.148
Interface	-1.0	34	-0.034	36.	-0.036	38	-0.038
Total			0.545		0.578		0.609

metallurgical
materials division

These data show that the 18-plate configuration is the closest
to the inner dimension of the cell case, viz. 0.585". The 17-
plate cells, having .040" clearance, could very well be so
loosely packed that the separator is not in sufficiently in-
timate contact with the electrodes for complete utilization
of available active material. On the other hand, the 19-plate
cores, 24 mils over, may require excessive compression to fit
into the case. This could result in permanent mechanical
damage to one or more components during assembly and further
mechanical damage induced by the excessive compression result-
ing from sterilization. With these points in mind, a number
of 18-plate cells were assembled and filled to the 80% pore
fill level with 30% potassium hydroxide. The assembled cells
were divided into three groups and studied in the following
manner.

Group A. Subjected to 5 charge-discharge cycles,
Routine R1.

Group B. Subjected to 5 charge-discharge cycles,
Routine R1, then sterilized and re-sub-
jected to 5 similar cycles.

Group C. Sterilized then subjected to 5 charge-
discharge cycles, Routine R1.

The complete data are shown in Table I-19 (delivered capacity)
and Table I-20 (end-of-charge voltage). As can be seen, the
behavior shows similar characteristics to that shown by the
17-plate cells. On pre-sterilization, after the first
atypical cycle, commonly observed in Ni-Cd cells, both the

I-81

metallurgical
materials division

TABLE I-19

Cell Capacity Before and After Sterilization

Ni-Cd, 18-Plate, Rectangular Cells, 30% KOH, 80% Pore Fill, FT2140 Separator

C.R. C/12.5 C.L. 137% D.R. C/2.5 CAPACITY, AH

Group	Cell #	Pre-Sterilization					Post-Sterilization				
		Cycle #1	Cycle #2	Cycle #3	Cycle #4	Cycle #5	Cycle #1	Cycle #2	Cycle #3	Cycle #4	Cycle #5
A	15	3.134	2.784	2.466	2.634	2.652					
A	16	3.418	3.052	2.784	2.900	2.918					
A	17	3.034	2.652	2.334	2.518	2.584					
B	1	3.400	3.200	3.000	2.784	2.866	4.052	4.018	3.934	4.039	3.952
B	2	3.584	3.300	3.018	2.784	2.834	4.018	3.952	3.818	3.900	3.752
B	3	3.600	3.318	3.052	2.834	2.918	3.952	3.918	3.834	3.952	3.866
B	5	3.418	3.152	2.884	2.634	2.766	4.084	4.034	3.966	4.118	4.052
C	9						4.018	4.052	3.818	3.900	3.866
C	10						4.100	4.184	4.000	3.984	3.918
C	11						4.152	4.200	4.118	4.052	3.966
Average		3.369 68%	3.065 62%	2.791 56%	2.727 55%	2.809 57%	4.061 82%	4.051 82%	3.927 80%	4.009 81%	3.910 79%
Stan. Dev.		0.214	0.256	0.285	0.134	0.131	0.058	0.107	0.112	0.081	0.095

TABLE I-20

ECV Data Before and After Sterilization

Ni-Cd, 18-Plate Rectangular Cells, 30% KOH, 80% Pore Fill,
FT2140 Separator

C.R. C/12.5 C.L. 137% D.R. C/2.5

END-OF-CHARGE VOLTAGE, VOLTS

Group	Cell #	Pre-Sterilization					Post-Sterilization				
		Cycle #1	Cycle #2	Cycle #3	Cycle #4	Cycle #5	Cycle #1	Cycle #2	Cycle #3	Cycle #4	Cycle #5
A	15	1.423	1.410	1.415	1.405	1.411					
A	16	1.423	1.412	1.416	1.407	1.414					
A	17	1.416	1.405	1.409	1.400	1.406					
B	1	1.447	1.420	1.409	1.415	1.402	1.489	1.506	1.474	1.473	1.472
B	2	1.445	1.418	1.409	1.413	1.404	1.488	1.499	1.470	1.468	1.467
B	3	1.446	1.418	1.410	1.414	1.405	1.488	1.509	1.478	1.477	1.479
B	5	1.443	1.416	1.409	1.413	1.404	1.487	1.505	1.475	1.476	1.477
C	9						1.486	1.475	1.473	1.460	1.462
C	10						1.487	1.472	1.471	1.460	1.465
C	11						1.484	1.472	1.471	1.460	1.465
Average		1.435	1.413	1.411	1.416	1.406	1.487	1.488	1.474	1.468	1.468
Stan. Dev.		0.0134	0.0059	0.0031	0.0056	0.0043	0.0017	0.016	0.0026	0.0026	0.0076

capacity and the end-of-charge voltage stabilize. Following sterilization, there is a 25-30% increase in capacity and an increase in ECV of the order of 60mv. The characteristic post-sterilization behavior appears to be independent of the pre-sterilization history of the cells, although there is a slight indication that the post-sterilization ECV is higher in cells which have undergone pre-sterilization charge-discharge cycles. These initial data indicate that, in comparison with 17-plate cells, 18-plate cells exhibit greater reproducibility. For this reason, these 18-plate cells were subjected to continued post-sterilization cycling.

Further post-sterilization cycling data up to 150 cycles are given in Table I-21, I-22 and I-23. Several observations can be made concerning the 18-plate cell performance --

1) Cell-to-cell and cycle-to-cycle uniformity is excellent. The difference between this result and the lack of uniformity in the 17-plate cells is remarkable.

2) As with 17-plate cells, the high end-of-charge voltage is in evidence, further confirming the profound effect that sterilization has upon the electrochemical properties of the cells.

3) The efficiency of the 18-plate cells is, on the average, about 83% as compared to 69% for the 17-plate cells after sterilization and shows far

TABLE 1-21

FT2140 SEPARATOR, POST-STERILIZATION DATA

Ni-Cd, Rectangular, 18-Plate Cells, 30% KOH, 80% Pore Fill

C.R. = C/12.5   C.L. - 137%   D.R. = C/2.5

Replicate 4 Cells

Cy-cle #	E.C.V. (V)		O.C.V. (V)		Cell Voltage at Various D. of D.						E.C.R. (mΩ)		E.D.R. (mΩ)		CAP (A.H.)		EFF. (%)	
					25%		50%		75%									
	Av.	σ	Av.	σ	Av.	σ	Av.	σ	Av.	σ	Av.	σ	Av.	σ	Av.	σ	Av.	σ
6	1.477	0.002	1.411	0.002	1.260	0.003	1.258	0.004	1.249	0.005	12.43	1.51	11.74	1.99	4.292	0.069	85.6	1.4
9	1.470	0.005	1.399	0.004	1.267	0.004	1.264	0.004	1.239	0.004	11.51	1.54	11.07	2.12	4.059	0.100	81.8	2.0
15	1.462	0.002	1.418	0.002	1.268	0.006	1.263	0.006	1.249	0.006	12.35	2.43	12.42	2.45	4.134	0.049	83.3	1.0
20	1.475	0.005	1.416	0.006	1.269	0.008	1.262	0.008	1.250	0.008	12.02	2.82	14.63	6.77	4.126	0.079	83.2	1.6
26	1.462	0.002	1.405	0.002	1.268	0.011	1.260	0.011	1.243	0.011	9.90	3.41	15.94	6.57	4.050	0.110	81.7	2.2
29	1.456	0.001	1.395	0.003	1.271	0.010	1.264	0.011	1.246	0.010	14.30	4.34	15.55	6.45	3.971	0.074	80.1	1.5

TABLE I-22

POST-STERILIZATION DATA

Ni-Cd, Rectangular, 18-Plate Cells, 30% KOH, 80% Pore Fill, FT2140 Separator

C.R. = C/12.5   C.L. = 137%   D.R. = C/2.5

Replicate: 4 Cells

Cycle #	E.C.V (v) Av.	σ	O.C.V. (v) Av.	σ	Cell Voltage at Various D. of D. 25% Av.	σ	50% Av.	σ	75% Av.	σ	E.C.R.(mΩ) Av.	σ	E.D.R.(mΩ) Av.	σ	Cap AH (AH) Av.	σ	Eff:(%) Av.
32	1.453	0.003	1.400	0.001	1.270	0.011	1.259	0.011	1.244	0.011	14.25	4.22	14.21	3.89	4.054	0.066	81.7 1.3
38	1.463	0.008	1.419	0.004	1.277	0.002	1.265	0.004	1.253	0.004	13.01	0.79	15.42	2.54	4.163	0.082	83.9 1.7
44	1.476	0.003	1.413	0.004	1.272	0.009	1.262	0.010	1.248	0.010	13.64	3.54	15.45	5.15	4.055	0.177	81.8 3.6
49	1.468	0.004	1.398	0.005	1.274	0.009	1.263	0.011	1.246	0.010	13.58	3.80	14.76	5.36	4.042	0.134	81.5 2.7
53	1.472	0.004	1.400	0.005	1.267	0.015	1.257	0.015	1.242	0.014	14.20	5.41	16.30	7.25	3.905	0.201	78.7 4.1
60	1.478	0.004	1.408	0.004	1.270	0.007	1.258	0.007	1.246	0.007	13.19	2.89	16.29	4.43	4.063	0.154	81.9 3.1
70	1.476	0.006	1.415	0.004	1.277	0.006	1.262	0.008	1.244	0.008	12.59	1.78	18.79	4.37	4.088	0.194	82.4 3.9
71	1.468	0.005	1.406	0.004							12.17	1.65	15.84	4.47	4.042	0.234	81.5 4.7
80	1.471	0.004	1.399	0.005							12.65	3.22	16.33	5.73	4.008	0.169	80.8 3.4
90	1.503	0.007	1.430	0.004							13.02	3.42	22.06	10.59	4.092	0.191	82.5 3.8

TABLE I-23

POST STERILIZATION CYCLE DATA

Ni-Cd, 18-Plate, FT2140 Separator, 30% KOH, 80% Pore Fill

C.R. = C/12.5   C.L. = 137%   D.R. = C/2.5   n = 4

Replicate: 4 Cells

Cycle #	ECV Volts		OCV Volts		ECR mΩ		EDR mΩ		Cap. (AH)		Effcy (%)	
	Ave.	σ	Ave.	σ	Ave.	σ	Ave.	σ	Ave.	σ	Ave.	σ
91	1.520	.003	1.423	.002	15.53	7.01	14.17	3.34	4.204	.152	84.8	3.1
95	1.469	.004	1.401	.002	15.99	8.54	16.34	7.50	4.046	.106	81.6	2.1
100	1.471	.006	1.396	.003	11.73	1.13	13.57	2.48	3.984	.143	80.3	2.9
105	1.458	.003	1.387	.004	11.43	.96	15.59	3.61	4.013	.159	80.9	3.2
110	1.453	.010	1.384	.009	12.08	1.23	15.05	3.24	3.967	.234	80.0	4.7
111	1.500	.007	1.434	.007	12.29	1.51	14.72	3.01	3.875	.250	78.1	5.0
115	1.486	.007	1.412	.003	11.34	1.04	13.66	3.11	4.025	.236	81.2	4.8
120	1.445	.016	1.375	.010	12.49	1.64	14.20	4.15	3.926	.380	79.2	7.7
125	1.487	.011	1.418	.005	13.62	3.92	16.53	6.02	4.042	.236	81.5	4.8
130	1.460	.011	1.389	.012	13.46	3.54	14.62	3.91	3.842	.413	77.5	8.3
131	1.455	.017	1.394	.016	12.42	2.34	14.62	5.20	3.737	.529	75.4	10.7
135	1.464	.007	1.399	.008			15.68	5.65	4.009	.355	80.8	7.2
140	1.462	.006	1.398	.009	13.67	2.86	16.45	6.49	3.992	.334	80.5	6.7
145	1.467	.006	1.384	.011	13.76	3.14	18.83	7.87	3.979	.293	80.2	5.9
150	1.469	.008	1.417	.007	15.28	4.34	19.40	8.39	4.184	.158	84.4	3.2
188	1.460	.012	----	---	13.00	6.00	17.00	----	4.100	.500	83.0	10.0

more reproducibility.

4)   Continued cycling produces greater cell-to-cell
     scatter of cell resistance data. Also, a gen-
     eral tendency of cell resistance to increase is
     evident.

The differences between 17-plate cells and 18-plate cells
noted above indicate that core compression is a significant
factor. An experiment was designed to assess this parameter
more directly. Twenty-four 17-plate cells were prepared with
304 stainless steel shims in thicknesses of .010" and .020"
placed as symmetrically as possible on the outside of the
cell packs. A 17-plate cell pack with a .033" shim would be
expected to be equivalent in thickness to an 18-plate cell.
The shim thickness and the resulting cell performance is
shown in Table I-24.

TABLE I-24

Core Compression Study With Shims

17-Plate Cell With FT2140 Separator, Cycle No. 3
Charge-Discharge Routine: Input: 1.00 amp, 5 hrs.
                            Output: 2.00 amps to 1V cut-off

Pre-Sterilization

Shim Ins.	ECV Volts	ECP* psia	ECR ohms	ECP psia	EDR ohms	ECC AH	Force to Flatten (lbs.)
0.00	1.456	79.7	11.20	26.7	11.14	3.518	5.4
0.01	1.468	57.7	10.09	23.7	10.24	3.472	5.1
0.02	1.460	75.7	10.10	39.7	10.62	3.539	6.2
0.03	1.458	62.7	10.45	32.7	11.28	3.583	4.7
0.04	1.456	80.7	9.11	43.2	9.87	3.463	6.4
0.05	1.458	62.7	10.02	29.7	10.84	3.571	7.2

* Value for 1 cell -- all other data average of 4 cells.

metallurgical
materials division

When prismatic cells are constructed, the walls of the case tend to bulge outward. When cycled, however, the cells are fixed between heavy, flat restraining plates. This would tend to place more compression on the thicker packs than on the thin packs. However, no correlation is evident between the shim thickness and the force to flatten, even though it was determined that the force to flatten empty cells filled with air at a known pressure was proportional to this pressure.

The poor correlation among the cell parameters and the shim thicknesses or the force to flatten seems to preclude the conclusion that cell compression is an important variable.

However, it should be noted that even the well-behaved 18-plate cells showed low efficiencies and poor reproducibility prior to sterilization. In fact, both groups showed pre-sterilization efficiencies of 60%. The most notable differences between 17-plate and 18-plate cells occurred after sterilization.

metallurgical
materials division

I. Separator-Electrolyte Absorption and Wettability Studies

The lack of reproducibility of cell data may result from poor absorption of electrolyte by the polypropylene separator materials. Poor wetting of the separator would be influenced by pressure on the plates, thereby accounting for the differences observed between 17- and 18-plate cells. The net result of poor wetting properties could be an uneven and irreproducible distribution of electrolyte which in turn would cause uneven utilization of the active electrode material. Initially, it was of interest to determine the amount of 30% KOH absorbed by the separators before and after heat sterilization.

The data for KOH absorption by Separators 14019 and FT2140 before and after heat sterilization at $135^{\circ}C$ for 64 hours in 30% KOH or 30% KOH saturated with CdO and with or without positive and negative plates are given in Table I-25. Without exception, all samples of the separator material absorbed more KOH after sterilization. The presence of CdO in the electrolyte or the positive and the negative plates in contact with the separator did not have any measurable effect on the amount of KOH absorbed by the separator. These results indicate that the effective porosity of the separator or the ability of the separator to retain KOH increases due to heat sterilization. This will result in effective lowering of the percent pore fill by KOH after cell sterilization and may account for increased resistance found in some cells following heat-sterilization

TABLE I-25

ABSORPTION OF KOH SOLUTIONS
BY TWO BEST POLYPROPYLENE SEPARATORS
BEFORE AND AFTER STERILIZATION

TEST MEDIA⟶	30% KOH	30% KOH & positive plate	30% KOH & negative plate	30% KOH sat'd with CdO	30% KOH sat'd with CdO & positive plate	30% KOH sat'd with CdO & negative plate
Separator FT 2140	Absorption of KOH Expressed in gmKOHsoln/gm sep.					
Presterilization	2.83	2.81	2.91	2.99	3.14	2.98
Poststerilization	4.70	5.15	4.33	4.60	4.40	4.85
Increase	1.87	2.34	1.42	1.61	1.26	1.87
14019 #2						
Presterilization	6.30	6.35	6.37	6.59	6.09	6.00
Poststerilization	13.90	17.00	17.10	17.60	9.40	11.00
Increase	7.60	10.65	10.73	11.01	3.31	5.00
14019 #3						
Presterilization	4.81	5.43	5.98	5.02	4.69	5.31
Poststerilization	16.50	16.60	16.40	10.80	12.60	13.20
Increase	11.69	11.17	10.42	5.78	7.91	7.89
Separator FT 2140	Absorption of KOH Expressed in cc KOH/in^2 separator					
Presterilization	0.105	0.104	0.108	0.110	0.116	0.110
Poststerilization	0.174	0.190	0.160	0.166	0.163	0.179
Increase	0.069	0.086	0.052	0.056	0.047	0.069
14019 #2						
Presterilization	0.202	0.203	0.204	0.211	0.195	0.192
Poststerilization	0.445	0.544	0.547	0.563	0.301	0.352
Increase	0.243	0.341	0.343	0.352	0.106	0.160
14019 #3						
Presterilization	0.144	0.163	0.179	0.151	0.141	0.159
Poststerilization	0.495	0.498	0.492	0.324	0.378	0.396
Increase	0.351	0.335	0.313	0.173	0.237	0.237

metallurgical
materials division

treatment. For these reasons, 60 and 70% pore fill levels appear inadequate since the effective pore fill level is reduced after sterilization.

Experimental data on the effect of heat sterilization of the positive and negative plates on KOH absorption characteristics are given in Table I-26. These results show that during the pre-sterilization cycling of the plates, the pickup of 30% KOH increases. After sterilization, there appears to be little change in KOH pickup. However, on cycling these plates following heat sterilization, the pickup by the positive plates shows an increase whereas the pickup by negative decreases. These results show that there is a shift in the electrolyte pore fill and distribution due to sterilization and cycling.

A series of electrolyte absorption studies were also performed on Gelman proprietary treated polypropylene. As can be seen in Figure I-17 the absorption rate of this as-received material is only slightly less than that exhibited by nylon. However, after sterilization in 30% KOH, washing and drying, the wetting properties deteriorate considerably. Other experiments measuring the grams of liquid electrolyte retained by a given weight of separator (pickup) showed that the weight retained by the unsterilized Gelman material was greater if withdrawn immediately after immersion in 30% KOH than if withdrawn after 64 hours. This indicates a possible change in wetting prop-

TABLE I-26

EFFECT OF STERILIZATION ON THE ABSORPTION OF 30% KOH

BY THE POSITIVE AND THE NEGATIVE PLATES

Plate	Initial	Pre-sterilization Pick up of KOH		Post-sterilization Pick up of KOH	
	Dry wt. as Received	g KOH/g Plate as Received	g KOH/g Plate Cycled	Not Cycled	Cycled After Sterilization
Neg. 1	6.3514	.127	.137	.144	.114
2	6.4344	.119	.143	.149	.110
3	6.2234	.123	.125	.132	.113
4	6.3688	.125	.148	.143	.104
Ave.	6.3445	.123	.138	.142	.110
Pos. 1	5.6122	.118	.139	.136	.200
2	5.9281	.124	.164	.158	..196
3	5.1690	.126	.145	.139	.202
Ave.	5.5697	.123	.149	.144	.199

metallurgical
materials division

FIGURE I-17

SEPARATOR ABSORPTION CHARACTERISTICS

(cm vs. time).

1 ○ Pellon (nylon)
2 ○ Sterilized FT2140 (with KOH + Pos.)
3 ▫ Unsterilized FT2140
4 ◇ Unsterilized 14019
5 ✕ Unsterilized Gelman
6 ▫ Sterilized Gelman
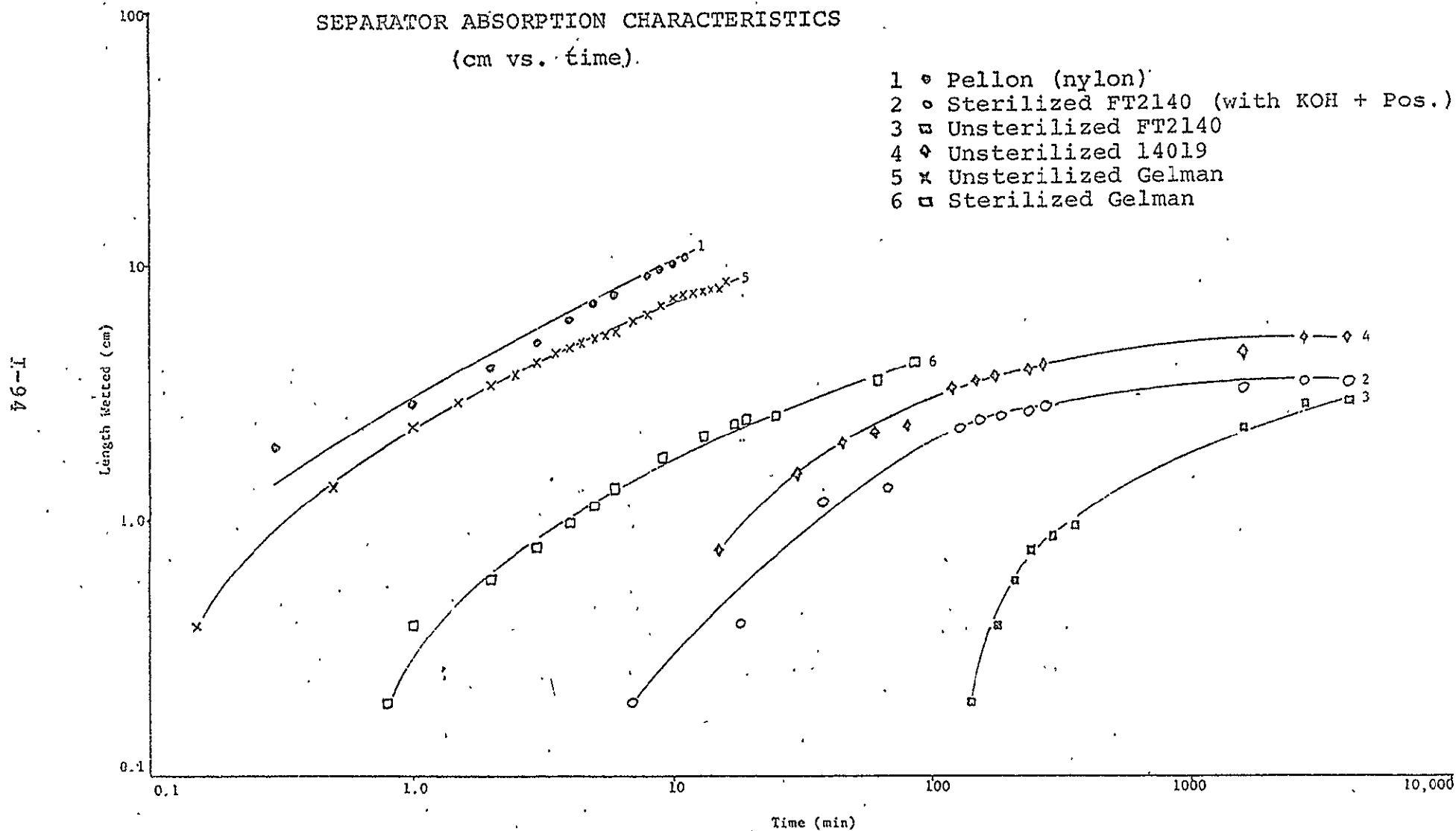
erties, and/or an attack upon the material by the electrolyte. Table I-27 gives results of pickup experiments for both FT2140 separator material and for the Gelman material under various conditions. It is noteworthy that the FT2140 does not show an immediate pickup and that an extended immersion is required.

TABLE I-27

30% KOH SOLUTION PICKUP
Gelman and FT2140 Polypropylene

Polypropylene Type	Conditions	Pickup (Grams KOH/Grams Separator) Sample #1	Sample #2
FT2140	64 hr. immersion	3.69	3.20
Gelman	Immediate	2.45	2.41
Gelman	64 hr. immersion	1.98	1.75
Gelman	Immediate	2.69	---

Four 17-plate cells employing the Gelman separator were constructed, two with the separator nap facing the positive plate (P-1 and P-2) and two with the nap facing the negative plate (N-1 and N-2). The cells were cycled 10 cycles prior to and 16 cycles after sterilization. Data for Cells P-2 and N-2 are shown in Table I-28. Prior to sterilization, Cells P-1 and P-2 yielded slightly higher efficiencies than Cells N-1 and N-2. After sterilization, the end-of-charge voltage was found to be increased. The efficiencies increased (6% for P-2 and 13% for N-2) over their pre-sterili-

metallurgical
materials division

TABLE I-28

CYCLE DATA FOR GELMAN SEPARATOR

17-Plate, Ni-Cd Pre-and Post-Sterilized Cells

Condition	Cycle #	CELL P-2					CELL N-2				
		ECV (v)	ECR (mΩ)	EDR (mΩ)	CAP (AH)	EFFCY (%)	ECV (v)	ECR (mΩ)	EDR (mΩ)	CAP (AH)	EFFCY (%)
Pre-Ster.	1	1.440	10.42	11.10	2.652	53.5	1.433	10.58	10.78	2.552	51.5
"	2	1.429	10.64	11.11	2.918	58.8	1.430	11.21	10.50	2.584	52.1
"	3	1.438	10.79	10.78	3.066	61.8	1.438	11.06	10.11	2.634	53.1
"	4	1.432	10.42	10.60	2.918	58.8	1.435	10.38	9.86	2.466	49.7
"	5	1.434	10.76	11.06	3.100	62.5	1.434	10.87	10.45	2.684	54.1
"	6	1.440	10.28	11.15	3.484	70.2	1.442	10.20	10.47	2.952	59.5
"	7	1.437	10.37	10.68	3.252	65.6	1.440	10.22	10.16	2.818	56.8
"	8	1.434	10.80	10.30	3.118	62.9	1.441	10.72	9.77	2.734	55.1
"	9	1.442	10.66	10.53	3.200	64.5	1.447	10.47	9.84	2.852	57.5
"	10	1.445	10.62	10.63	3.218	64.9	1.449	10.40	10.00	2.866	57.8
Post-Ster.	1	1.512	9.12	9.86	3.552	71.6	1.507	9.32	10.06	3.534	71.2
"	2	1.482	8.47	9.54	3.500	70.6	1.479	8.72	9.71	3.484	70.2
"	3	1.474	10.25	11.11	3.334	67.2	1.471	10.59	11.28	3.366	67.9
"	4	1.464	20.50	10.72	3.134	63.2	1.459	10.55	10.98	3.200	64.5
"	5	1.493	9.78	11.00	3.166	63.8	1.483	10.00	10.92	3.166	63.8
"	6	1.466	7.07	10.89	3.084	62.2	1.462	7.25	11.14	3.118	62.9
"	7	1.469	10.15	10.74	3.066	61.8	1.465	10.39	10.85	3.100	62.5
"	8	1.464	9.99	11.30	2.966	59.8	1.461	10.23	11.50	3.018	60.8
"	9	1.462	10.04	10.42	3.066	61.8	1.458	10.15	10.55	3.084	62.2
"	10	1.489	10.12	10.83	3.166	63.8	1.481	10.22	10.92	3.200	64.5
"	11	1.457	10.25	10.85	3.118	62.9	1.453	10.32	11.01	3.166	63.8
"	12	1.454	10.11	11.23	3.134	63.2	1.452	10.24	11.21	3.184	64.2
"	13	1.464	9.73	10.95	3.166	63.8	1.461	9.97	10.98	3.200	64.5
"	14	1.470	10.47	10.27	3.084	62.2	1.466	10.37	10.38	3.152	63.5
"	15	1.473	10.08	10.83	3.184	64.2	1.469	10.21	10.86	3.218	64.9
"	16	1.473	11.21	10.26	3.100	62.5	1.469	9.78	10.46	3.166	63.8

zation values. With continued post-sterilization cycling the ECV decreased from highs of 1.512V for Cell P-2 and 1.507V for Cell N-2 to average (Cycles 7-16) of 1.467 and 1.464, respectively, but never attained the pre-sterilization levels of 1.437 and 1.439, respectively. The efficiency of Cell P-2 did drop from a high of 71.6 on the first cycle after sterilization to the pre-sterilization level of 62.3% after 6 cycles. (The average efficiency for Cell P-2 on post-sterilization cycles, 7 through 16, was 62.6%.) However, Cell N-2 achieved a high of 71.2% after sterilization and dropped only to an average (Cycles 7-16) of 63.5 as opposed to its pre-sterilization average (over 10 cycles) of 52.4%. These cells showed far less scatter than that previously observed in the cycled factorial design 17-plate cells. Post-sterilization cycling studies are being continued.

The differences observed between cells with separator nap facing positive or negative plate cells warranted further investigation. Therefore, a number of 17-plate and 18-plate cells with FT2140 separator were constructed such that the nap faced:

     a)   negative plates;

     b)   positive plates;

     c)   both negative and positive plates.

The cells were cycled five times charging at the $C/12.5$ rate to 137% charge level and discharging at the $C/2.5$ rate to a

metallurgical
materials division

1 V cut-off. Following these cycles, the cells were steri-
lized and cycling continued. The results do not show any
marked differences between the various separator-electrode
configurations, but the differences between before and after
sterilization data, and 17-plate and 18-plate cells are sig-
nificant.

A summary of data taken from the fifth cycle before and the
fifth cycle after sterilization is given in Table I-29.
Each entry for a given configuration (e.g. nap facing nega-
tive, 17-plate, pre-sterilization) is an average for the three
cells constructed with that configuration. The average values
for all pre-sterilization 17-plate cells are therefore for a
total of nine cells and all pre-sterilized cells total 18
cells. The post-sterilization values are for the same 18
cells after sterilization. The same trends that were noted
previously are apparent here; that is, ECV, OCV and effi-
ciency all increase upon sterilization. It is also note-
worthy that a very low efficiency of 42.5 occurs for 18-
plate cells prior to sterilization and that the efficiency of
these cells increases to the highest value after steriliza-
tion. Since no marked effect was observed to result from
differences in separator nap configurations, however, this
series of tests was terminated.

Experiments to study the wetting rates of separator materials
were performed as follows: A 1 cm x 25 cm strip of the

TABLE I-29

DATA FROM 5th CYCLE BEFORE & 5th CYCLE AFTER STERILIZATION

Ni-Cd Rectangular Cells 30% KOH, 80% Pore Fill

C.R. = C/12.5   C.L. = 137%   D.R. = C/2.5

Condition	ECV (volts)	OCV (volts)	Effcy. (%)
Nap Facing Neg., 17-Plate, Pre-sterilization	1.421	1.372	66.6
Nap Facing Pos., 17-Plate, Pre-sterilization	1.438	1.376	76.0
Nap Facing Both, 17-Plate, Pre-sterilization	1.425	1.372	61.1
Average of above, 17-Plate, Pre-sterilization	1.428	1.373	67.3
Nap Facing Neg., 18-Plate, Pre-sterilization	1.410	1.368	43.7
Nap Facing Pos., 18-Plate, Pre-sterilization	1.406	1.366	40.3
Nap Facing Both, 18-Plate, Pre-sterilization	1.412	1.369	43.5
Average of Above, 18-Plate, Pre-sterilization	1.409	1.368	42.5
Average of All, Pre-sterilization	1.418	1.371	54.9
Nap Facing Neg., 17-Plate, Post-sterilization	1.496	1.405	73.3
Nap Facing Pos., 17-Plate, Post-sterilization	1.488	1.403	64.6
Nap Facing Both, 17-Plate, Post-sterilization	1.498	1.406	72.6
Average of Above, 17-Plate, Post-sterilization	1.494	1.405	70.2
Nap Facing Neg., 18-Plate, Post-sterilization	1.489	1.411	77.4
Nap Facing Pos., 18-Plate, Post-sterilization	1.485	1.410	76.2
Nap Facing Both, 18-Plate, Post-sterilization	1.481	1.413	75.3
Average of Above, 18-Plate, Post-sterilization	1.485	1.411	76.3
Average of All, Post-sterilization	1.489	1.408	73.2

material under investigation was suspended in a 100 ml graduated cylinder. The lower end of the strip was immersed just below the surface of a reservoir of a 30% potassium hydroxide solution. The distance between the surface of KOH reservoir and the point on the strip to which the electrolyte had risen was measured as a function of time. Since data extended over several orders of magnitude, it is presented as a log-log plot in Figure I-17.

It is immediately apparent from Figure I-17 that all of the "as-received", untreated polypropylene separators show lower rates of absorption than the nylon (Pellon) separator material. Also, the wetting properties of the FT2140 separator are poorer than unsterilized 14019 whether the FT2140 has been sterilized or not. Even though sterilization improves the wetting properties of the FT2140 separator, they are so poor in comparison with nylon that the poor observed performance of the cells is understandable on the basis of this factor alone. Since, however, the FT2140 separator has shown an ability to stand up under sterilization (while nylon and the 14019 polypropylene have not) attempts were made to enhance the wetting properties of the FT2140 material.

Three approaches to the improvement of the FT2140 wetting properties were considered:

metallurgical
materials division

1) Oxidative Surface Treatment of the Separator
   Material;

2) Modification of the Wetting Properties of
   the Electrolyte by Surfactant Addition;

3) Use of Proprietary Treatments on the Separator
   Material.

Oxidative Surface Treatment

Chromic acid oxidative treatments have been reported to modify
the hydrophillic character of the surface and to control the
wettability of polyethylene films. Acetic/sulphuric acid
solutions of dichromate have been shown to effect oxidations
of saturated hydrocarbons.

The wetting properties of Type FT2140 separator, however,
were found to be essentially unaffected by oxidative surface
treatments. This was shown by the results of the following
experiments.

Four solutions were prepared, each consisting of a solution
of 10 ml 2N sodium dichromate/10 ml concentrated sulphuric
acid, added to 90 ml of A) deionized water, B) acetone,
C) acetic acid, D) concentrated sulphuric acid. Solution B
was quickly eliminated because of oxidation of the acetone.
Samples of as-received FT2140 material were immersed at room
temperature for varying periods of time. Following immer-
sion, the samples were leached in deionized water for 1-¼

metallurgical
materials division

hours and then dried at 70°C for 1-½ hours. Absorption rate studies were then performed on the several treated samples.

The results of the absorption studies are listed in Table I-30.

TABLE I-30

Comparison of Wetting Properties of FT2140 Separator with 30% KOH After Various Treatments

Treatment	Immersion Time (Minutes)	Time (Min.) to Reach Height of:		
		0.5 cm	1.0 cm	2.0 cm
None	---	200	400	>400
Steriliza- tion	---	20	44	>44
Sol. A	30	1500	>1500	>1500
Sol. A	60	130	150	200
Sol. A	90	800	1500	>1500
Sol. A	120	1700	>1700	>1700
Sol. C	60	110	160	400
Sol. D	60	290	400	>400

The times required for the 30% potassium hydroxide to rise to a height of 0.5, 1.0 and 2.0 cm in the separator above the reservoir level are given. After 60 minutes' immersion, the treatments with the aqueous and acetic acid Solutions A and C have comparable effects. Treatment with the concentrated chromic acid, Solution D, has no beneficial effect. With Solution A, an optimum immersion time of approximately

metallurgical
materials division

sixty minutes is indicated. However, in comparison with the effects produced by sterilization, the enhancement of the absorption rate by chemical oxidation is not very significant.

Modification of Electrolyte by Surfactant Addition

Absorption studies were carried out with electrolyte solutions (30% KOH) containing various surfactants. The surfactants were chosen for their known ability to remain stable under electrochemical oxidizing or reducing conditions. The electrolyte solutions were prepared as follows.

Five cc of 0.1% surfactant solution were added to 50 cc of 34% KOH giving a resulting solution of 30 to 31% in KOH and .01% in surfactant. The surfactants were:

> Rohm & Haas Triton X-100
>
> 3M Company FC-98
>
> 3M Company FC-128
>
> 3M Company FC-170
>
> 3M Company FC-172
>
> 3M Company FC-176

Of these only Types FC-128 and FC-176 were efficient enough in enhancing the electrolyte wetting properties to warrant further investigation.

Therefore, a series of absorption studies using several concentrations of these two surfactants were performed on FT2140 separator. The experiments were performed on the

separator in the "as-received" condition and after an oxida-
tive pre-treatment. The pre-treatment used was that described
above -- immersing for sixty minutes in a dilute chromic acid
solution (Solution A). As can be seen from Table I-31, the
FC-128 surfactant is most effective in enhancing the wettabil-
ity properties of the FT2140 separator.

TABLE I-31

Effect of Surfactants on Wetting Properties of
As-Received and Pre-Treated FT2140 with 30% KOH

Surfactant	Concentration ppm	FT2140 Pretreat.	Time to Attain a 0.5 cm (min.)	1.0 cm (min.)	Height of 1.5 cm (min.)
None	----	None	200	400	>400
FC-128	100	None	14	80	650
	100	Chromic Acid	2	7	34
	200	None	16	45	200
	200	Chromic Acid	1	5	21
	500	None	1	6	46
	500	Chromic Acid	1	4	21
	Saturated	None	1	4	45
	Saturated	Chromic Acid	1	3	21
FC-176	100	None	300	150	1500
	100	Chromic Acid	100	1000	1000
	200	None	50	120	1000
	200	Chromic Acid	40	130	600
	500	None	40	95	600
	500	Chromic Acid	30	85	500
	1000	None	35	75	300
	1000	Chromic Acid	2	80	500

metallurgical
materials division

Furthermore, the wettability increases concentration of the surfactant, and is ultimately limited only by the solubility of the surfactant in 30% KOH. The solubility limit is only slightly higher than 500 ppm. Again it can be seen that the oxidation treatment of the separator offers only a slight improvement of the wetting properties.

The effect of 500 ppm additions of the FC-128 and the FC-176 surfactants on cell operational behavior was studied. Four groups of five 18-plate cells each were constructed:

Group (1) Control -- no surfactant, no oxidative treatment of FT2140 separator;

Group (2) Chromic Acid Treatment -- No surfactant;

Group (3) 500 ppm FC-128 added -- no chromic acid treatment;

Group (4) 500 ppm FC-176 added -- no chromic acid treatment.

Following sterilization, one of the control and one of the FC-128 cells failed to accept charge, probably due to the development of an internal short. During this period, the cells were subjected to twelve pre-sterilization cycles, 12.5 hour charge rate to 137% charge input level, discharge at the 2.5 hour rate to the 1.0V cut-off. Representative data after various cycles is shown in Table I-32. The average parameter values for the five cells, and the standard deviations, are given. The discharge voltage data are shown at

I-105

TABLE I-32

EFFECT OF SURFACTANT ADDITION AND SEPARATOR PRETREATMENT ON CELL OPERATIONAL BEHAVIOR

Ni-Cd, 18-Plate Cells. FT2140 Separator. 30% KOH. 30% Pore Fill Level

C.R. = C/12.5   C.L. = 137%   D.R. = C/2.5

PRE-STERILIZATION DATA

Cell Group	Cycle #	E.C.V. (v) Av.	σ	O.C.V. (v) Ave.	σ	25% Av.	σ	50% Av.	σ	75% Av.	σ	E.C.R.(mΩ) Av.	σ	E.D.R.(mΩ) Av.	σ	Cap.(AH) Av.	σ	Effcy (%) Av.	σ
Control	2	1.416	0.002	1.385	0.001	1.257	0.002	1.244	0.003			12.21	0.71	11.72	0.73	3.140	0.156	63.3	3.1
Pretreat	"	1.414	0.002	1.384	0.001	1.270	0.001	1.257	0.002			10.08	0.25	10.50	0.35	3.580	0.086	72.2	1.7
FC-128	"	1.410	0.001	1.381	0.001	1.269	0.002	1.254	0.001			10.19	0.68	11.92	0.97	3.317	0.082	66.9	1.7
FC-176	"	1.414	0.003	1.384	0.001	1.267	0.004	1.252	0.004			10.85	0.40	11.12	0.35	3.354	0.175	67.6	3.5
Control	5	1.421	0.004	1.379	0.002	1.259	0.004	1.229	0.009	1.188	0.037	11.17	1.06	11.86	1.10	2.640	0.235	53.2	4.7
Pretreat	"	1.425	0.002	1.383	0.002	1.270	0.002	1.250	0.003	1.223	0.007	9.69	0.38	10.34	0.22	3.364	0.173	67.8	3.5
FC-128	"	1.418	0.002	1.379	0.001	1.267	0.002	1.242	0.002	1.167	0.040	10.16	0.66	10.67	0.85	2.831	0.069	57.1	1.4
FC-176	"	1.422	0.004	1.380	0.001	1.265	0.004	1.241	0.005	1.192	0.022	10.24	0.33	11.34	0.45	2.827	0.153	57.0	3.1
Control	7	1.431	0.005	1.379	0.003	1.256	0.004	1.231	0.010	1.175	0.051	12.72	0.98	12.42	1.36	2.958	0.276	59.6	5.6
Pretreat	"	1.436	0.003	1.383	0.003	1.268	0.001	1.255	0.002	1.242	0.003	9.30	0.37	9.79	0.26	3.627	0.210	73.1	4.2
FC-128	"	1.435	0.001	1.382	0.001	1.268	0.002	1.252	0.002	1.232	0.003	10.24	0.85	11.70	1.17	3.167	0.061	63.9	1.2
FC-176	"	1.436	0.002	1.381	0.003	1.262	0.004	1.246	0.006	1.226	0.012	10.26	1.16	10.66	1.10	3.104	0.221	62.6	4.5
Control	9	1.425	0.006	1.379	0.003	1.261	0.006	1.238	0.010	1.187	0.049	11.90	1.40	13.98	1.76	2.843	0.281	57.3	5.7
Pretreat	"	1.432	0.002	1.387	0.002	1.275	0.001	1.259	0.002	1.241	0.003	9.67	0.30	10.48	0.29	3.811	0.124	76.8	2.5
FC-128	"	1.423	0.002	1.380	0.002	1.272	0.002	1.248	0.002	1.222	0.003	10.38	1.03	10.98	1.13	3.109	0.073	62.7	1.5
FC-176	"	1.428	0.004	1.382	0.002	1.270	0.005	1.247	0.005	1.221	0.011	10.76	0.99	11.18	0.95	3.138	0.283	63.3	5.7
Control	11	1.425	0.006	1.374	0.003	1.259	0.007	1.236	0.011	1.197	0.027	12.20	1.64	12.77	2.09	2.864	0.291	57.7	5.9
Pretreat	"	1.431	0.002	1.382	0.001	1.272	0.003	1.255	0.004	1.231	0.006	9.65	0.38	9.69	0.28	3.794	0.176	76.5	3.5
FC-128	"	1.422	0.002	1.376	0.001	1.270	0.002	1.246	0.003	1.207	0.007	10.64	1.12	11.33	1.17	3.146	0.089	63.4	1.8
FC-176	"	1.428	0.004	1.377	0.002	1.266	0.004	1.242	0.007	1.210	0.011	10.27	0.87	10.64	0.96	3.237	0.307	65.3	5.2

Cell Voltage at Various D. of D. (v) — columns 25%, 50%, 75%

25%, 50%, and 75% depth-of-discharge, based upon the average
capacity delivered in the first cycle. These data show that,
prior to sterilization, those cells employing pre-treated
FT2140 as separator yield the highest delivered capacity,
above 75% of theoretical formation capacity after eight
cycles. It is to be noted that such efficiency is significantly greater than has been achieved in the pre-sterilization stage with polypropylene separators up to this time.
Furthermore, it is to be noted that these cells exhibit the
lowest end-of-charge, and end-of-discharge resistances, with
the least amount of scatter. Although the "pre-treated"
cells yielded the greatest capacity, it is to be noted that
those cells containing the FC-128 surfactant showed the
least amount of scatter in the efficiency data. Following
sterilization, the four groups of cells were cycled according
to the same charge-discharge routine. The post-sterilization
data for the first four cycles are shown in Table I-33. The
high end-of-charge and open-circuit voltages are again in
evidence. The efficiency for all four groups of cells
increases noticeably after sterilization. Post-sterilization
data for Cycles 5, 10, 15, 20 and 25 are shown in Table I-34A
and I-34B. All of the cells in the control and pre-treated
group leaked on cycles immediately after sterilization. The
leaks disappeared after changing the "O" rings on the vent
seals, but some loss of electrolyte resulted in low capacity
in these cells. Eighteen-plate sterilized cells normally

metallurgical
materials division

TABLE I-33

EFFECT OF SURFACTANT ADDITION AND SEPARATOR PRETREATMENT ON CELL OPERATIONAL BEHAVIOR

Ni-Cd, 18-Plate Cells   FT2140 Separator   30% KOH   80% Pore Fill Level
C.R. = C/12.5   C.L. - 137%   D.R. = C/2.5

POST-STERILIZATION DATA

Cell Group	Cycle #	E.C.V. (v) Av.	σ	O.C.V. (v) Av.	σ	Cell Voltage at Various D. of D. (v) 25% Av.	σ	50% Av.	σ	75% Av.	σ	E.C.R.(ma) Av.	σ	E.D.R.(ma) Av.	σ	Cap.(AH) Av.	σ	Effcy.(%) Av.	σ
Control	1	1.505	0.002	1.415	0.001	1.247	0.002	1.242	0.002	1.228	0.005	11.50	0.70	11.76	0.93	3.680	0.257	74.2	5.2
Pretreat	"	1.503	0.001	1.415	0.001	1.254	0.005	1.246	0.003	1.235	0.006	9.53	0.25	10.31	0.29	3.472	0.237	70.0	4.8
FC-128	"	1.497	0.002	1.413	0.001	1.252	0.001	1.247	0.000	1.238	0.001	10.30	0.45	10.32	0.51	4.051	0.065	81.7	1.3
FC-176	"	1.504	0.003	1.413	0.002	1.255	0.006	1.245	0.004	1.235	0.008	10.30	0.55	11.21	0.66	3.688	0.275	74.4	5.5
Control	2	1.486	0.004	1.414	0.001	1.250	0.001	1.243	0.002	1.220	0.008	11.50	0.79	13.06	0.79	3.738	0.271	75.4	5.5
Pretreat	"	1.493	0.005	1.418	0.002	1.252	0.003	1.246	0.004	1.223	0.009	10.96	0.30	10.42	0.57	3.560	0.246	71.8	5.0
FC-128	"	1.486	0.003	1.414	0.001	1.255	0.001	1.252	0.001	1.239	0.002	10.46	0.42	11.10	0.58	4.067	0.082	82.0	1.6
FC-176	"	1.501	0.005	1.419	0.003	1.252	0.001	1.247	0.004	1.229	0.012	12.00	0.94	10.79	0.94	3.907	0.308	78.8	6.2
Control	3	1.473	0.004	1.405	0.003	1.256	0.001	1.247	0.002	1.221	0.011	11.81	0.63	13.51	1.12	3.517	0.282	70.9	5.7
Pretreat	"	1.474	0.004	1.404	0.003	1.256	0.003	1.246	0.006	1.219	0.013	10.73	0.89	10.43	0.36	3.620	0.247	73.0	5.0
FC-128	"	1.476	0.003	1.407	0.002	1.259	0.000	1.243	0.002	1.243	0.002	10.56	0.34	10.35	0.57	3.858	0.126	77.8	2.5
FC-176	"	1.489	0.005	1.409	0.005	1.256	0.001	1.248	0.005	1.230	0.013	11.49	0.84	10.82	1.06	4.107	0.342	82.8	6.9
Control	4	1.470	0.004	1.389	0.019	1.259	0.002	1.249	0.004	1.217	0.013	11.96	1.38	11.44	0.54	3.288	0.308	66.3	6.2
Pretreat	"	1.472	0.006	1.407	0.004	1.262	0.001	1.256	0.004	1.226	0.013	10.85	0.42	10.02	0.47	3.251	0.240	65.5	4.8
FC-128	"	1.482	0.004	1.416	0.001	1.263	0.001	1.261	0.000	1.247	0.002	10.97	0.34	12.69	0.80	4.013	0.117	80.9	2.4
FC-176	"	1.488	0.004	1.413	0.004	1.260	0.002	1.256	0.003	1.237	0.012	12.14	0.92	10.87	0.84	3.758	0.314	75.8	6.3

TABLE I-34A

EFFECT OF SURFACTANT ADDITION AND SEPARATOR PRETREATMENT ON CELL OPERATIONAL BEHAVIOR

POST-STERILIZATION DATA

Ni-Cd, 18-Plate Cells   FT2140 Separator   30% KOH 80% Pore Fill Level
C.R. = C/12.5   C.L. = 137%   D.R. = C/2.5

		ECV(v)		OCV(v)		Cell Voltage at Various D. of D. (v) 25%		50%		75%		ECR(mΩ)		EDR(mΩ)		Cap.(AH)		Effcy(%)	
Cycle	Group	Av.	S	Av.	S	Av.	S	Av.	S	Av.	S	Av.	S	Av.	S	Av.	S	Av.	S
5	Control	1.452	.003	1.399	.003	1.264	.001	1.249	.004	1.218	.013	11.95	0.63	11.80	1.06	3.183	.302	64.2	6.1
5	Pretreat	1.447	.007	1.395	.003	1.267	.003	1.258	.005	1.225	.012	10.58	0.51	10.60	0.56	3.364	.232	67.8	4.7
5	FC128	1.451	.004	1.399	.002	1.269	.001	1.264	.001	1.252	.002	11.16	0.63	11.64	0.68	4.203	.130	84.3	2.3
5	FC176	1.458	.003	1.400	.004	1.267	.002	1.260	.004	1.240	.011	11.63	0.87	11.73	1.49	3.737	.233	75.3	5.7
10	Control	1.452	.004	1.390	.002	1.264	.001	1.254	.002	1.224	.009	12.26	0.94	11.50	0.72	3.075	.250	62.0	5.1
10	Pretreat	1.460	.005	1.387	.003	1.269	.003	1.260	.007	1.233	.013	10.79	1.03	10.66	0.82	3.160	.335	63.7	6.8
10	FC128	1.455	.003	1.393	.002	1.271	.002	1.265	.002	1.243	.005	10.77	0.73	10.67	0.63	3.713	.175	74.9	2.5
10	FC176	1.456	.002	1.392	.003	1.269	.003	1.262	.004	1.245	.010	11.19	1.22	11.88	1.45	3.644	.311	73.5	6.3
15	Control	1.478	.005	1.407	.003	1.266	.001	1.257	.002	1.229	.007	11.84	0.34	14.39	0.60	3.234	.215	65.2	4.3
15	Pretreat	1.430	.004	1.404	.003	1.270	.003	1.261	.005	1.233	.015	10.97	0.58	11.96	1.40	3.393	.365	68.5	7.4
15	FC128	1.473	.003	1.407	.001	1.271	.002	1.267	.002	1.255	.003	11.22	0.91	11.40	0.02	3.867	.166	78.0	3.3
15	FC176	1.481	.003	1.407	.003	1.269	.003	1.263	.004	1.246	.009	11.63	1.55	13.47	2.61	3.810	.315	76.6	6.3
20	Control	1.467	.003	1.386	.002	1.267	.002	1.258	.002	1.231	.007	11.59	0.78	13.65	0.73	3.203	.171	64.7	3.4
20	Pretreat	1.466	.003	1.387	.003	1.271	.006	1.261	.009	1.239	.016	11.10	2.06	10.23	1.77	3.331	.335	66.2	6.7
20	FC128	1.472	.003	1.395	.002	1.271	.003	1.267	.002	1.260	.002	10.42	0.78	10.91	0.73	3.871	.177	78.0	3.6
20	FC176	1.470	.001	1.391	.003	1.267	.003	1.260	.003	1.244	.010	12.75	3.76	12.17	3.66	3.804	.314	76.7	6.3
25	Control	1.472	.002	1.410	.000	1.265	.002	1.255	.002	1.229	.004	13.74	1.56	13.61	1.99	3.159	.135	63.7	2.3
25	Pretreat	1.480	.003	1.416	.002	1.271	.005	1.261	.007	1.240	.014	11.60	1.53	10.93	0.93	3.430	.322	69.2	5.6
25	FC128	1.472	.002	1.416	.002	1.275	.001	1.269	.002	1.252	.004	11.10	0.72	13.84	1.15	4.051	.155	81.7	3.1
25	FC176	1.478	.001	1.417	.003	1.268	.009	1.260	.009	1.244	.011	13.33	4.42	13.24	3.86	3.817	.295	77.0	5.9

TABLE I-34B.

COMPARISON OF CELLS WITH AND WITHOUT SURFACTANT ADDITION

POST-STERILIZATION DATA

Ni-Cd, 18-Plate Cells   FT2140 Separator   30% KOH 80% Pore Fill Level
  C.R. = C/12.5   C.I. - 137%   D.R. = C/2.5

	Group	n	ECV(v) Av.	S	OCV(v) Av.	S	Cell Voltage at Various D. of D. (v) 25% Av.	S	50% Av.	S	75% Av.	S	ECR(mΩ) Av.	S	EDR(mΩ) Av.	S	Cap.(AH) Av.	S	Effcy(%) Av.	S
25	"B"	3	1.487	.002	1.411	.002	1.264	.012	1.254	.012	1.238	.012	17.75	9.57	16.67	6.61	4.085	.125	82.4	2.
25	FC128	4	1.472	.002	1.416	.002	1.275	.001	1.269	.002	1.252	.004	11.10	0.72	13.84	1.15	4.051	.155	81.7	3.
25	FC176	4	1.478	.001	1.417	.003	1.268	.009	1.260	.009	1.244	.011	13.33	4.42	13.24	3.86	3.817	.295	77.0	5.
25	*	2	1.487	.002	1.411	.001	1.273	.005	1.263	.005	1.246	.006	10.99	0.20	11.99	0.48	4.018	.200	81.0	4.

* Group "B" cells without the cell with high resistance.

yield 4.0 AH, while these two groups yielded 3.0 to 3.4 AH. Since there appears to be little improvement in general with the surfactant addition or separator pre-treatment on cell performance after sterilization, no further work was carried out with these surfactants or pre-treatments. The addition of FC-128 does show some improvement in the capacity. However, the data are not statistically significant to draw firm conclusions.

Other Treatment of Separator Material

Samples of FT2140 separator material were sent to RAI Research Corporation, New York, and Southwest Research Institute (SRI), San Antonio, Texas, to be given their respective irradiation treatments to improve the surface wetting properties. In Table I-35 are shown some pertinent physical properties of the as-received and treated materials. The FT2140 polypropylene treated by the Southwest Research Institute presents a drastic change in appearance from the original material. Even the mildest treatment results in a 10% shrinkage in the cross-fibre direction, a marked increase in the thickness and in the mass per unit area. Although this treatment enhances the KOH electrolyte pickup, only the most severe treatment results in an increase in the absorption rate, which, however, is not too significant. On the other hand, the RAI treated FT2140 exhibits greatly enhanced wettability properties, without any marked change on the other physical properties of the material.

metallurgical
materials division

TABLE I-35

PHYSICAL PROPERTIES OF AS-RECEIVED AND TREATED FT2140 POLYPROPYLENE SEPARATOR

Sample	Mass/Unit Area (gm/in.^{2})	Thickness (in.)	Shrinkage	KOH Pick-up (gm KOH/gm Sep)	Time(min) to Attain a Height of:		
					0.5 cm	1.0 cm	2.5 cm
As-Received	0.044	0.0075		-	200	400	>400
RAI Treatment	0.047	0.0090	None	2.54	0.2	0.5	1.7
SWRI Treatment* 1	0.102	0.023	~10%	4.79	100	340	>24 hrs
" " 2	0.096	0.022	"	3.46	160	700	>24 hrs
" " 3	0.073	0.018	"	3.61	650	1290	>24 hrs

* Southwest Research Institute - Treatment 1 - Most severe
                                        "   2 - Intermediate severity
                                       "   3 - Least severe

Two rectangular, 18-plate cells, incorporating RAI-treated

FT2140 separator have been prepared and cycled 11 times. The

data tabulated in Table I-36 show only one significant effect

of the RAI treatment. The pressure developed during over-

charge is greater than in the control cell. This is under-

standable since the treatment reduces the effective porosity

of the material, resulting in greater resistance to oxygen

diffusion from the positive to the negative plate and its

recombination rate during overcharge. Other effects of the

RAI treatment on the cell performance are all minor. Post-

sterilization cycling data for RAI treated and control cells

are given in Table I-37. The results obtained do not war-

rant any further work with RAI treated separator.

TABLE I-36

Effect of RAI Treated Separator

PRE-STERILIZATION.

Ni-Cd   18 Plates   FT2140 Separator   30% KOH   80% Pore Fill

C.R. = C/12.5

C.L. = 137%

D.R. = C/2.5

Separator	Cell #	Cycle #	ECV volts	ECR mΩ	EDR mΩ	ECP psia	EDP psia	ECC A.H.	EFF. %
RAI	1	1	1.427	10.96	12.31	65.7	34.7	3.066	61.8
RAI	2	1	1.426	10.79	12.12			3.084	62.2
Control	1	1	1.445	10.51	12.46	23.7	<14.7	3.384	68.2
Control	2	1	1.443	10.53	12.17			3.300	66.5
RAI	1	6	1.442	11.02	10.58	134.7	<14.7	2.800	56.5
RAI	2	6	1.445	10.71	10.42			2.918	58.8
Control	1	6	1.438	11.41	11.37	46.7	<14.7	2.818	56.8
Control	2	6	1.436	11.04	11.13			2.100	42.3
RAI	1	11	1.476	11.11	11.65	154.7	40.7	3.800	76.6
RAI	2	11	1.482	10.82	11.22			4.100	82.7
Control	1	11	1.463	11.71	13.26	86.7	<14.7	3.800	76.6
Control	2	11	1.474	11.69	12.23			3.952	79.7

metallurgical
materials division

TABLE I-36 (Cont'd.)

Effect of RAI Treated Separator

PRE-STERILIZATION

Ni-Cd   18 Plate   FT2140 Separator   30% KOH   80% Pore Fill

$$C.R. = C/12.5$$

$$C.L. = 137\%$$

$$D.R. = C/2.5$$

Separator Type	Cell #	Cycle #	ECV Volts	ECR m Ω	EDR m Ω	ECP psia	EDP psia	ECC AH	Effcy. %
RAI	1	12	1.433	10.72	11.14	114.7	14.7	3.652	73.6
RAI	2	12	1.435	10.40	10.77			3.934	79.3
Control	1	12	1.432	9.94	12.41	82.7	14.7	3.634	73.3
Control	2	12	1.436	10.28	11.69			3.887	78.3
RAI	1	16	1.455	12.22	12.55	134.7	42.7	3.852	77.7
RAI	2	16	1.454	11.43	11.78			3.984	80.3
Control	1	16	1.461	13.71	15.02	42.7	14.7	4.166	84.0
Control	2	16	1.454	12.90	13.00			4.034	81.3
RAI	1	20	1.437	11.41	15.00	118.7	44.7	3.566	71.9
RAI	2	20	1.433	10.67	14.11			3.800	76.6
Control	1	20	1.441	12.34	19.03	54.7	44.7	4.000	80.6
Control	2	20	1.441	12.00	15.42			4.000	80.6
RAI	1	24	1.429	12.26	13.66	118.7	52.7	3.584	72.3
RAI	2	24	1.430	11.31	12.69			3.934	79.3
Control	1	24	1.435	12.77	19.44	52.7	44.7	3.934	79.3
Control	2	24	1.431	12.49	14.23			4.052	81.7
RAI	1	29	1.451	11.78	13.14	124.7	67.7	3.918	79.0
RAI	2	29	1.441	10.89	12.10			4.016	81.0
Control	1	29	1.449	12.55	18.01	48.7	14.7	4.084	83.7
Control	2	29	1.447	11.95	13.30			4.152	81.5

metallurgical
materials division

TABLE I-37

Effect of RAI Treated Separator

POST STERILIZATION

Ni-Cd   18 Plate   FT2140 Separator   30% KOH   80% Pore Fill

C.R. = C/12.5   C.L. = 137%   D.R. = C/2.5

Separator Type	Cell #	Cycle #	ECV Volts	ECR mΩ	EDR mΩ	ECP psia	EDF psia	ECC AH	Effcy. %
RAI	2	1	1.496	11.65	11.14	--	--	3.434	69.2
Control	1	1	1.503	15.45	19.94	54.7	--	3.084	62.2
Control	2	1	1.499	16.18	15.22	--	--	3.152	63.5
RAI	2	3	1.477	11.12	11.19	54.7	14.7	3.200	64.5
Control	1	3	1.473	13.04	15.46	104.7	18.7	2.700	54.4
Control	2	3	1.515	16.66	17.26	--	--	2.852	57.5
RAI	2	7	1.465	9.44	11.90	94.7	14.7	2.984	60.2
Control	1	7	1.471	10.52	16.69	104.7	25.7	2.556	51.7
Control	2	7	1.479	15.38	19.53	--	--	3.100	62.5
RAI	2	15	1.471	10.79	11.38	81.7	14.7	3.352	67.6
Control	1	15	1.475	11.69	16.96	97.7	24.7	2.852	57.5
Control	2	15	1.492	16.70	20.52	--	--	3.666	73.9
RAI	2	25	1.464	--	10.65	73.7	14.7	3.518	70.9
Control	1	25	1.460	--	19.20	75.7	19.7	2.934	59.2
Control	2	25	1.459	--	18.37	--	--	3.518	70.9
RAI	2	35	1.469	11.58	12.34	68.7	14.7	3.634	73.3
Control	1	35	1.463	12.03	23.38	67.7	21.7	3.000	60.5
Control	2	35	1.465	24.94	31.09	--	--	3.584	72.3
RAI	2	45	1.468	11.62	12.26	62.7	14.7	3.684	74.3
Control	1	45	1.459	12.31	24.86	58.7	18.7	3.084	62.2
Control	2	45	1.463	24.46	42.02	--	--	3.652	73.6
RAI	2	55	1.471	12.04	11.36	59.7	14.7	3.752	75.6
Control	1	55	1.457	12.63	22.66	56.7	18.7	3.118	62.9
Control	2	55	1.467	31.06	32.59	--	--	3.684	74.3

metallurgical
materials division

J. <u>Physico-Chemical Characterization of Cell Components: Effect of Sterilization</u>

Optical Microscopy of the Plates:

The purpose of this phase of the investigation was to determine what visible changes occurred in the plates as a result of heat sterilization. Since nickel metal is known to corrode in alkaline media under certain anodic conditions and/or at elevated temperatures according to the reaction:

$$Ni + 2OH^- \longrightarrow Ni(OH)_2 + 2e^-$$
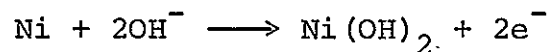
both the nickel mesh and sintered nickel are subject to attack. In fact, during the manufacturing process of the positive plate a noticeable proportion of the nickel sinter is attacked. This reaction is accelerated by temperature and thus the heat sterilization process (with the positive and negative electrodes short circuited) may cause a further attack of the substrate. This would result in a loss of some strength and electronic conductivity of the plate and lower utilization of active material (loss in capacity).

To determine these possible effects, both the positive and negative plates were examined by optical microscopy in various stages. The plate conditions included:

1) As-received from the manufacturing process;

2) After cycling in a sealed cell;

3) After heat sterilization;

4) After heat sterilization and cycling in a sealed cell.

metallurgical
materials division

In Figures I-18 through I-21 the full cross sections of the

positive and negative plates are shown. These views include:

1) The longitudinal and cross-sectional areas of

   the woven nickel mesh support;

2) The sintered nickel substrate (white areas);

3) The porous active material (gray and black

   areas).

These cross sections show visible changes, notably in the

positive electrode. The texture and coloring of the positive

active material undergoes several transformations. After

sterilization the positive (nickel oxide) plate has a blue-

gray coloration (appears gray in the photo-micrographs) as

opposed to the normal black color. The negative (cadmium)

electrode also undergoes a change in coloration from dark to

a light gray. These color, shade and texture changes are

more readily visible in Figures I-22 through I-25 which were

taken at a higher magnification. These figures (I-18 through

I-25) show no appreciable loss in the nickel sinter structure

through corrosion.

Since corrosion quite often occurs at grain boundaries,

these samples were etched to show the microstructure of the

nickel wire grid. Photographs of these samples are shown in

Figures I-26 through I-29. There is some evidence of grain

boundary attack of the wire as shown in Figure I-26. This

slight intergranular corrosion occurred in the manufacturing

metallurgical
materials division

.The cross-section photomicrographs of positive and

negative plate materials at various stages before and

after heat-sterilization treatment are shown in the

following pages, I-119 through I-130.

metallurgical
materials division

FIGURE I-18

AS MANUFACTURED
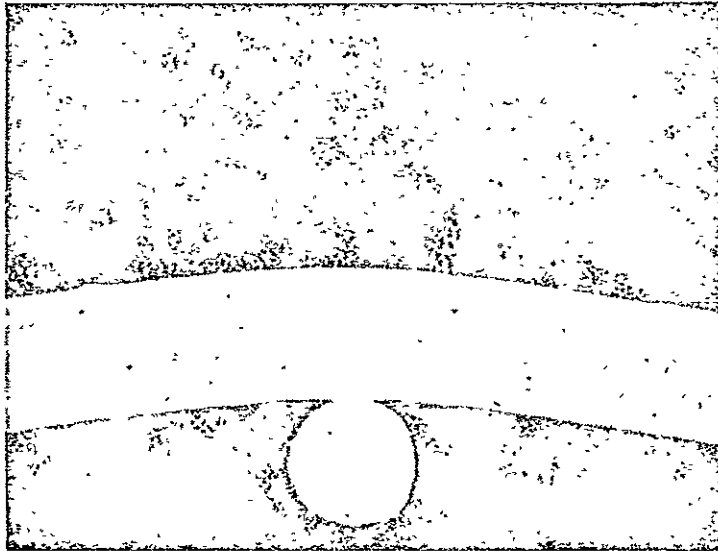
POS 68   MAG. 100X
AS POLISHED
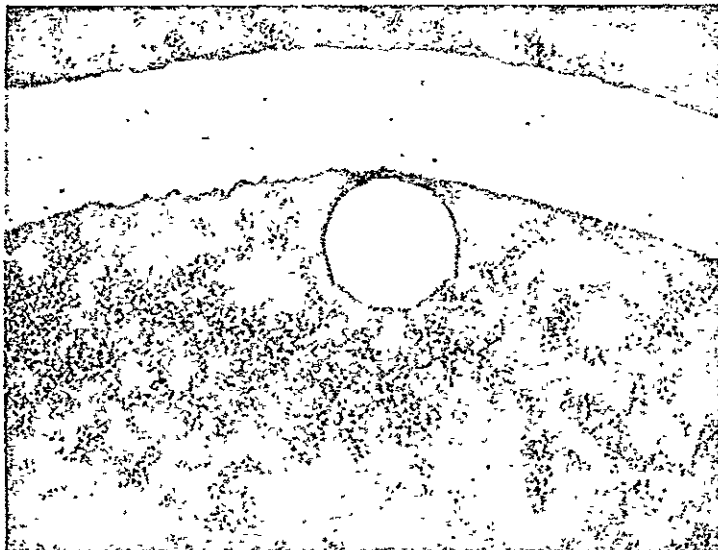
NEG 85   MAG. 100X
AS POLISHED
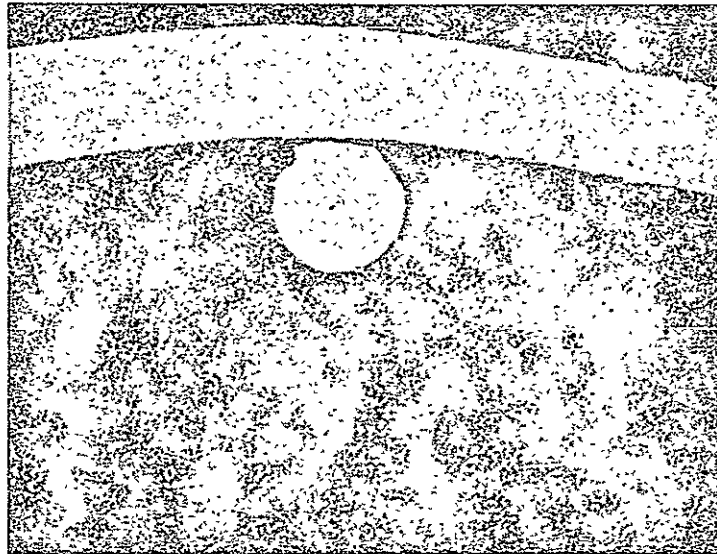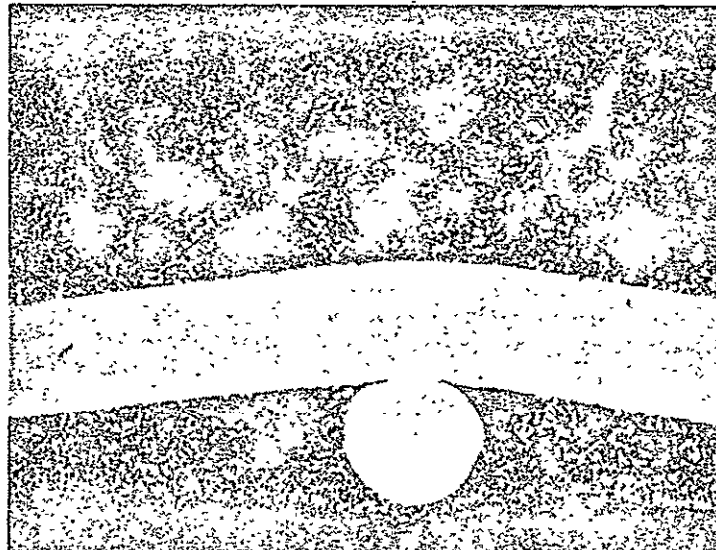
FIGURE I-19

CYCLED PRE-STERILIZED

POS 68 100X MAG.
AS POLISHED

NEG 85 100X MAG.
AS POLISHED

FIGURE I-2Q
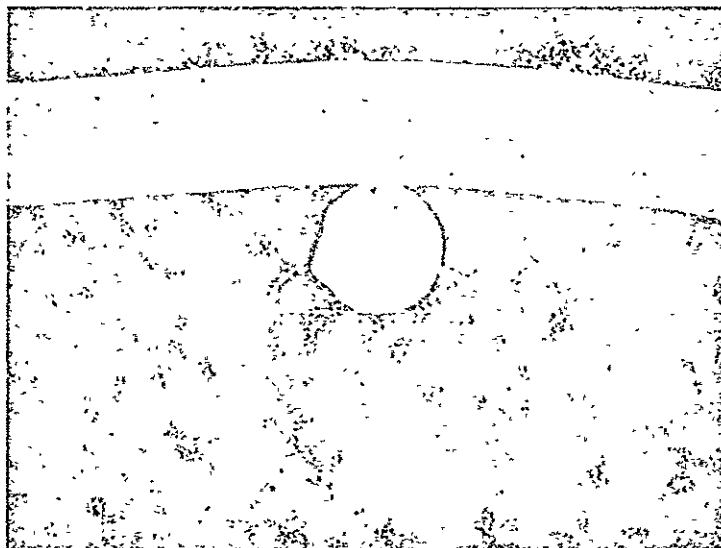
STERILIZED

POS 68   100X MAG.
AS POLISHED
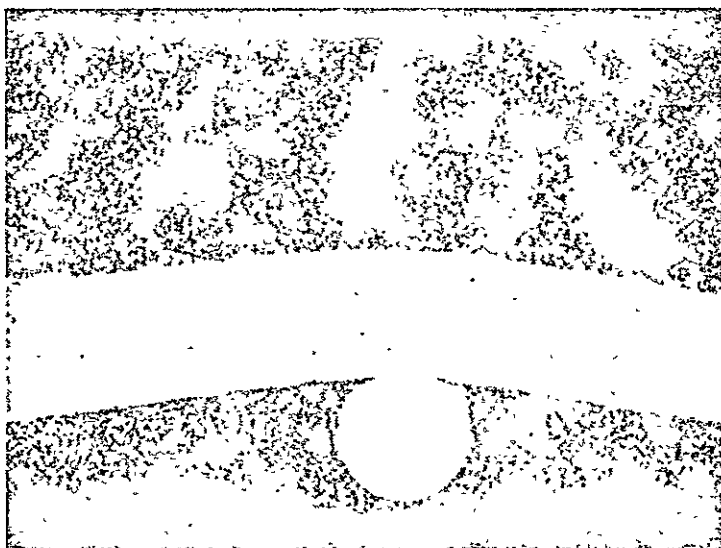
NEG 85   100X MAG.
AS POLISHED

FIGURE I-21

STERILIZED & CYCLED
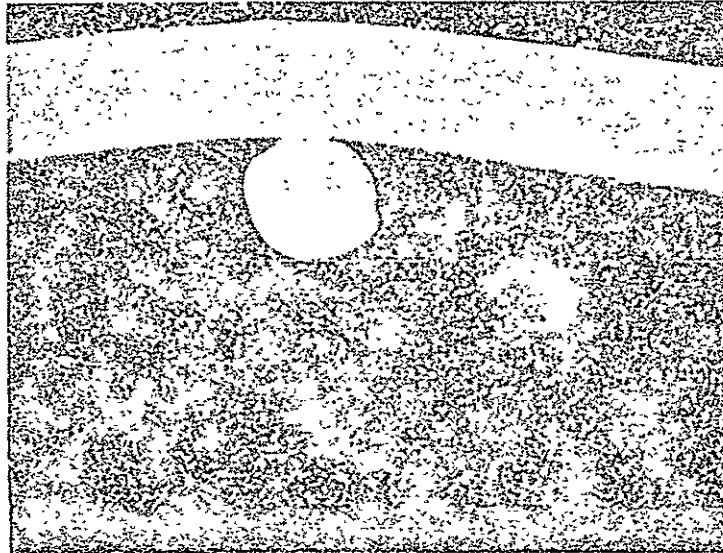
POS 68 500X MAG.
AS POLISHED
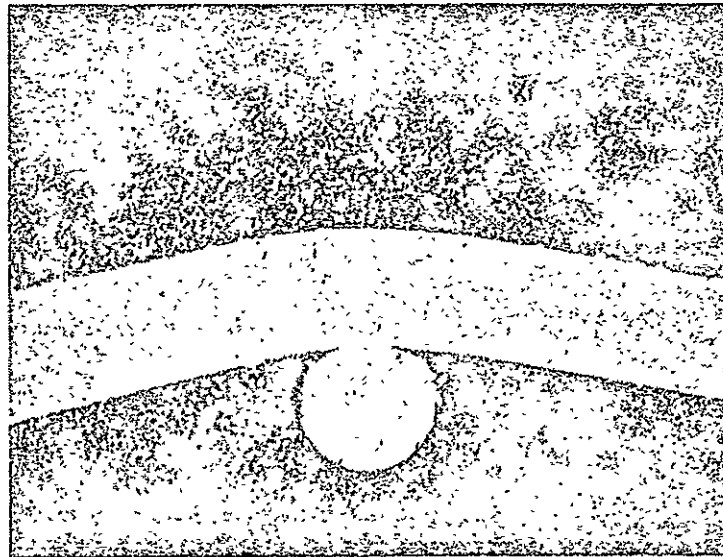
NEG 85 500 X MAG.
AS POLISHED

FIGURE I-22

AS MANUFACTURED
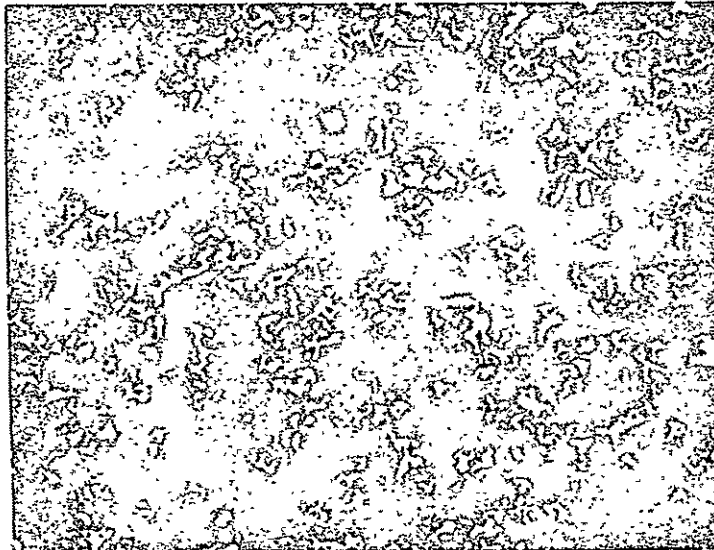
AS POLISHED
POS 68   MAG. 250X
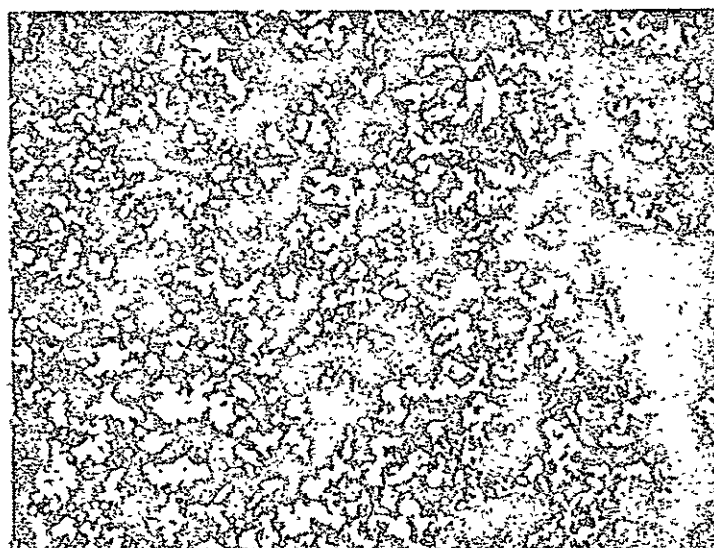
AS POLISHED
NEG 85   MAG. 250X

FIGURE I-23

CYCLED PRE-STERILIZED
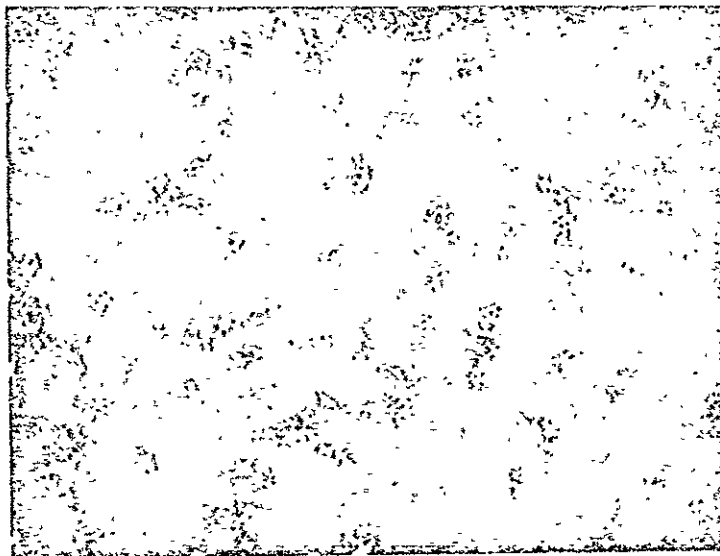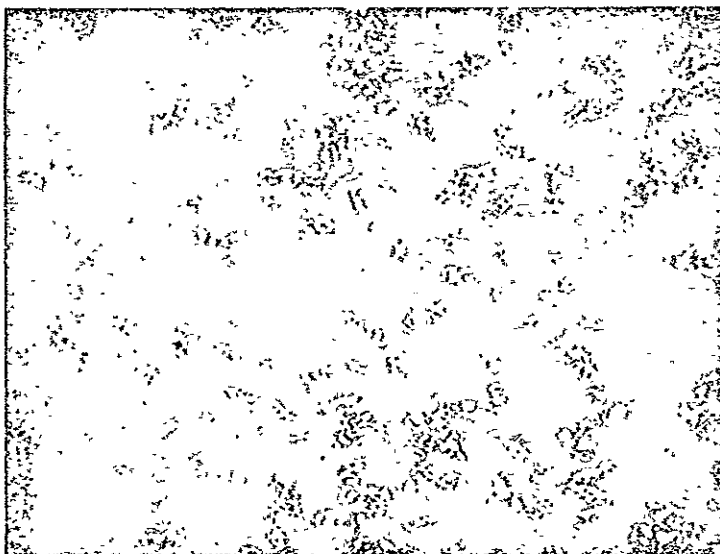
POS 68   250X MAG.
AS POLISHED

NEG 85   250X MAG.
AS POLISHED

FIGURE I-24
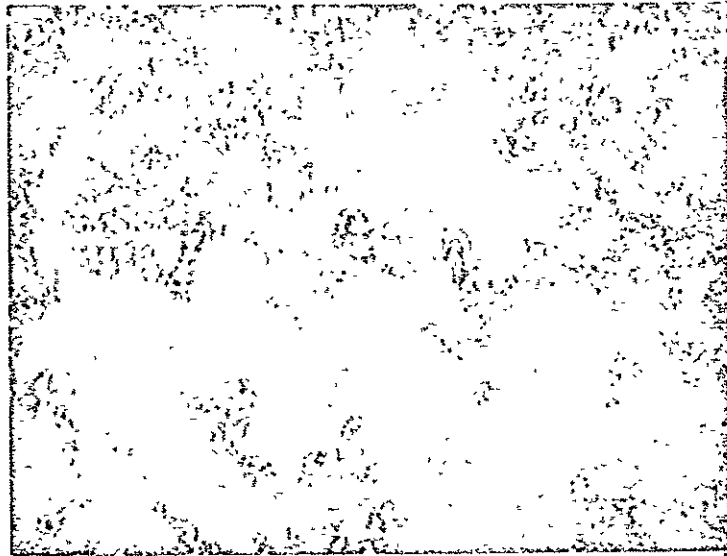
STERILIZED

POS 68 250X MAG.
AS POLISHED
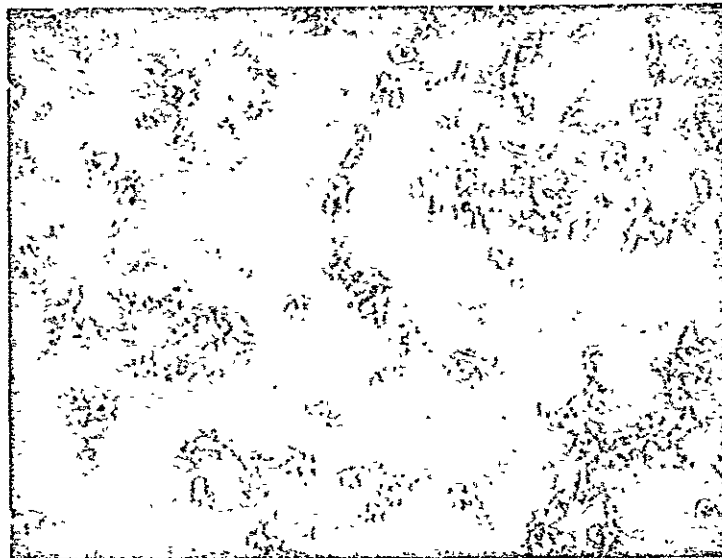
NEG 85 250X MAG.
AS POLISHED

FIGURE I-25

STERILIZED & CYCLED
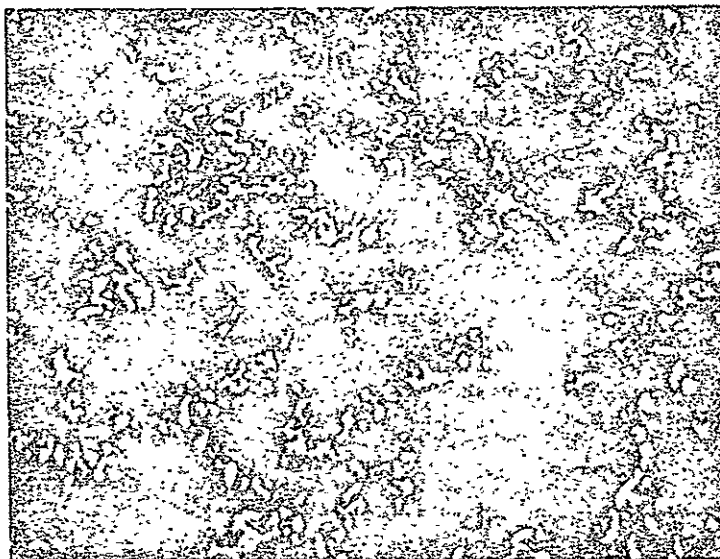
POS 68 250X MAG.
AS POLISHED
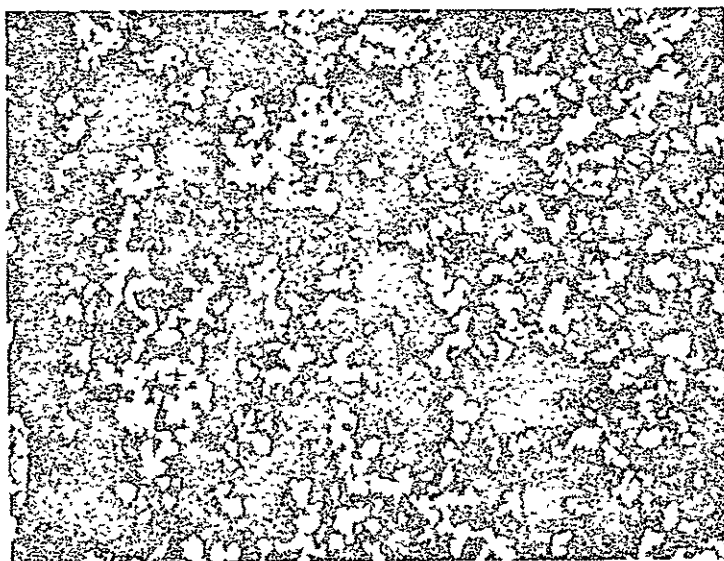
NEG 85 250X MAG.
AS POLISHED

FIGURE I-26

AS MANUFACTURED

POS 68   MAG. 100X
ETCHED
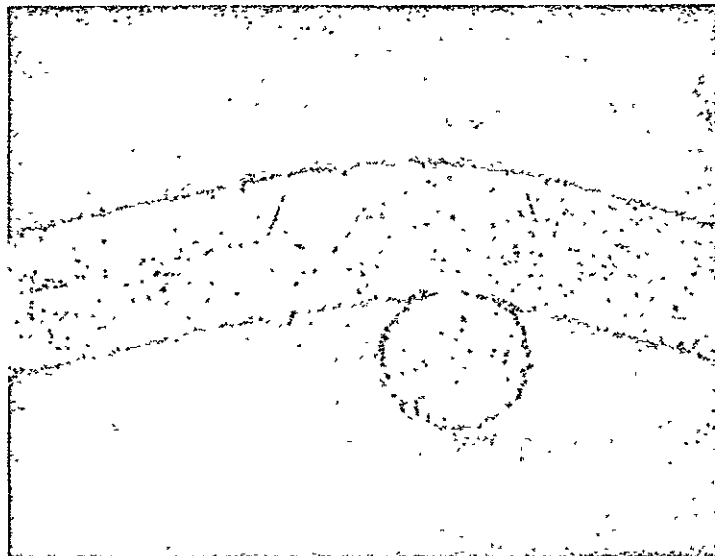
NEG 85   MAG. 100X
ETCHED

FIGURE I-27

CYCLED PRE-STERILIZED
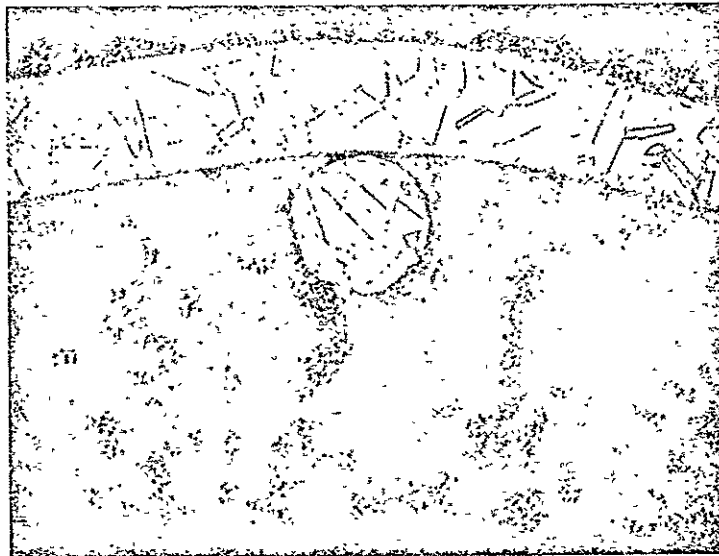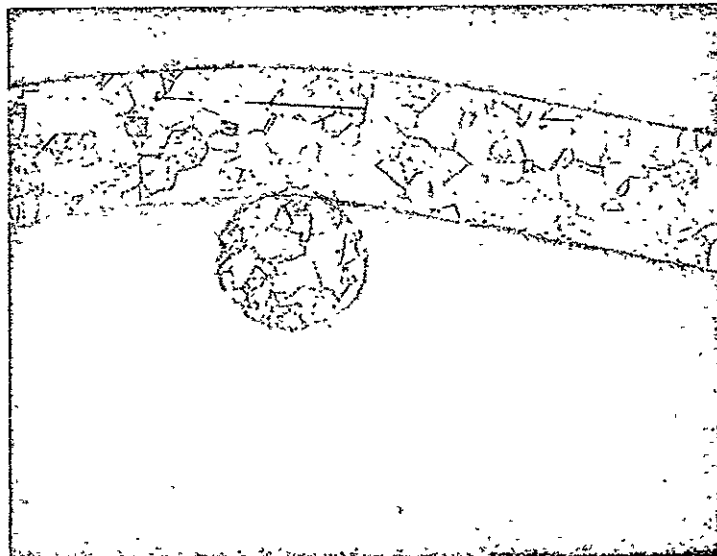
POS 68   100X MAG.
ETCHED
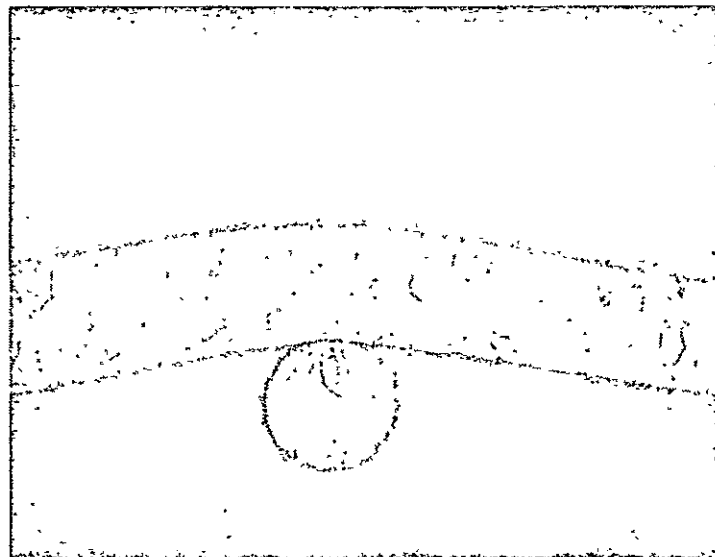
NEG 85   100X MAG.
ETCHED

FIGURE I-28

STERILIZED

POS 68   100X MAG.

ETCHED

NEG 85   100X MAG.

ETCHED

I-129

FIGURE I-29

STERILIZED & CYCLED
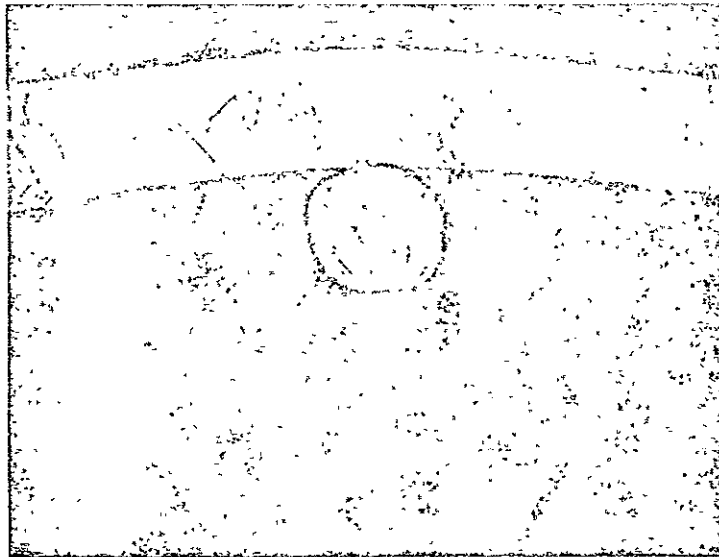
POS 68 100X MAG.
ETCHED

NEG 85 100X MAG.
ETCHED

process but there is no further corrosion of the grid either before or after the heat sterilization cycle.

Thus optical microscopic studies have shown that there is no appreciable attack on the nickel grid or nickel sinter substrate as a result of the heat sterilization process. Also, the color, shade, and texture changes which occur in both the positive and negative electrodes are visible and are believed to be morphological in nature.

Porosity and Pore Size Distribution:

The wetting and electrolyte retention properties of porous materials (e.g. battery plates) are affected by: (1) the wettability of the surface (inherent property of the material); (2) the total porosity; and (3) the pore sizes (distribution) in the plates.

Both porosity and pore size distribution of positive and negative plates were determined at the several stages previously mentioned. An Aminco-Winslow mercury porosimeter, Model No. 5-7118, was used for these determinations. A summary of the porosity data is shown in Table I-38.

TABLE I-38

Porosity of Dry Positive and Negative Plates

	Condition of Plate When Evaluated			
	As Manufactured	Cycled Pre-Sterilized	Sterilized	Cycled Post-Sterilized
Positive	33.4%	26.9%	45.2%	39.1%
Negative	55.9%	57.8%	55.5%	58.6%

I-131

metallurgical
materials division

These data indicate that there are measurable changes in the
porosity of the positive plate, whereas the porosity of the
negative plate is essentially unchanged, under the conditions
studied. In addition, heat sterilization causes a marked and
apparently irreversible change in the pore size distribution
of the positive plate. These data are shown in Figures I-30
and I-31. After sterilization the majority of the pores in
the positive plate are one micron or less. Continued cycling
after sterilization does not restore the original (presterili-
zation) pore diameter distribution of the positive plate.

Independent studies conducted in these laboratories indicate
that in battery plates, pores with very small diameters do not
effectively participate in electrochemical reactions. Thus a
shift to a larger number of very small pores may cause a loss
in useable capacity of a plate. The change in pore diameter
distribution also affects the capillarity of the positive
plate, which can alter the electrolyte retention of the plate
and cause a shift in electrolyte distribution throughout the
cell.

One may therefore speculate a mechanism for capacity degrada-
tion and other changes for heat-sterilized cells according to
the following scheme.

1) The average pore size of the positive plate
decreases during sterilization and may hold
less electrolyte even though porosity may

metallurgical
materials division

FIGURE I-30

PORE SIZE DISTRIBUTION OF POSITIVE PLATES

FIGURE I-31

PORE SIZE DISTRIBUTION OF POSITIVE PLATES

Pore Diameter --- Microns

Cumulative Percent

Plates Sterilized
Then Cycled

Cycled Plates
Not Sterilized
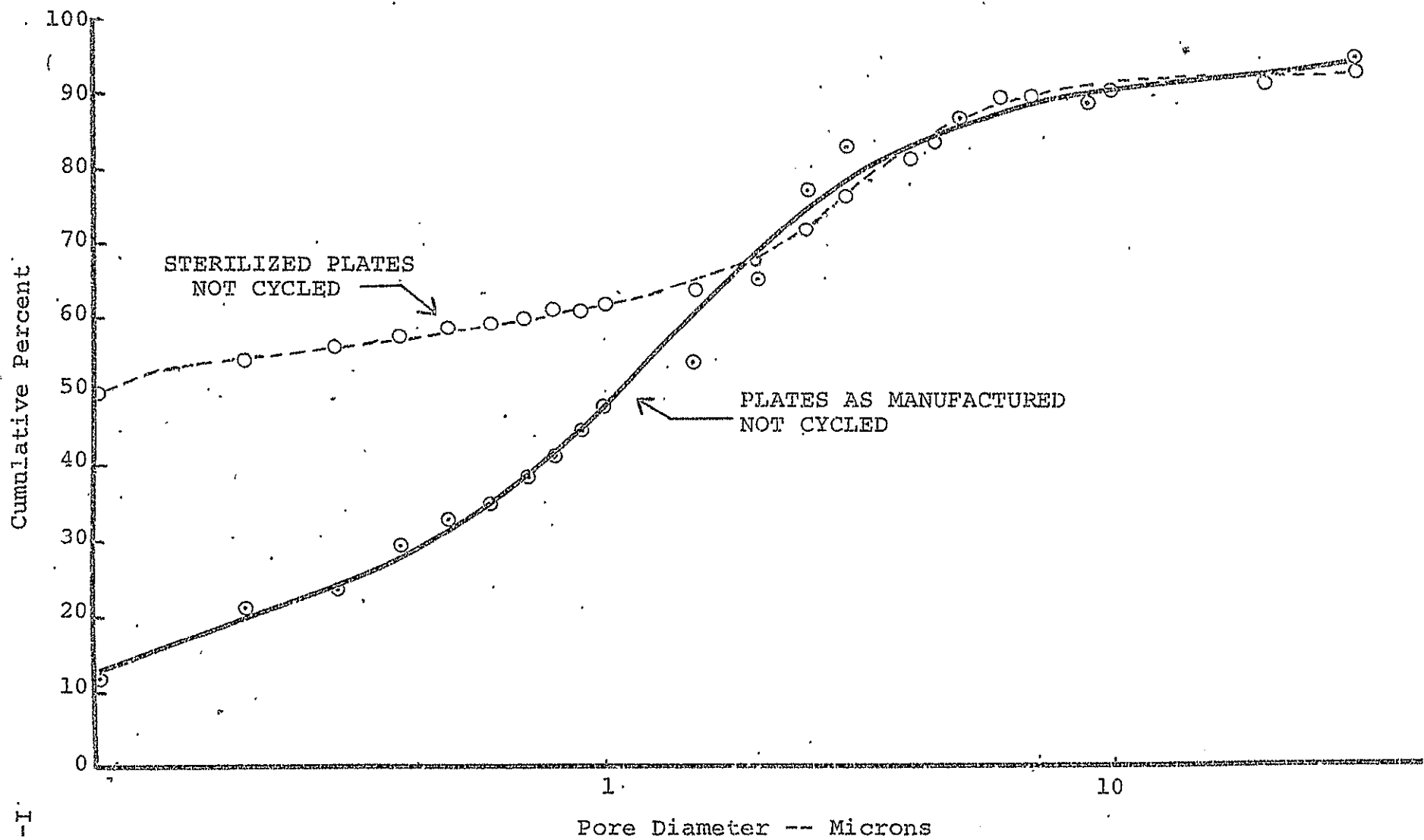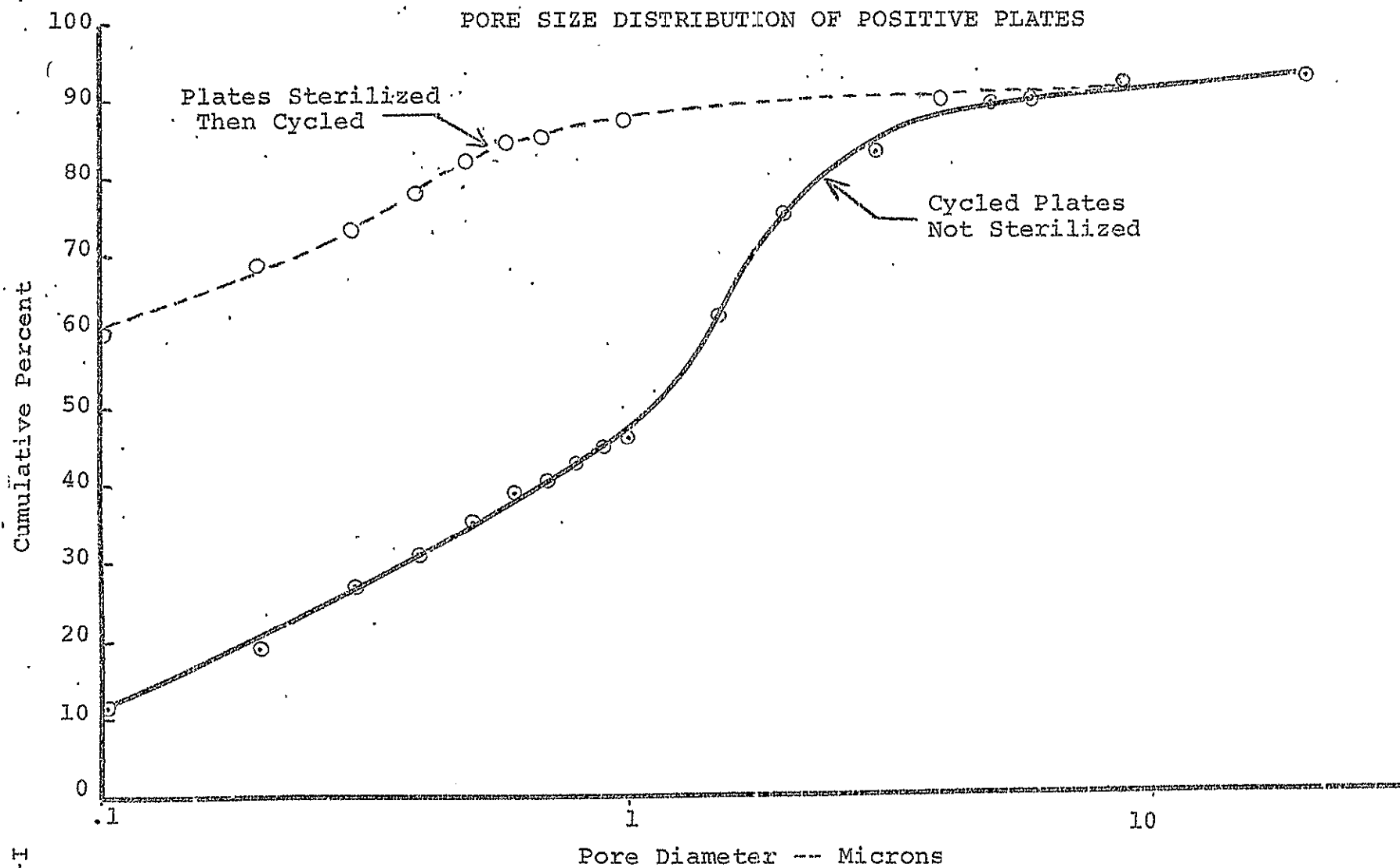
increase somewhat.

2) The available capacity of the positive plate decreases due to electrolyte limitation. The cadmium plate absorbs some of the electrolyte rejected by the positive plate in the sealed cell.

3) Since the positive plate capacity falls, then for a given coulombic charge input (e.g. 5 ampere-hours) a greater proportion of oxygen gas is evolved.

4) If the cadmium plate absorbs the additional electrolyte, its oxygen recombination rate is lowered, since recombination rate is controlled predominantly by the oxygen diffusion through the electrolyte film.

5) This results in a rapid buildup of oxygen gas pressure during overcharge.

6) Under these conditions the negative (cadmium) electrode can evolve hydrogen gas as a parallel reaction particularly if excess cadmium hydroxide is not accessible for reduction during constant current charging and oxygen diffusion is impeded by the electrolyte film resistance.

This hypothesis appears valid even if there are no changes in the porosity or pore diameter distribution of the negative

metallurgical
materials division

plate. The data presented in Figures I-32 and I-33 indicate that certain shifts in the pore size distribution of the negative plate occur during heat sterilization. These changes are apparently reversible and upon post-sterilization cycling the pore size distribution apparently returns to its original (pre-sterilization) values.

X-Ray Diffraction:

X-ray diffraction spectra were taken of positive and negative electrodes at various stages (of condition) previously mentioned. Spectra were taken using a Norelco diffractometer Model No. 5-210M. The scan rate for these initial runs was 2 degrees per minute using CuK α radiation. The major peaks and relative intensities of these spectra are presented in Table I-39. These data have been analyzed and compared to values available in the literature.

A preliminary analysis of the data shown in Table I-39 reveals changes in bandwidth, intensity and slight shifting in some reflection peaks indicating that crystallographic or morphological changes occur in both positive and negative plates as a result of the heat sterilization process. However, the x-ray spectrum of the positive plate taken after sterilization and subsequent cycling is similar to spectra obtained before heat sterilization. This indicates that during post-sterilization cycling the crystallography or morphology of the positive plate returns to its original state (i.e.,

metallurgical
materials division

FIGURE I-32

PORE SIZE DISTRIBUTION OF NEGATIVE PLATES
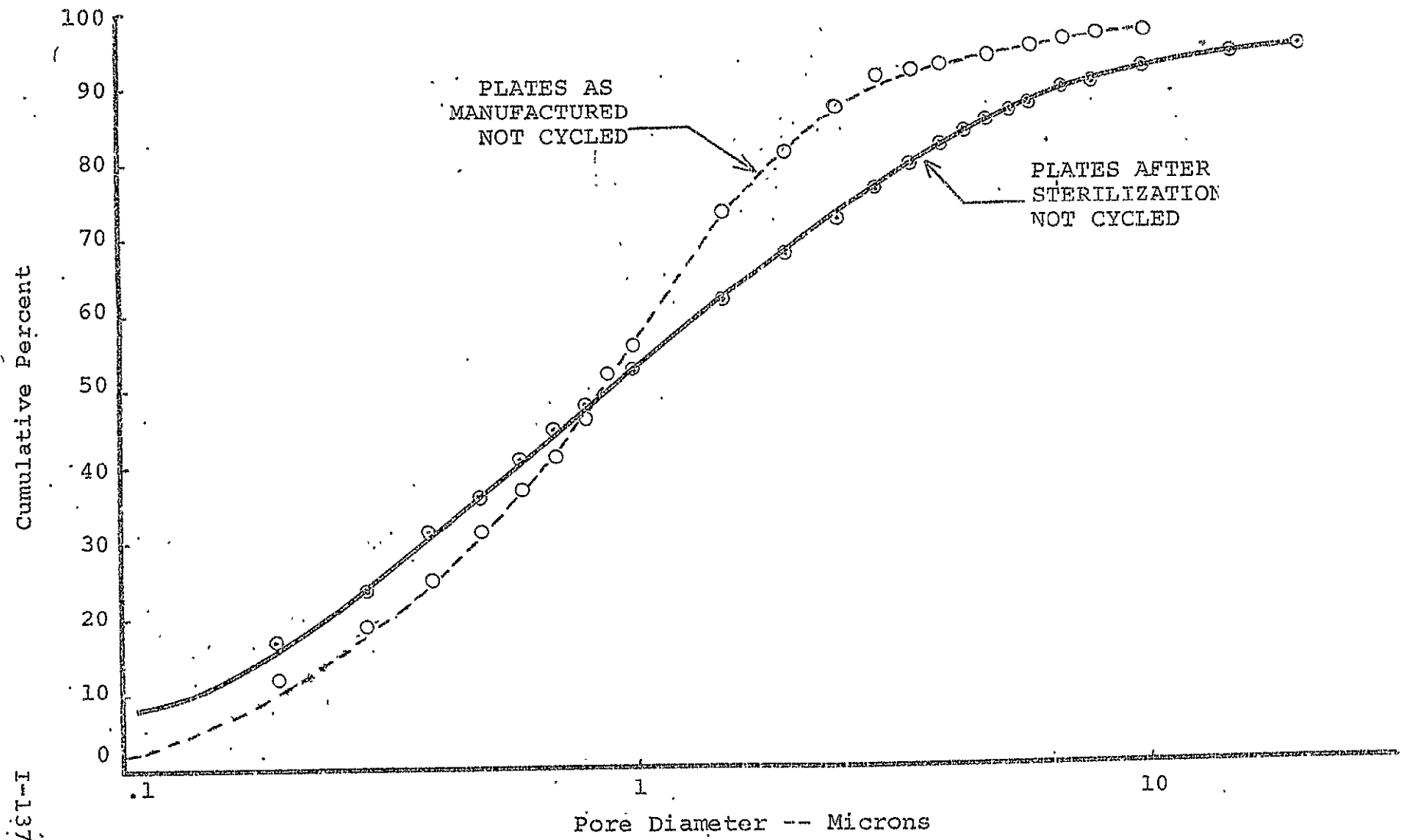
FIGURE I-33

PORE SIZE DISTRIBUTION OF NEGATIVE PLATES

I-138
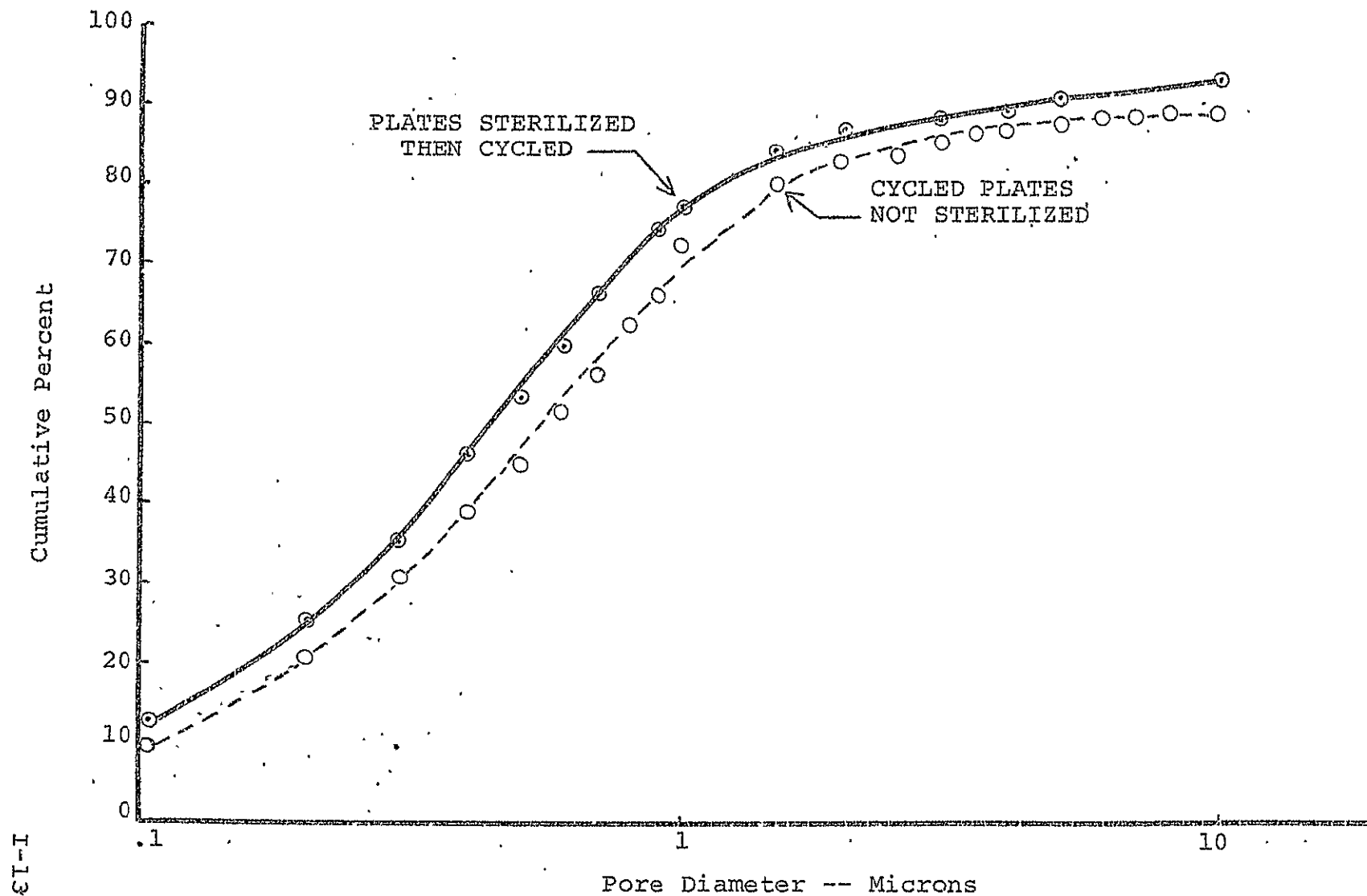
TABLE I-39

X-RAY DIFFRACTION DATA - NEGATIVE PLATES

Plate Condition											
As Received			Cycled			Sterilized			Sterilized and Cycled		
2θ	I	B.W.	2θ	I	B.W.	2θ	I	B.W.	2θ	I	B.W.
18.85	≥100	---	18.80	15.9	1.5	18.80	≥100	---	18.75	≥100	---
29.45	85.0	1.5	29.50	10.8	1.3	29.45	≥100		29.45	≥100	---
31.90	8.4	1.4	31.80	34.8	1.8	-----	----	---	31.75	8.0	1.7
-----	----	---	-----	----	---	33.00	5.0	2.0	-----	----	---
35.30	≥100	---	*34.70 / 35.20	31.2 / 19.8	1.6 / 2.3	35.20	≥100	---	35.20	≥100	
38.40	39.0	1.8	38.35	≥100	---	38.20	19.3	1.9	38.30	29.8	1.7
44.50	2.0	2.0	44.50	2.0	2.0	44.40	8.6	1.3	44.50	6.0	1.5
47.90	6.0	1.8	47.80	18.6	2.0	-----	----	---	47.80	6.2	1.7
49.10	53.8	1.9	49.00	6.0	1.8	49.00	82.0	1.7	49.00	66.0	1.7
52.40	29.3	2.0	52.40	3.8	2.2	52.30	48.6	1.5	51.25	36.0	1.8
56.20	25.4	2.0	56.15	5.0	2.0	56.10	53.0	1.5	56.10	35.0	1.8
59.0	5.0	1.8	-----	----	---	58.80	6.4	2.0	58.70	7.4	1.4
61.20	13.0	2.3	61.10	19.5	2.3	61.20	14.2	1.7	61.15	16.8	1.6
62.40	6.4	4.7	62.35	19.0	2.0	-----	----	---	62.35	7.8	2.0
64.75	16.5	2.0	64.70	3.0	1.4	64.60	29.4	2.0	64.50 / 64.70	22.5 / 64.7	2.0
66.70	8.5	2.5	66.60	3.0	2.0	66.60 / 66.80	17.0 / 15.0	1.4 / 1.6	66.60	11.0	2.0
77.20	12.8	2.6	-----	----	---	67.15	24.0	1.9	67.20	19.3	1.8
71.80	5.0	2.0	71.70	18.4	2.4	-----	----	---	71.70	6.8	2.8
74.60	10.4	2.5	75.70	12.0	2.4	74.40	20.5	2.0	74.50	14.3	2.0
82.60	6.5	2.8	82.40	4.0	2.5	82.60	8.2	2.8	82.40 / 82.80	8.50 / 6.20	2.0 / 2.0
84.65	5.0	2.6	84.50	2.0	2.0	84.60 / 84.80	11.3 / 7.5	1.8 / 2.0	84.60	7.5	3.0
87.70	10.6	2.7	87.70	2.8	3.0	87.60 / 87.90	21.8 / 14.8	1.4 / 1.0	87.60 / 87.90	13.0 / 12.2	2.8
90.00	5.0	3.0	-----	----	---	89.20 / 90.00	7.40 / 9.00	3.5 / 3.0	89.20 / 89.90	6.50 / 8.10	2.5 / 3.0

2θ = Reflection angle, I = Relative intensity, B.W. = Band width at 1/2 I

* $\frac{34.7}{35.2}$ for example indicates doublet

TABLE I-39 CONT'D.

Plate Condition											
As Received			Cycled			Sterilized			Sterilized and Cycled		
2θ	I	B.W.	2θ	I	B.W.	2θ	I	B.W.	2θ	I	B.W.

X-RAY DIFFRACTION DATA - NEGATIVE PLATES

2θ	I	B.W.	2θ	I	B.W.	2θ	I	B.W.	2θ	I	B.W.
93.00	3.4	2.7	93.00	6.0	3.3	-----	----	---	-----	----	---
96.80 97.10	12.1 11.0	2.0 1.5	96.90 97.20	4.60 3.00	3.0 3.0	96.90 97.20	18.5 14.60	1.8 1.5	96.80 97.10	12.0 9.3	3.2
-----	----	---	97.80	4.0	4.7	-----	----	---	-----	----	---
-----	----	---	-----	----	---	99.50	6.0	3.0	99.30	5.1	2.0
102.50	4.0	2.0	-----	----	---	102.60	9.0	3.0	102.60	6.1	2.0
104.60	4.0	2.0	-----	----	---	104.20	9.7	4.0	104.20	7.0	3.5
-----			106.60	7.4	4.6	-----	----	---	106.60	5.8	3.0

X-RAY DIFFRACTION DATA - POSITIVE PLATES

2θ	I	B.W.	2θ	I	B.W.	2θ	I	B.W.	2θ	I	B.W.
19.1	42.0	6.3	19.0	55.5	5.2	19.2	▷100	---	19.0	77.4	2.7
33.1	16.0	3.2	33.2	28.0	3.8	33.0	57.7	3.0	33.0	24.7	3.0
38.5	39.0	5.4	38.5	57.8	6.7	38.5	▷100	---	38.4	56.0	4.2
44.5	▷100	---	44.6	▷100	---	44.5	▷100	---	44.6	▷100	---
51.8	▷100	---	51.9	▷100	---	51.9	▷100	---	51.9	▷100	---
59.1	10.0	5.5	59.2	19.5	4.0	59.0	36.4	3.0	58.9	13.8	6.0
62.7	7.8	5.0	62.8	11.4	4.2	62.6	28.0	3.0	62.5	10.0	7.0
69.7	4.4	12.0	69.7	5.0	8.0	69.4	6.0	3.0	69.0	7.0	7.0
----	----	---	----	----	---	70.4	11.8	3.6	70.2	10.0	6.0
72.7	4.5	6.0	72.7	5.6	7.5	72.7	13.3	4.2	72.5	9.0	6.0
* 76.2 76.4	40.4 42.4	2.5	76.4 76.5	39.3 39.3	2.5	76.4 76.5	43.3 43.8	2.7	76.4 76.6	63.6 43.5	2.1
82.5	3.0	5.0	82.5	4.0	3.8	82.5	7.8	4.4	82.5	5.0	5.5
92.8 93.1	47.0 44.0	3.0	92.9 99.2	46.0 38.6	3.0	92.8 93.1	48.0 38.9	3.2	92.8 93.2	67.8 45.6	2.5
98.2 98.6	14.5 12.4	3.2	98.4 98.8	15.0 12.2	3.0	98.4 98.6	17.7 15.2	3.3	98.4 98.8	22.0 15.7	3.0
100.8	2.0	5.0	100.9	3.0	3.5	100.7	9.0	5.6	----	----	---

2θ = Reflection angle, I = Relative intensity, B.W. = Band width at 1/2 I

* $\frac{76.2}{76.4}$ for example indicates doublet

before heat sterilization). The same effect is not apparent·
in the negative electrode since spectra obtained for sterilized
and cycled negatives retain many of the intensity and band-
width changes characteristic of the post-sterilization spectra.
Therefore heat sterilization produces long-term crystallo-
graphic· changes in the negative electrode which may impair its
electrochemical efficiency.

X-Ray Diffraction and Electron Microscopic Studies:
In order to get a better understanding of the changes in the
sterilized plates, further x-ray diffraction studies were
carried out as described below.

Eight samples of· fully discharged positive and negative plate
materials representing (1) as-received, (2) cycled (3 dis-
charge-charge cycles), (3) sterilized, and (4) cycled after
sterilization were washed free of KOH, dried at $100^{o}C$ and
stored in a vacuum desiccator. X-ray diffraction patterns
were made of. the surface of each sample under the experimental
conditions stated in Table I-40. The· patterns of plates and
plaque materials are shown in Figures I-34-I-42.

Data from these figures and from the preceding tables were
compared with data from the ASTM "Powder Diffraction File."
Table I-41 lists principle lines for the specific compounds
sought and reveal the following observations:

Positive Plates: An examination of the patterns for the ·

I-141

TABLE I-40

X-RAY DIFFRACTION INSTRUMENTAL CONDITIONS

Radiation	CuK_2	Cu Tube 45KV 35ma full wave rectified with focusing monochromator at detector
Goniometer	Norelco Verticle	Take off angle 3° S_D 1^O S_R 1^O S_S 4°
Detector	Norelco transistorized Scintillation with PHA	850 volts 1.50 base 3.00 window
Data	6°/in Log Output	Scan 1^O/min Chart 10 in/hour +.25 offset

metallurgical
materials division

TABLE I-41

Principle Lines from ASTM Standards
for CuKα Radiation

Compound Card No	°2θ	I/I_1
Cd 5-0674	38.45	100
	31.86	65
	34.77	32
	47.85	32
CdO 5-0640	33.03	100
	38.32	88
	55.30	43
	63.81	28
Cd(CO)$_3$ 8-456	30.27	100
	23.51	60
	46.49	35
	43.78	25
Ni 4-0854	44.45	100
	51.84	42
	76.34	21
NiO 4-0835	43.30	100
	37.30	91
	62.90	57
Ni(OH)$_2$ 14-117	19.27	100
	38.57	100
	33.09	45
	52.14	35
Cd(OH)$_2$ 1-0305	18.86	100
	29.55	63
	35.02	100
Cd(OH)$_2$ 13-226	18.88	70
	29.48	65
	35.19	100
BNiOOH 6-0141	18.38	100
	37.30	80
	66.77	80
γNiOOH 6-0075	12.81	100
	25.96	80
	37.93	80
	43.25	80

X-RAY DIFFRACTION OF Ni PLAQUE
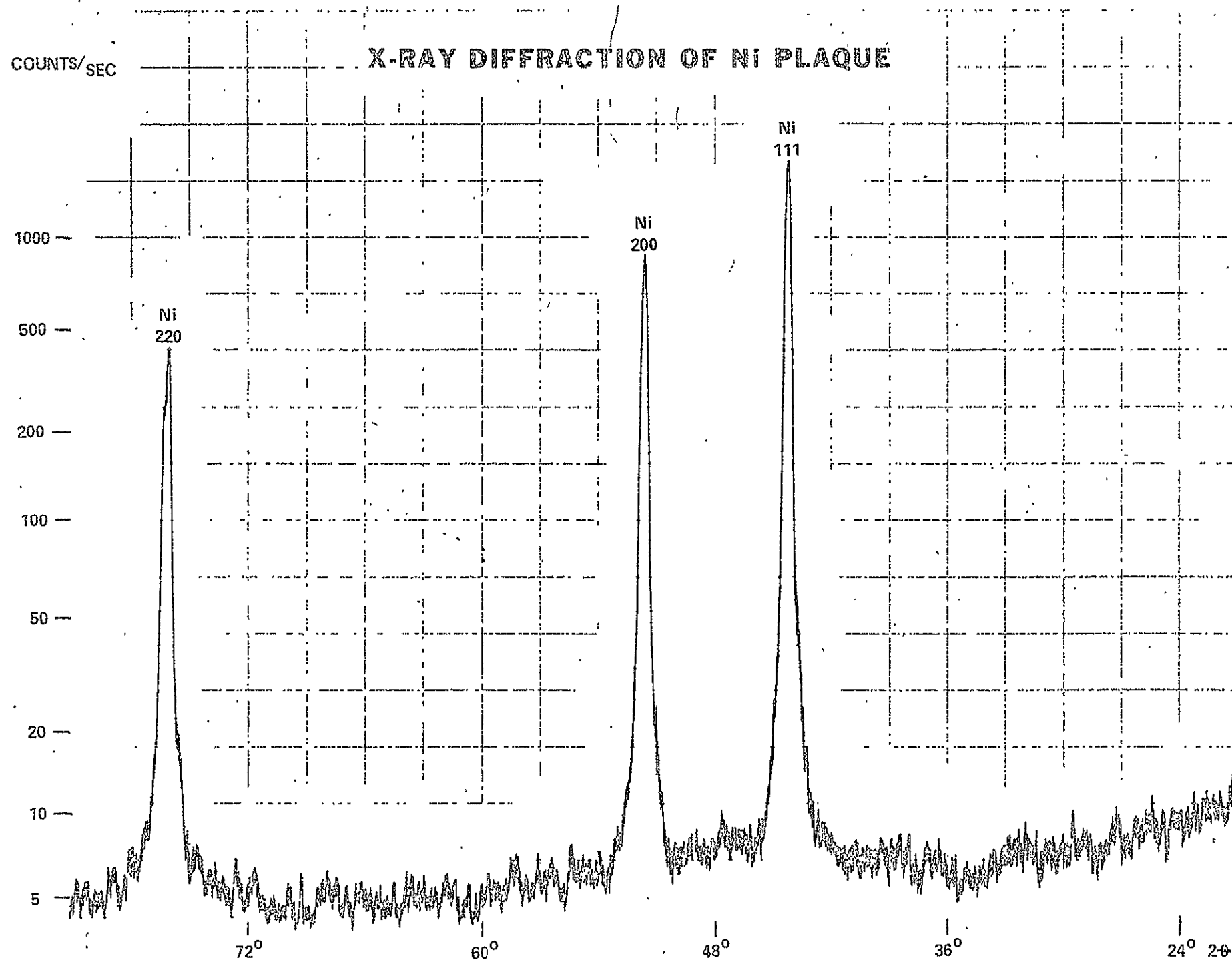
FIGURE I-34

I-144

X-RAY DIFFRACTION OF POSITIVE (AS RECEIVED)
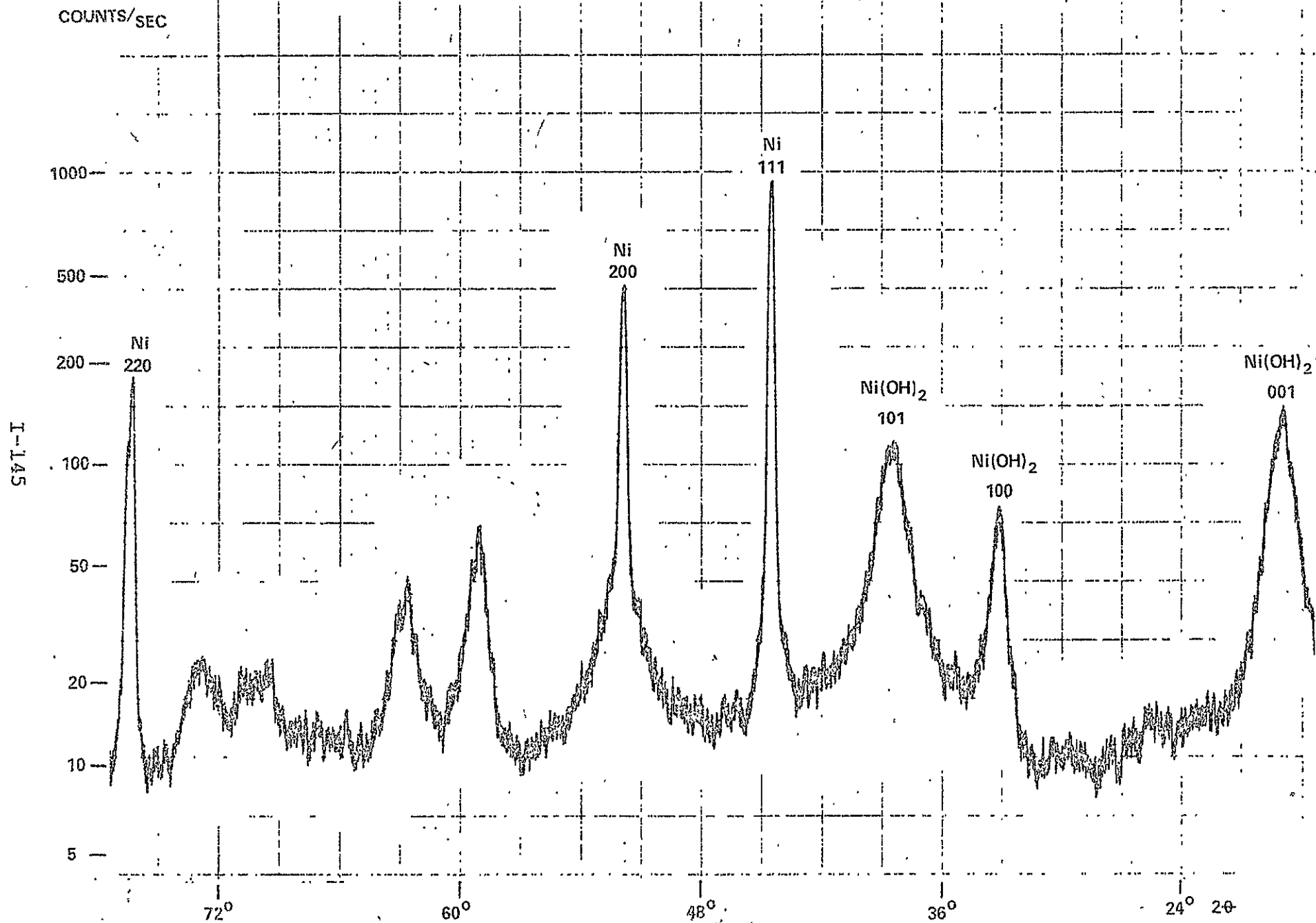
FIGURE I-35

I-145

X-RAY DIFFRACTION OF POSITIVE (CYCLED)
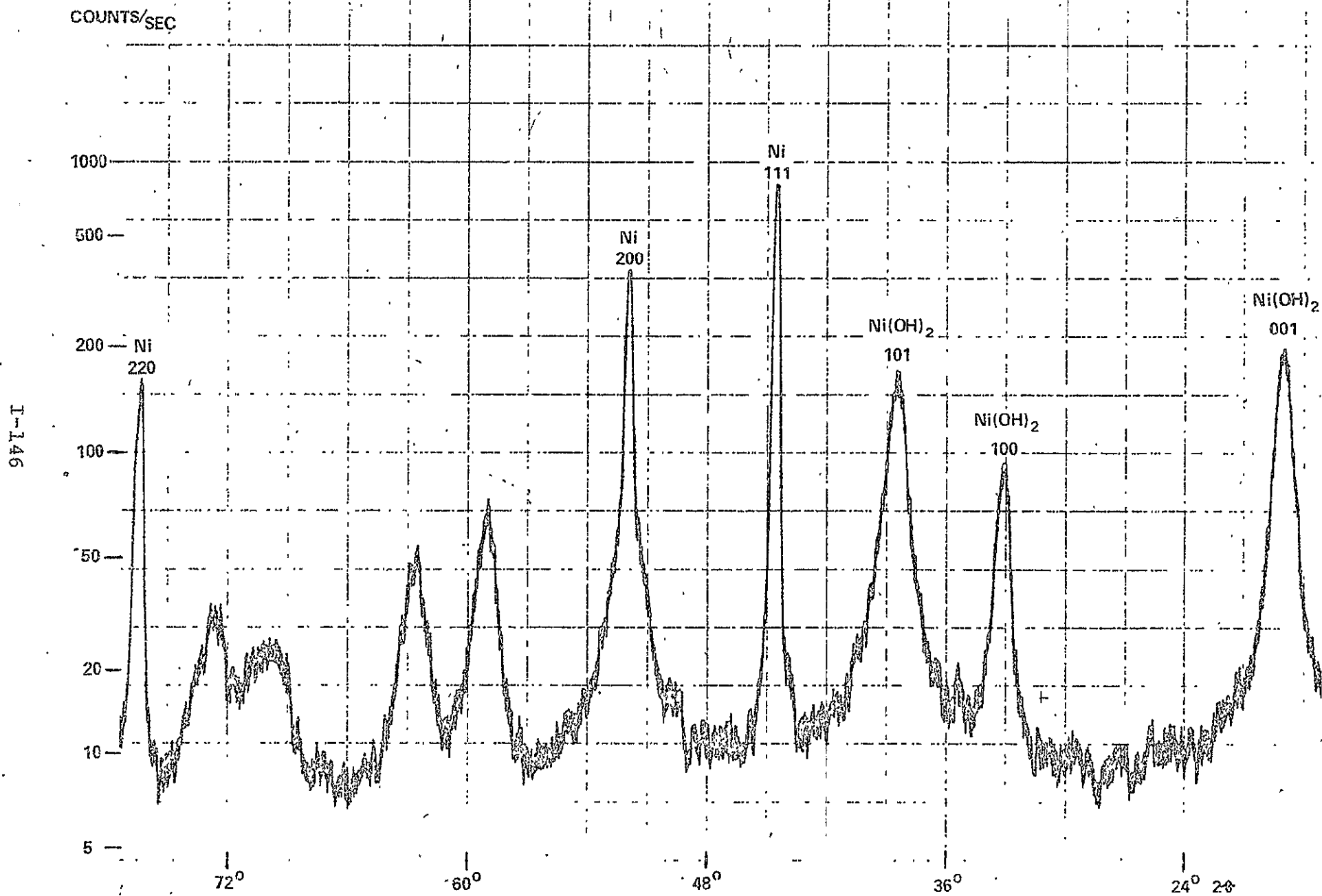
FIGURE I-36

X-RAY DIFFRACTION OF POSITIVE (STERILIZED)
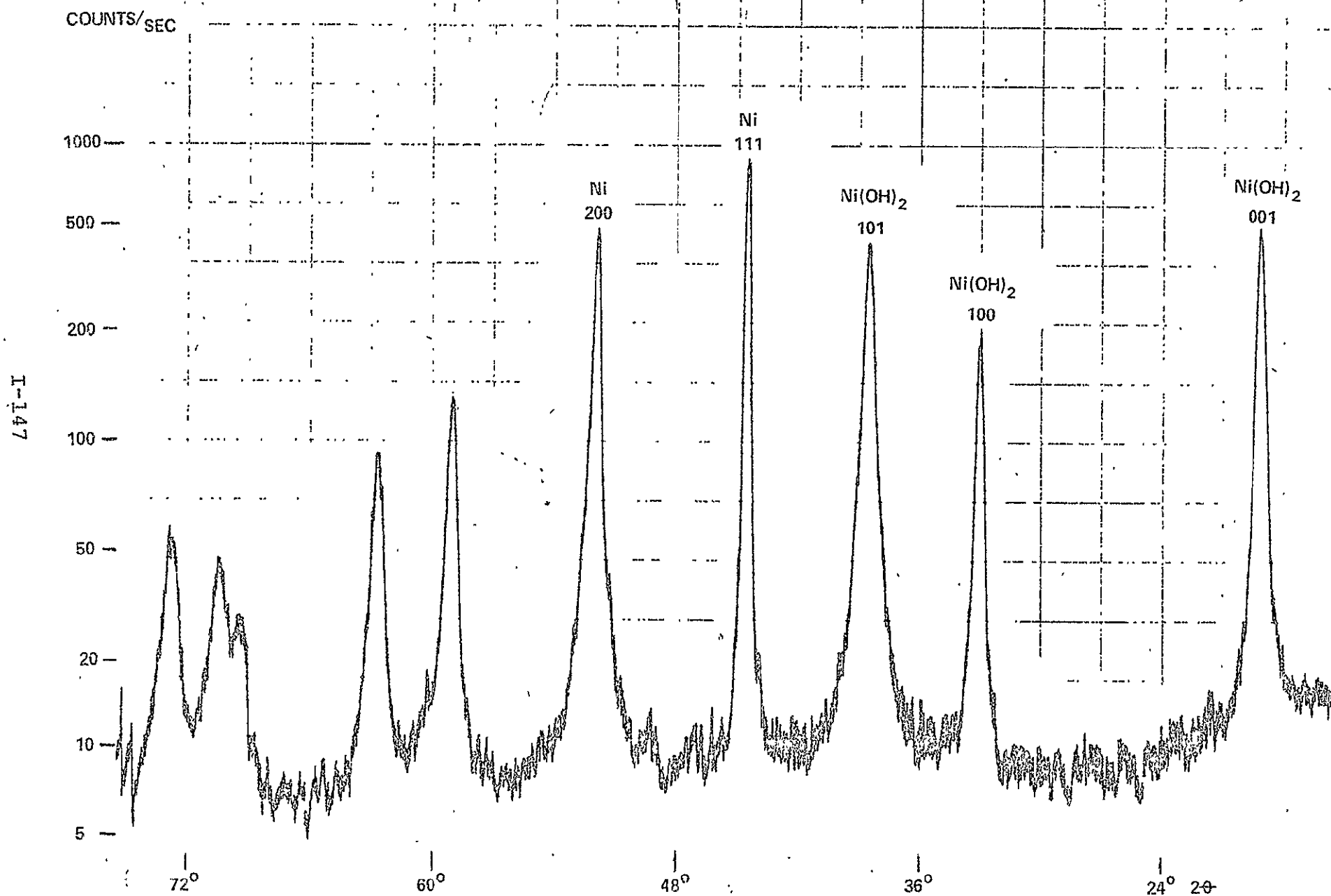
FIGURE I-37

X-RAY DIFFRACTION OF POSITIVE (STERILIZED AND CYCLED)
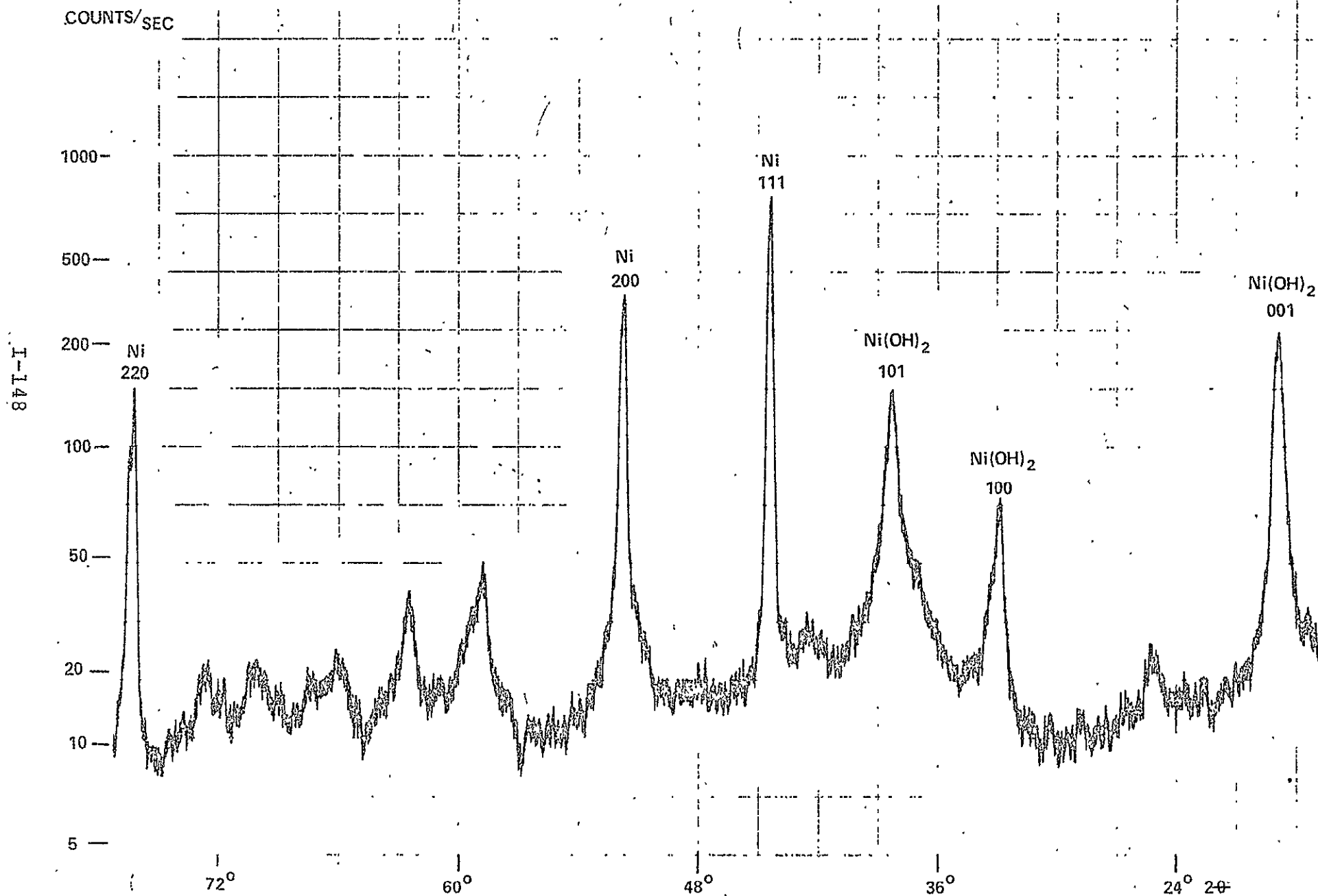
FIGURE I-38

FIGURE I-39

X-RAY DIFFRACTION OF NEGATIVE (CYCLED)

FIGURE I-40
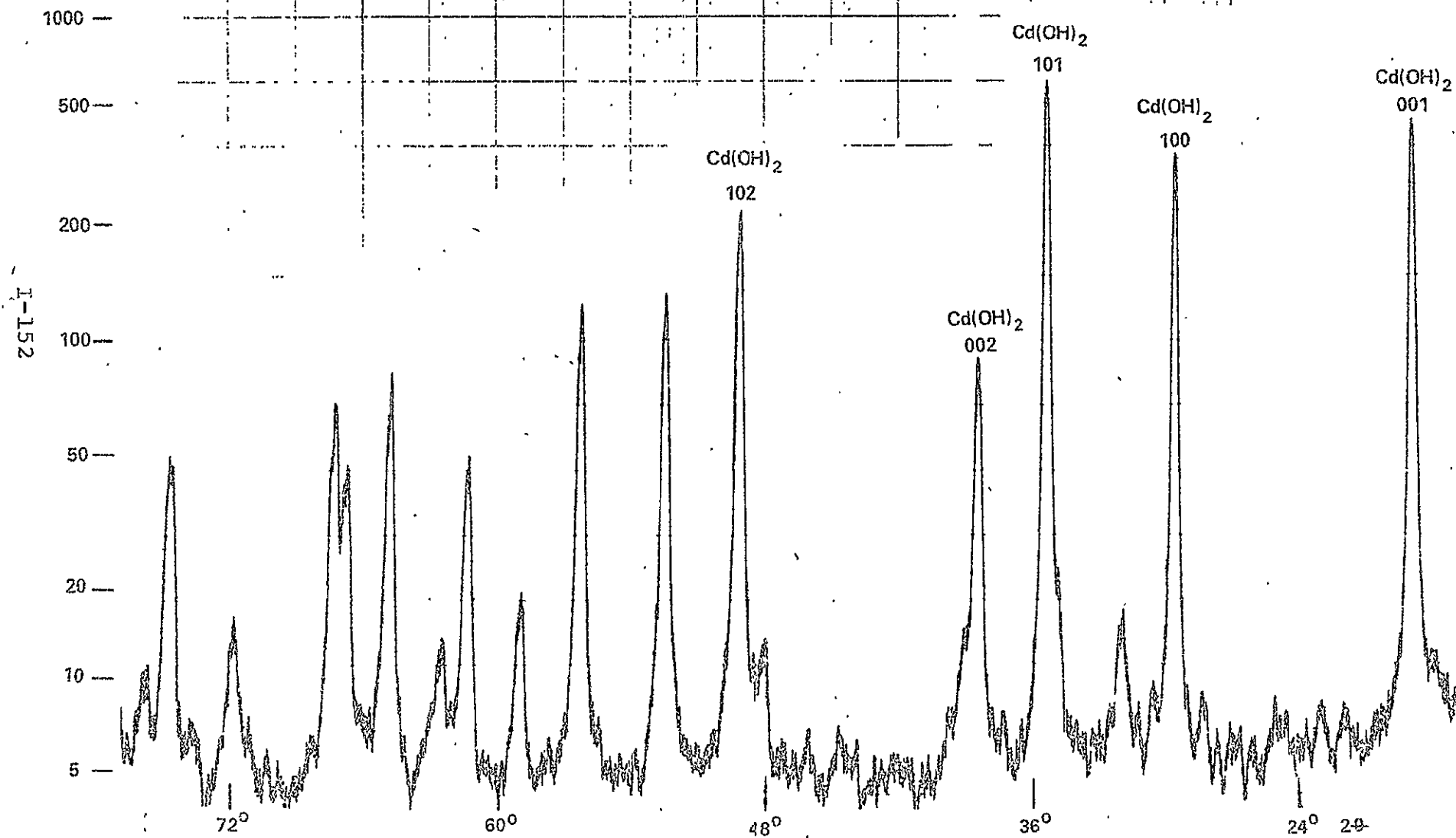
FIGURE I-41

FIGURE I-42

positive plates shows the presence of $Ni(OH)_2$ and Ni metal. The significant intensity of the Ni peaks (1/3 to 1/2 of those of the Ni plaque) implies either a relatively thin layer of $Ni(OH)_2$ or exposed Ni plaque.

All $Ni(OH)_2$ lines show broadening implying either small crystallite size or disorder. The presence of the relatively sharp 100 line can be interpreted in two ways. Either the compound exists as relatively thin plates whose base is the 001 plane or in layers in which the spacing in the C direction varies.

An examination of the positive plates after different treatments shows that the $Ni(OH)_2$ lines are sharpest, i.e. most ordered or largest size, for the sterilized sample. Cycling after sterilization again broadens the lines returning the material almost to its presterilized condition.

Negative Plates: The lines of patterns from the negative plates show little evidence of broadening. The identification of compounds from these patterns is more complex. There is disagreement as to the accepted patterns, the residual spectra due to compounds other than $Cd(OH)_2$ are obtained. These are tabulated in Table I-43 with their most probable origin. The variable, low intensity of the Ni lines, shows that the nickel substrate is thickly covered with $Cd(OH)_2$. Traces of Cd are found in all samples except

TABLE I-42

X-RAY DIFFRACTION LINES OF Cd(OH)$_2$

FOR CuKα RADIATION

I/I$_1$	hkl	°2θ
Card No. 1-0305		
100	001	18.86
63	100	29.55
100	101	35.02
40	102	48.93
30	110	52.55
30	111	56.40
13	200	61.34
20	201	64.53
20	112	66.60
15	202	74.68
Card No. 13-226		
70	001	18.88
65	100	29.48
100	101	35.19
7	002	38.47
35	102	49.05
20	110	52.34
6	200	61.26
8	201	64.68
8d	103	66.93
	112	
6	202	74.47
As Received Sample		
59		18.8
54		29.2
100		35.0
10		38.1
37		48.6
22		52.1
20		55.9
6		60.9
12		64.3
3		66.4?
6		67.0
6		74.5

TABLE I-43

X-RAY DIFFRACTION DATA (NEG. PLATE)

PEAKS OTHER THAN $Cd(OH)_2$

As Received		Cycled		Sterilized		Sterilized and Cycled		Assignment
°2θ	c/sec I	°2θ	c/sec I	°2θ	c/sec I	°2θ	c/sec I	ment
31.9	6	31.9	4	----	----	31.9	5	Cd
32.9	3	----	----	33.1	4	----	----	CdO
----	----	39.2	4	22.9	3	----	----	
----	----	44.5	9	44.6	3	----	----	Ni
48.0	2	----	----	----	----	48.0	3	Cd
----	----	51.8	1	----	----	----	----	Ni
58.9	10	58.8	10	58.9	13	58.9	8	
62.2	2	62.4	3	62.7	3	62.5	5	
----	----	----	----	----	----	71.8	7	

From TABLE V 2nd Quarterly Report

31.9	8	31.8	35	----	----	31.8	8	Cd
----	----	----	----	33.0	5	----	----	CdO
----	----	34.7	31?	----	----	----	----	Cd
44.5	2	44.5	2	44.4	9	44.5	6	Ni
47.9	6	47.8	19	----	----	47.8	6	Cd
59.0	5	----	----	58.8	6	58.7	7	
62.4	6	62.4	19	----	----	62.4	8	
71.8	5	71.7	18	----	----	71.7	7	

metallurgical
materials division

those immediately after sterilization and CdO is found in both of the sterilized samples and in one of the samples as received.

The Scanning Electron Microscopy:

The scanning electron microscopy pictures in Figures I-43 and I-44 show that sterilization results in increased crystal size in the cadmium plate.

DTA and TGA Studies:

In order to get a better understanding of the changes occurring particularly in the state of hydration and degree of oxidation of the active material, during thermal sterilization of the Ni-Cd cells, techniques of differential thermal analysis (DTA) and thermogravimetric analysis (TGA) were employed.

Typical DTA curves for the positive plates under the following stages are given in Figures I-45 to I-48.

Figure I-45:   Positive Plate As-Received;

Figure I-46:   Positive Plate Cycled Prior to Sterilization;

Figure I-47:   Positive Plate After Heat Sterilization;

Figure I-48:   Positive Plate Cycled After Sterilization.

Shape of the curve of Figure I-48 has been confirmed on other plates.   Similar DTA curves for the negative plates in (a) as-received, (b) cycled, (c) after sterilization, and (d) cycled after sterilization are given in Figures I-49, I-50, I-51, and I-52 respectively.

An interpretation and correlation of these data with other

metallurgical
materials division
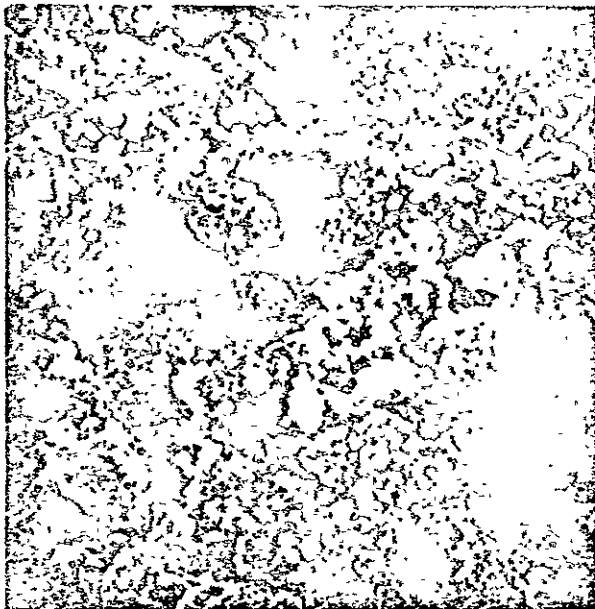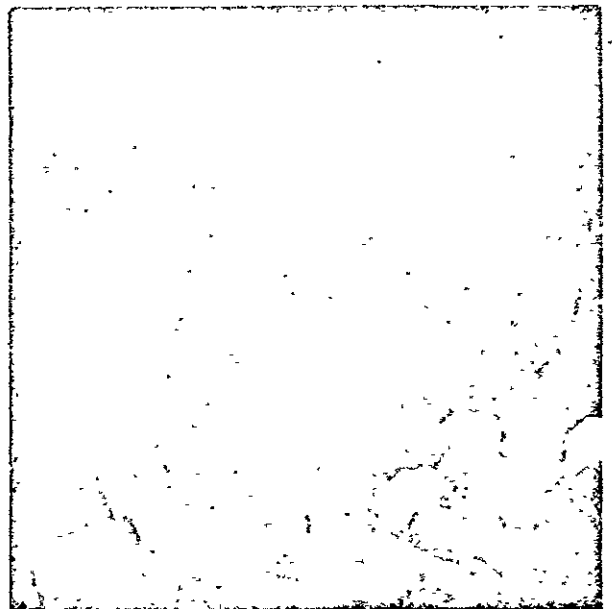
1000X   5000X

NEGATIVE MATERIAL - AS RECEIVED
(FLAT SURFACE)

1000X   5000X

NEGATIVE MATERIAL - STERILIZED
(FLAT SURFACE)

FIGURE I-43
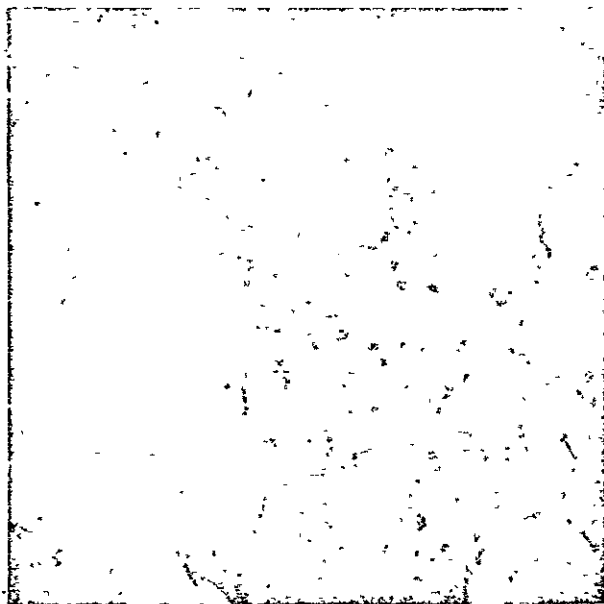
NEGATIVE MATERIAL
AS RECEIVED
(TRANSVERSE SECTION)
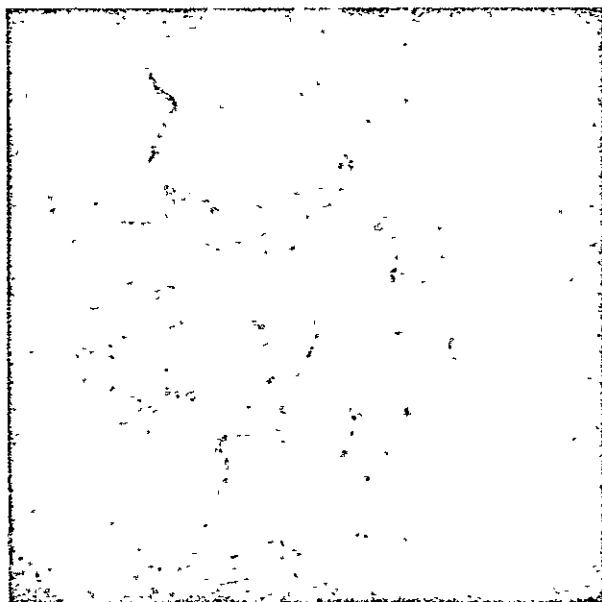
5000X

NEGATIVE MATERIAL
STERILIZED
(TRANSVERSE SECTION)

5000X

FIGURE I-44

electrochemical and physico-chemical data has not been possi-

ble.

metallurgical
materials division
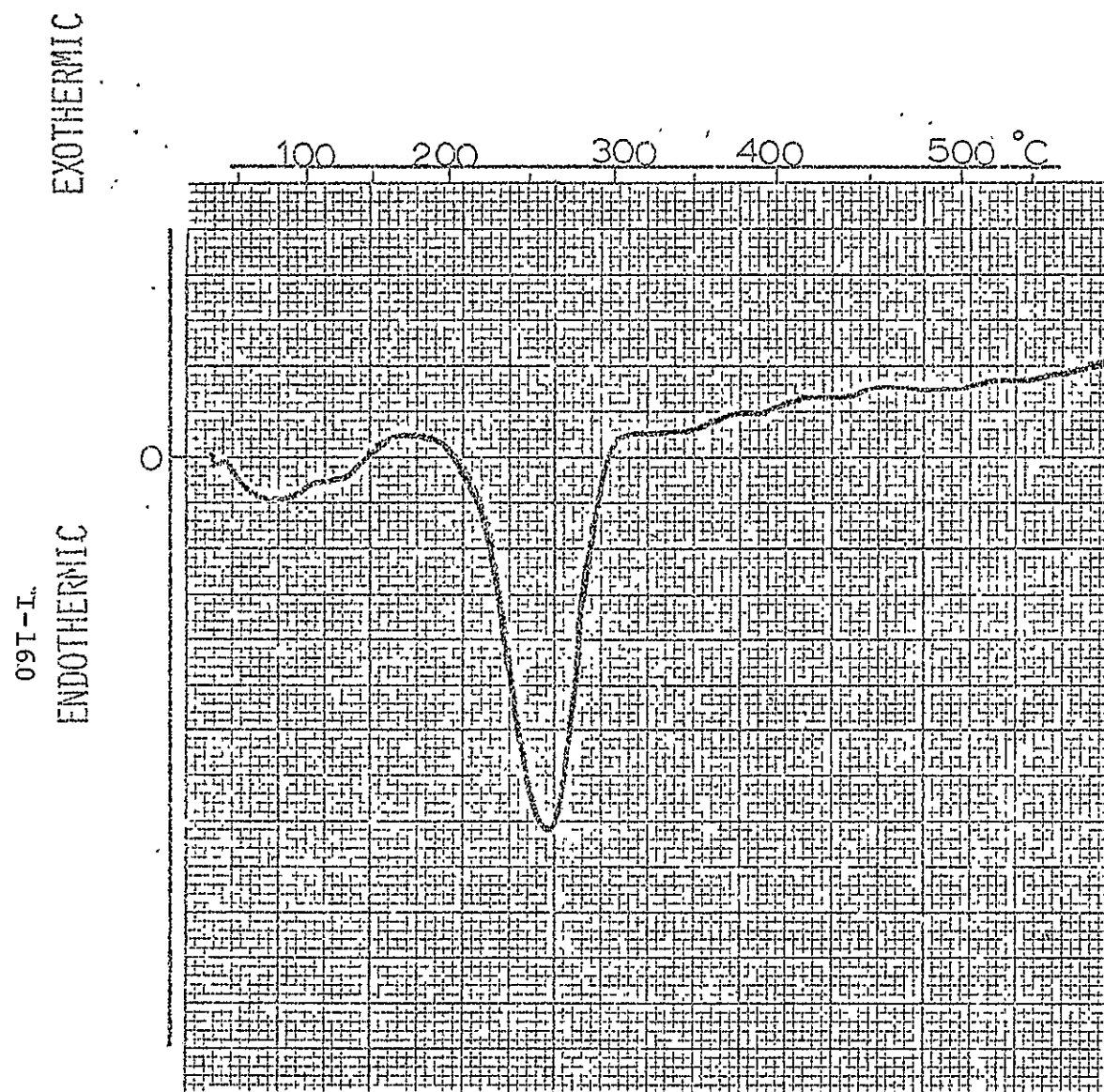
FIGURE I-45
DTA #153

SAMPLE: POSITIVE (AS RECEIVED)

SAMPLE WT.: 10 MG

CONDITIONS: 10°C MIN^{-1}
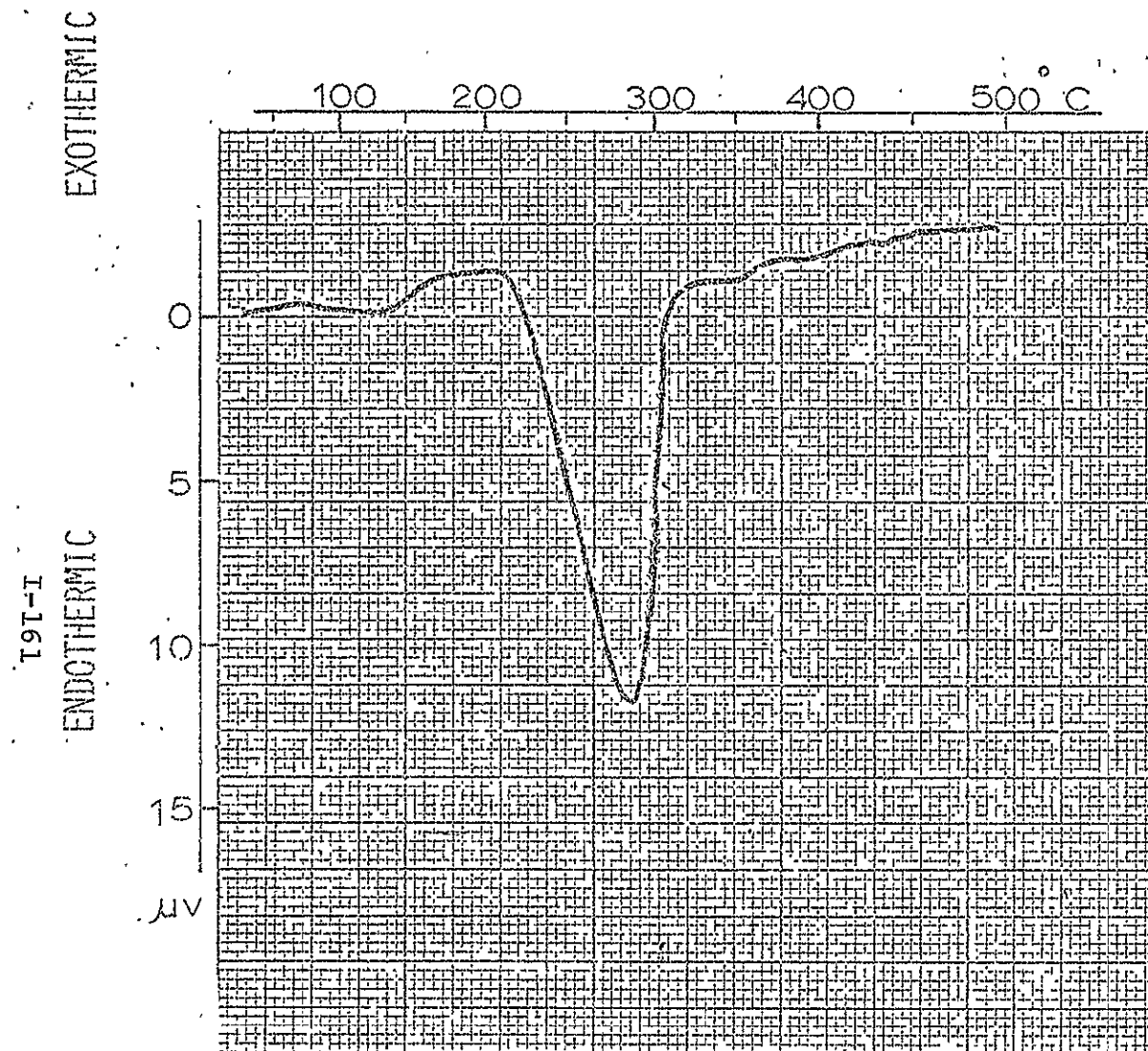
0.10 SCFM AR

FIGURE I-46

DTA #116

SAMPLE: #68 POSITIVE CYCLED PRIOR
           TO STERILIZATION

SAMPLE WT.: 8.4 MG

CONDITIONS: 10°C MIN^{-1}
              0.10 SCFM Ar

EXOTHERMIC

ENDOTHERMIC

I-162
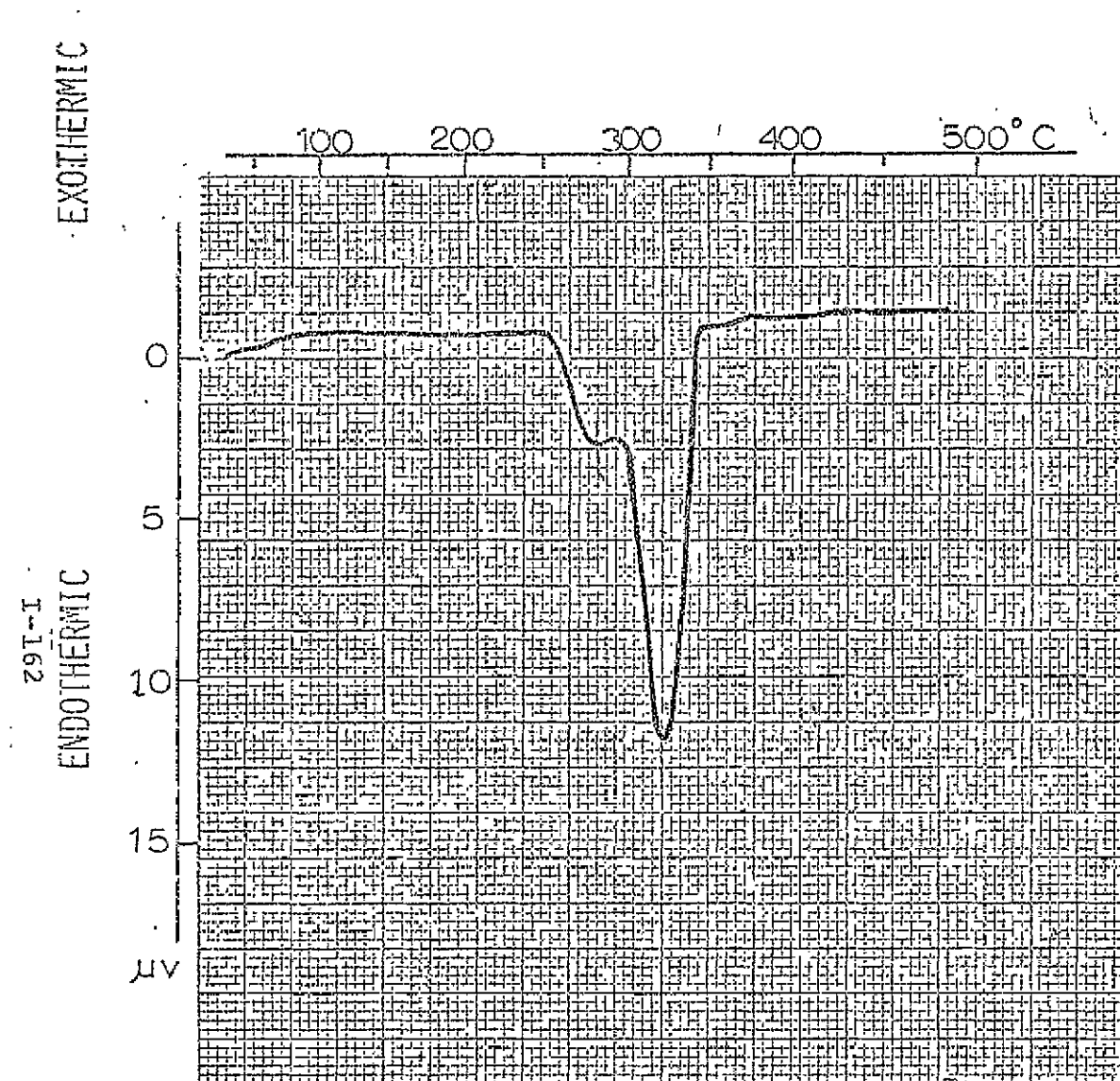
FIGURE I-47

DTA #124

SAMPLE: #68 POSITIVE STERILIZED

SAMPLE WT.: 8.5 MG

CONDITIONS: $10°C \cdot MIN^{-1}$
0.10 SCFM Ar
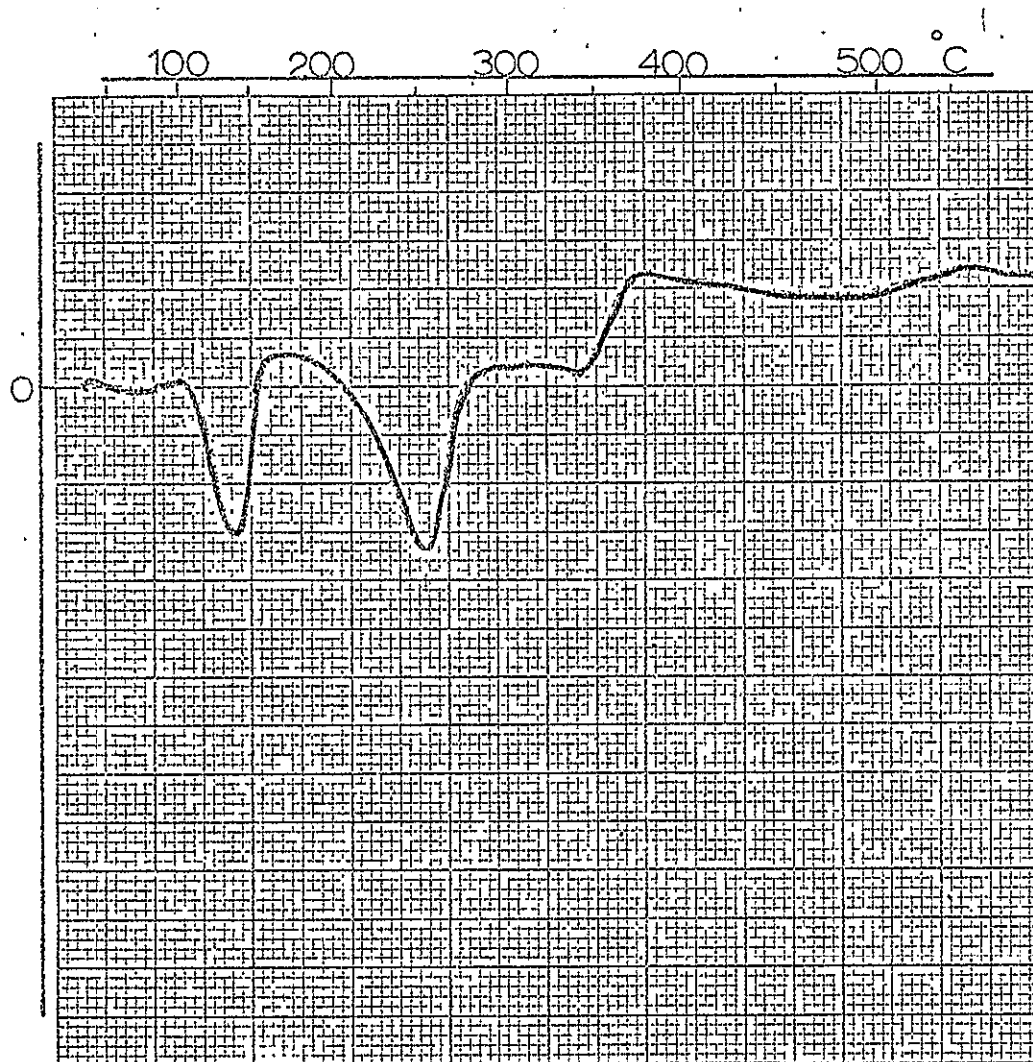
FIGURE I-48

DTA #155

SAMPLE: POSITIVE (STERILIZED AND CYCLED)

SAMPLE WT.: 10 MG

CONDITIONS: 10°C MIN^{-1}
0.10 SCFM Ar
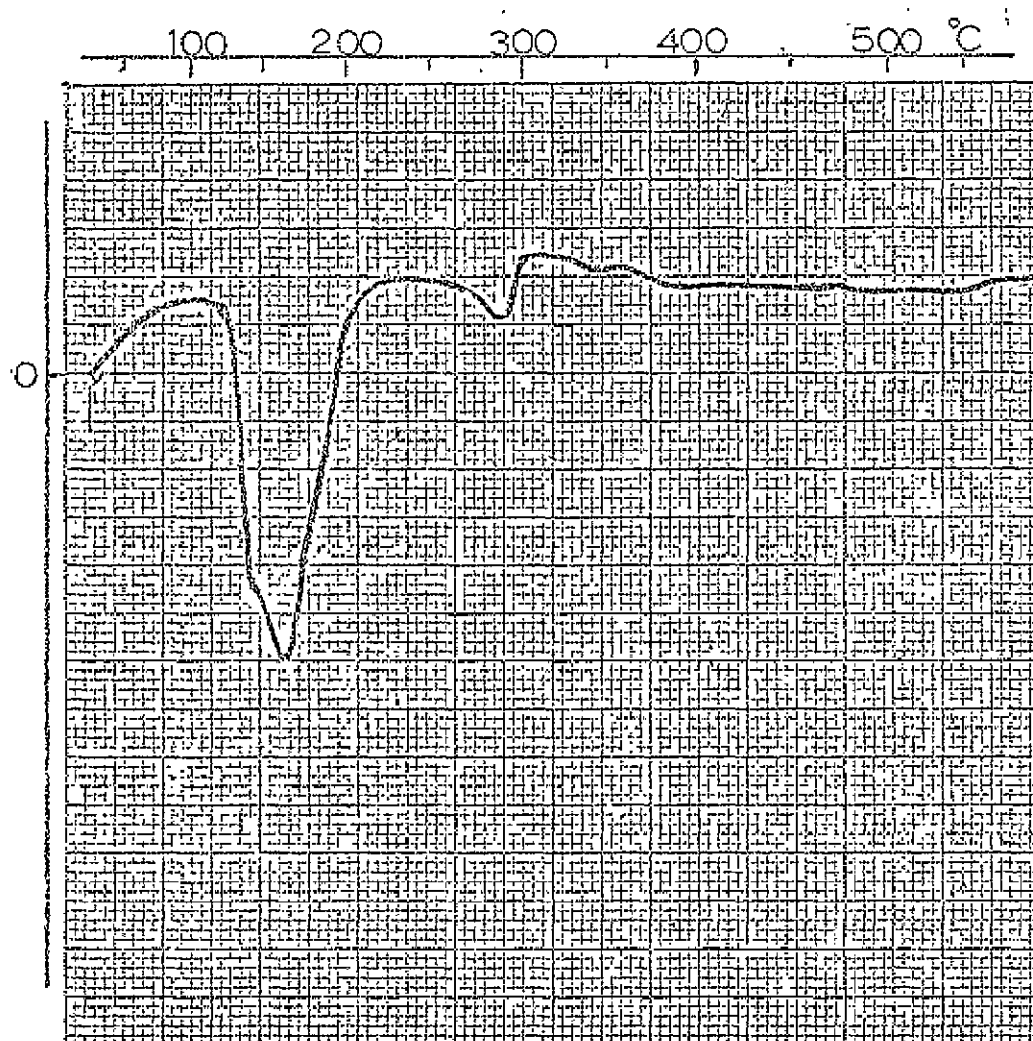
FIGURE I-49

DTA #154

SAMPLE: NEGATIVE (AS RECEIVED)

SAMPLE WT.: 10 MG

CONDITIONS: 10°C MIN^{-1}
0.10 SCFM AR

EXOTHERMIC — ENDOTHERMIC

I-165
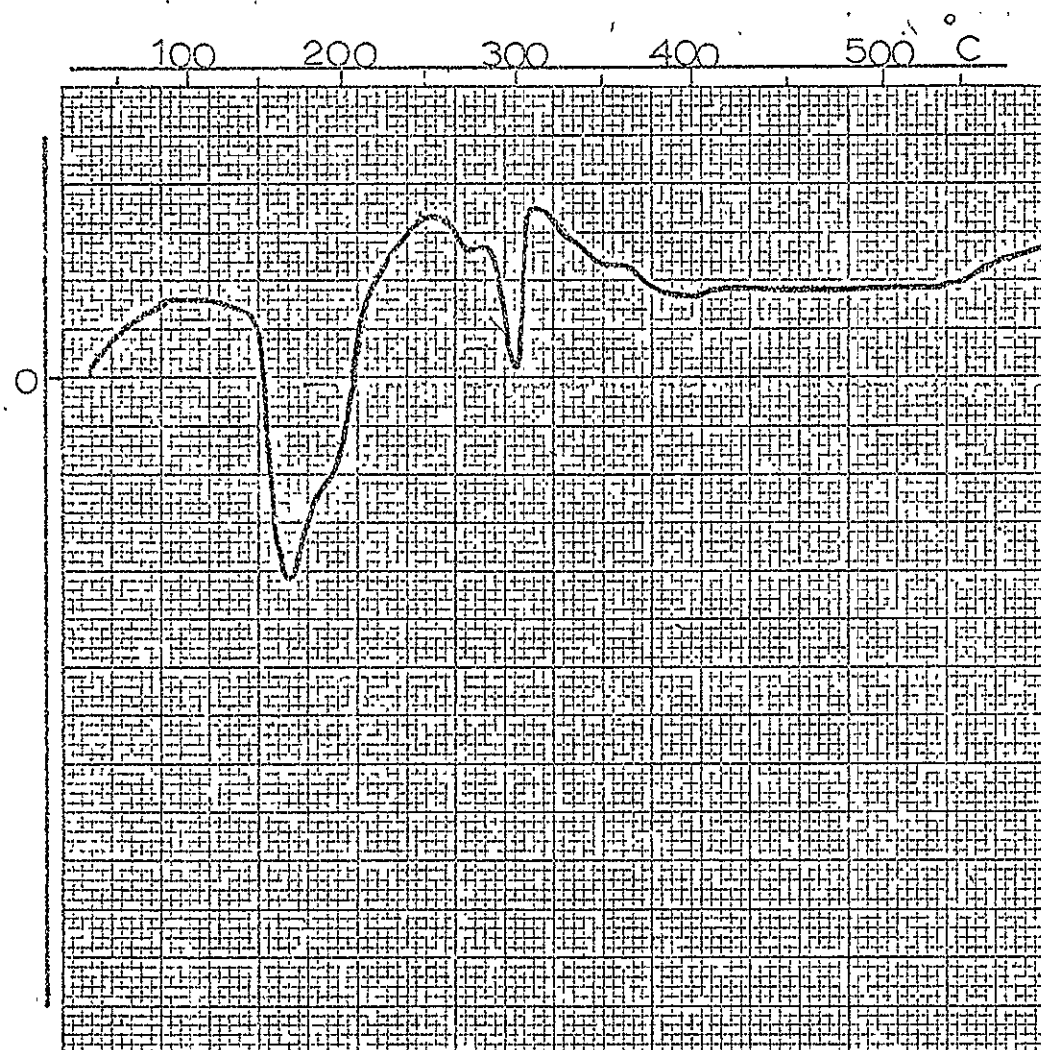
FIGURE I-50

DTA #158

SAMPLE: NEGATIVE (CYCLED)

SAMPLE WT.: 10 MG

CONDITIONS: 10°C MIN^{-1}
0.10 SCFM AR

EXOTHERMIC

ENDOTHERMIC

T-166
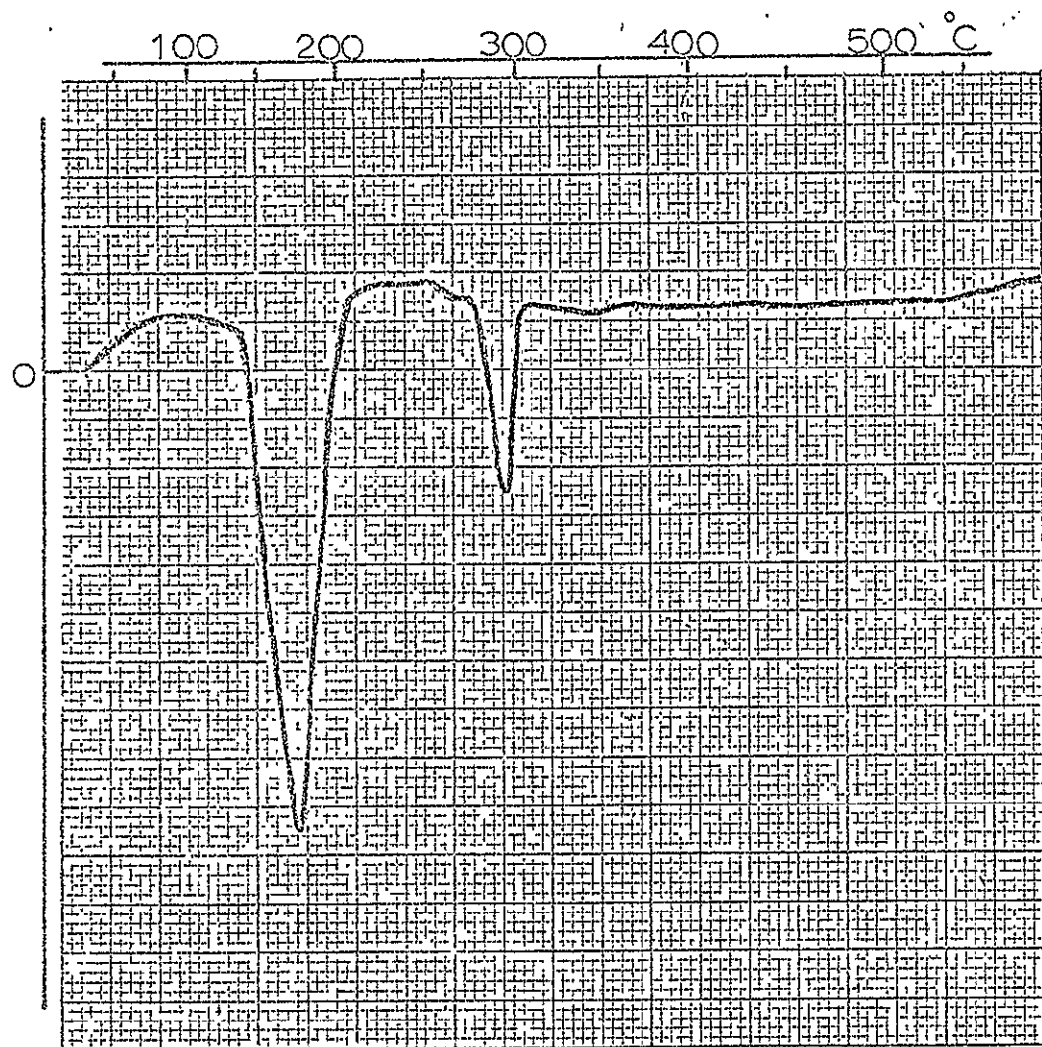
FIGURE I-51

DTA #160

SAMPLE: NEGATIVE (STERILIZED)

SAMPLE WT.: 10 MG

CONDITIONS: 10°C MIN^{-1}
0.10 SCFM AR
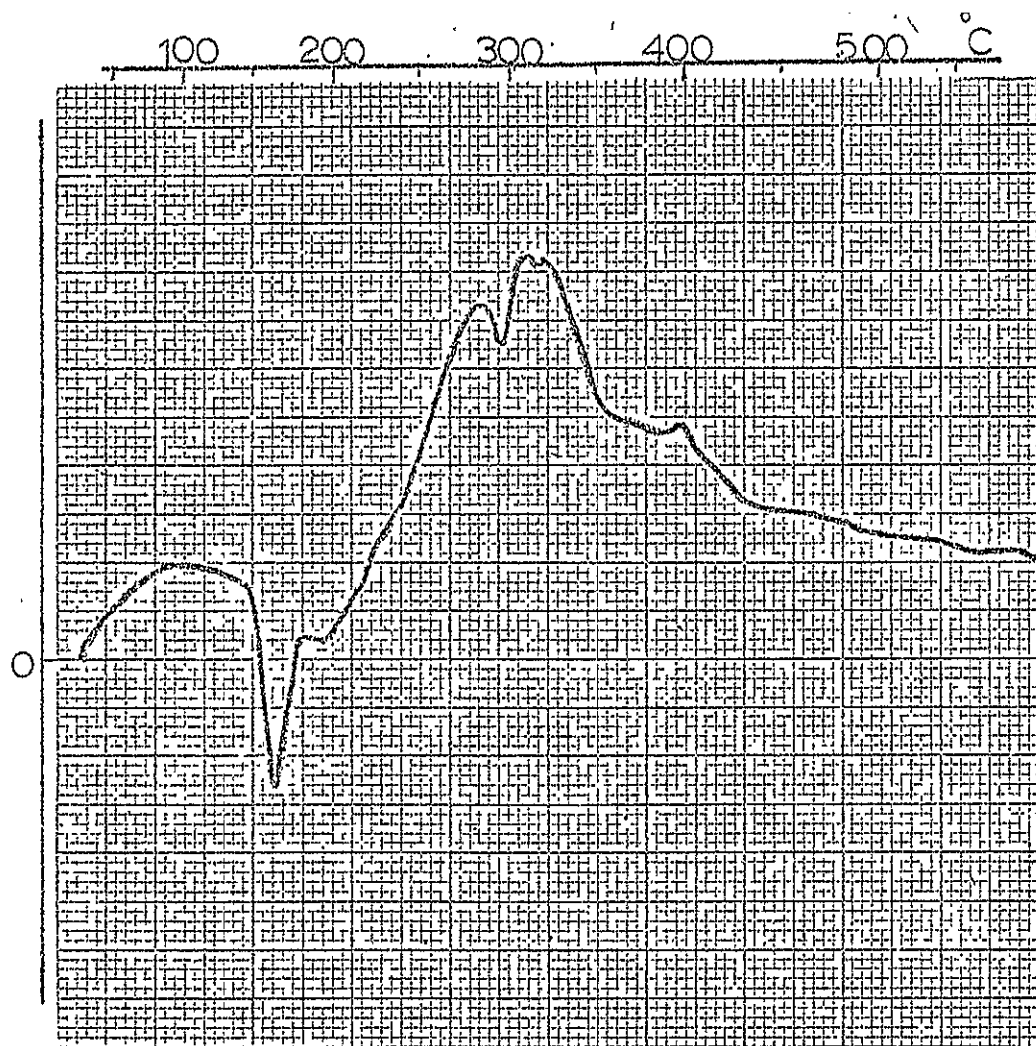
FIGURE I-52

DTA #156

SAMPLE: NEGATIVE (STERILIZED AND CYCLED)

SAMPLE WT.: 10 MG

CONDITIONS: 10°C MIN^{-1}
0.10 SCFM Ar

EXOTHERMIC

ENDOTHERMIC

I-167

K. Causes of Higher End-of-Charge Voltage of Sterilized Cells

   1. Effect of Sterilization Time on Cell Performance

        In order to study the effect of varying sterilization
        times on the relevant cell operational parameters, eight
        rectangular, 4 AH cells were fabricated. Each cell em-
        ployed 18 plates, untreated FT2140 separator, and 30%
        KOH at the 80% pore fill level. Seven of the cells were
        heat sterilized at 135°C for 1, 2, 4, 8, 16, 32 and 64
        hours, respectively. Each cell together with the eighth
        unsterilized control cell, was subjected to the normal
        cycling routine (charge at the 12.5 hour rate to 137%
        level; discharge at the 2.5 hour rate to the 1.0V cut-
        off). As can be seen from the data shown in Figure I-53,
        the time during which the cells are subjected to steri-
        lization has a marked effect on the cell voltages, both
        at end-of-charge and on open circuit, and on the effi-
        ciency. There is no analogous effect observed with the
        cell resistance data. This type of variation persisted
        throughout the eleven tests performed. These data indi-
        cate that sterilization in the cell environment produces
        increasing changes in the electrochemical characteristics
        of one or both of the electrodes.

    2. Single Electrode Potential Studies in the Cell Environment

        In order to investigate the source and causes of the high
        end-of-charge voltage exhibited by all cells following

metallurgical
materials division

FIGURE I-53

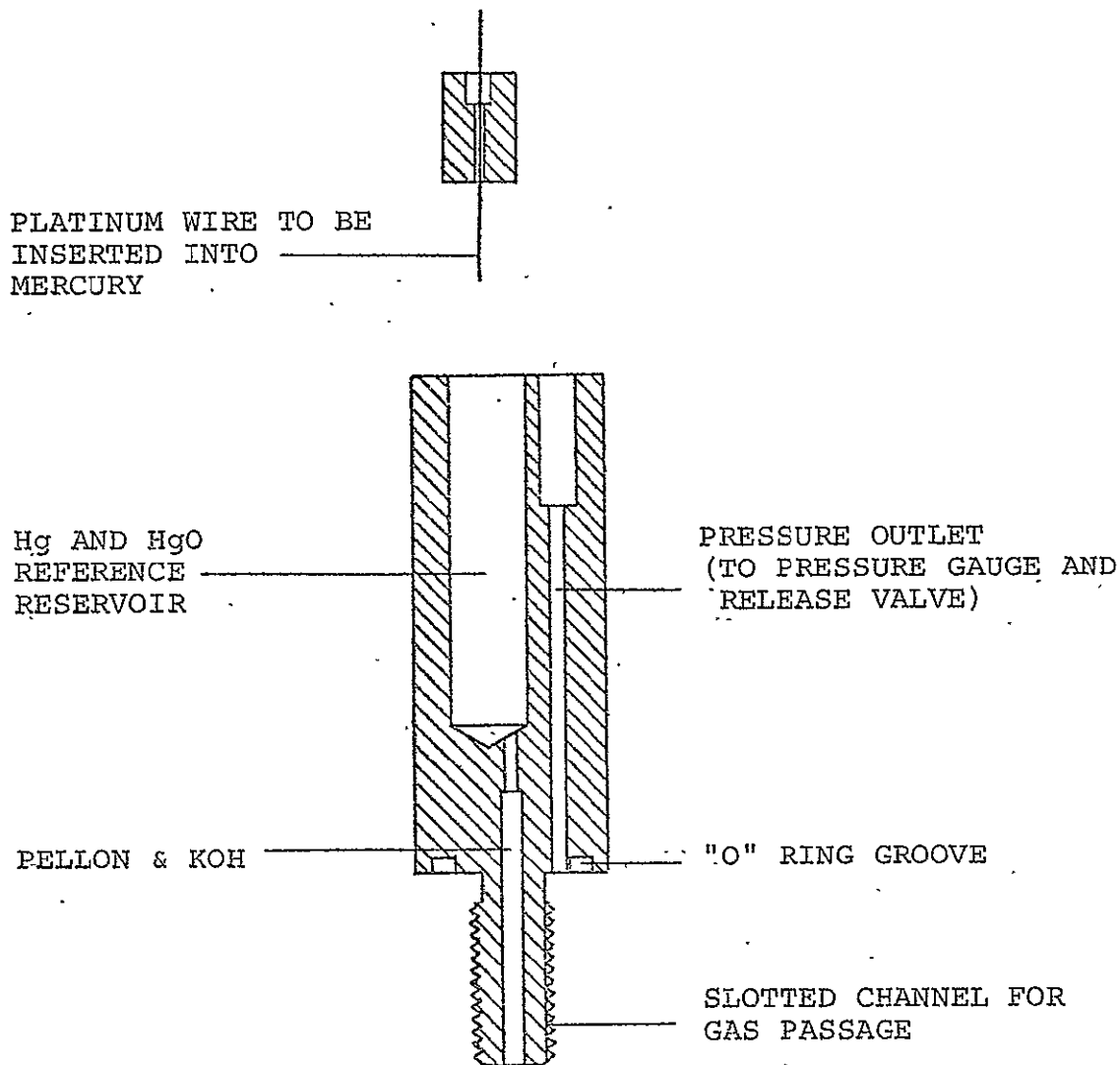## EFFECT OF STERILIZATION TIME ON CELL PERFORMANCE
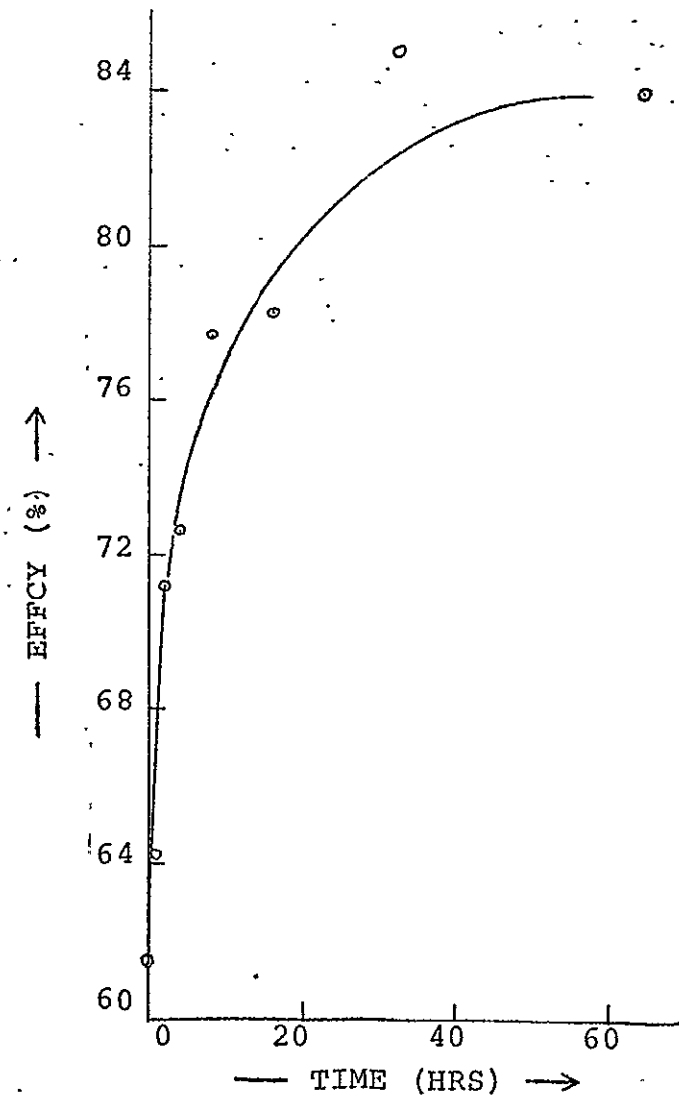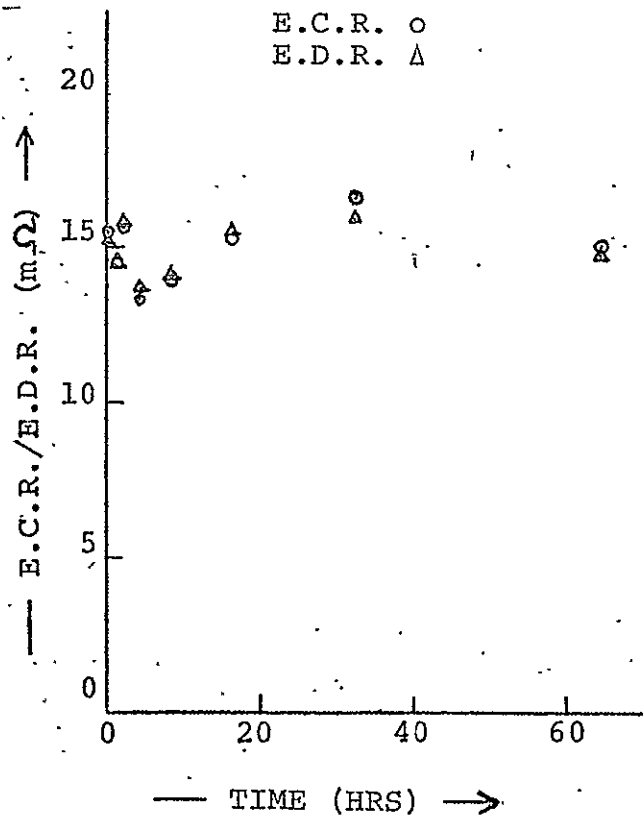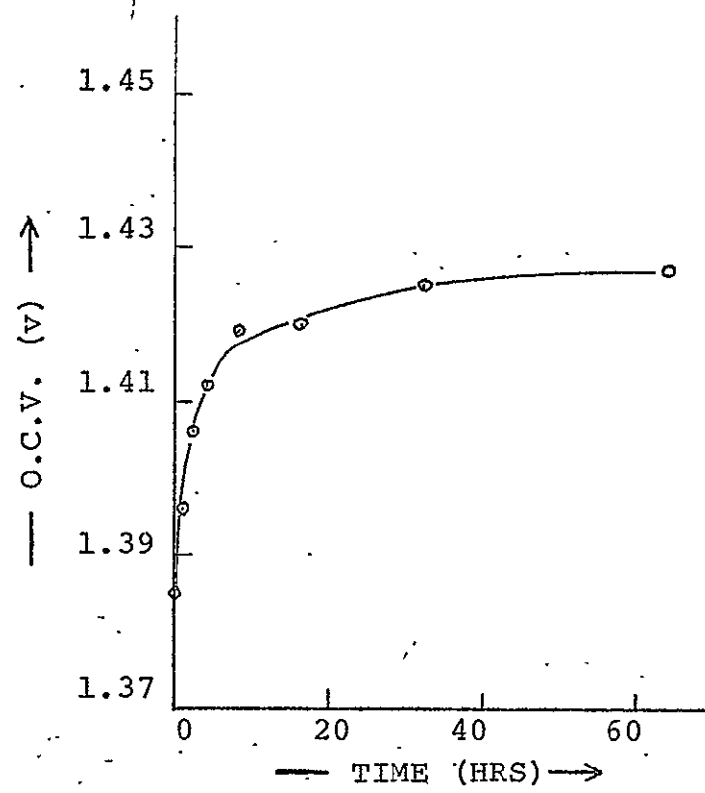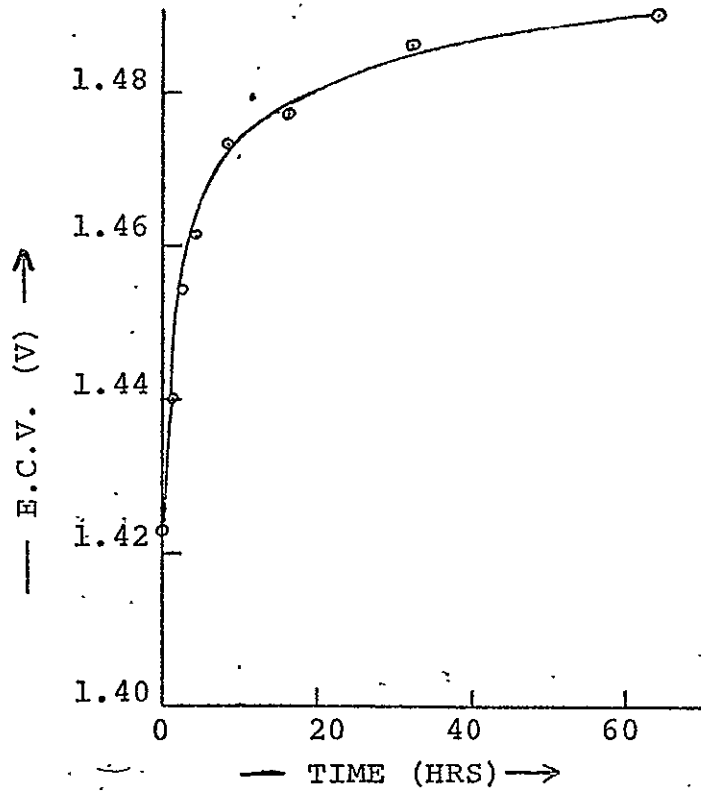
heat sterilization, it was considered of prime importance

to design and test an externally located reference elec-

trode capable of being inserted into a "sealed" cell in

order to monitor the separate potentials of the positive

and negative electrodes. Such an electrode was designed,

and after some modification, it worked satisfactorily for

"sealed" cells.

A diagram of the modified Lucite electrode assembly is

shown in Figure I-54. The electrode proper consists of

the Hg/HgO/KOH system set up in the wider section of the

Lucite container, as shown. External contact to the mer-

cury is made by means of the platinum wire cemented into

the cap (shown separated in the diagram). The narrow,

cylindrical base section of the assembly is packed with

separator material (Pellon-nylon or FT2140 -- Polypro-

pylene), pre-soaked with cell electrolyte, 30% KOH. This

section, acting as a salt-bridge, extends into the

threaded part of the Lucite body, and protrudes slightly

at the base. The cap is finally cemented into the main

body. A rubber O-ring fits into a groove, located

just above the threaded section. The entire reference

electrode system is screwed into a threaded hole, tapped

into the top plate of the cell. When tightened, the

lower section presses firmly against the cell separator

protruding from between the alternate electrode plates

FIGURE I-54

An Hg/HgO Reference Electrode Design for
"Sealed Cell" Studies

PLATINUM WIRE TO BE
INSERTED INTO
MERCURY

Hg AND HgO
REFERENCE
RESERVOIR

PRESSURE OUTLET
(TO PRESSURE GAUGE AND
RELEASE VALVE)

PELLON & KOH

"O" RING GROOVE

SLOTTED CHANNEL FOR
GAS PASSAGE

forming the cell pack. There is provision for gas
passage by way of a slot cut into the threads. This
modified reference electrode is suitable for simultane-
ous measurement of pressure and each electrode potential
in sealed cells. The electrode assembly, as described,
is capable of being used to monitor the positive and
negative electrode potentials simultaneously, and is
capable of withstanding the high pressures, (up to
80 psig), commonly developed on overcharge, without
disrupting or leaking. In Figure I-55 are shown some
typical positive and negative electrode potentials
and cell voltage-time curves, monitored during a
normal charge-discharge routine, i.e. charge at the
12.5 hour rate to 137% level, discharge at the 2.5
hour rate. The full lines are for an unsterilized cell,
the dashed lines are for a post-sterilized cell. The
reference electrode is at ground potential. The positive
reference, and negative reference potential differences
are fed to the recorder via two separate, operational
amplifiers, voltage follower circuits, with separate
power supplies. The cell voltage is monitored directly.
This data indicates that the high end-of-charge voltage
is associated mainly with the positive electrode.
Sterilization appears to have little or no effect on
either electrode potentials during discharge. As can be
seen, in the case of the unsterilized cell, the cell

metallurgical
materials division

FIGURE I-55

CELL VOLTAGE AND INDIVIDUAL ELECTRODE POTENTIALS
FOR UNSTERILIZED AND STERILIZED CELLS DURING
CHARGE AND DISCHARGE
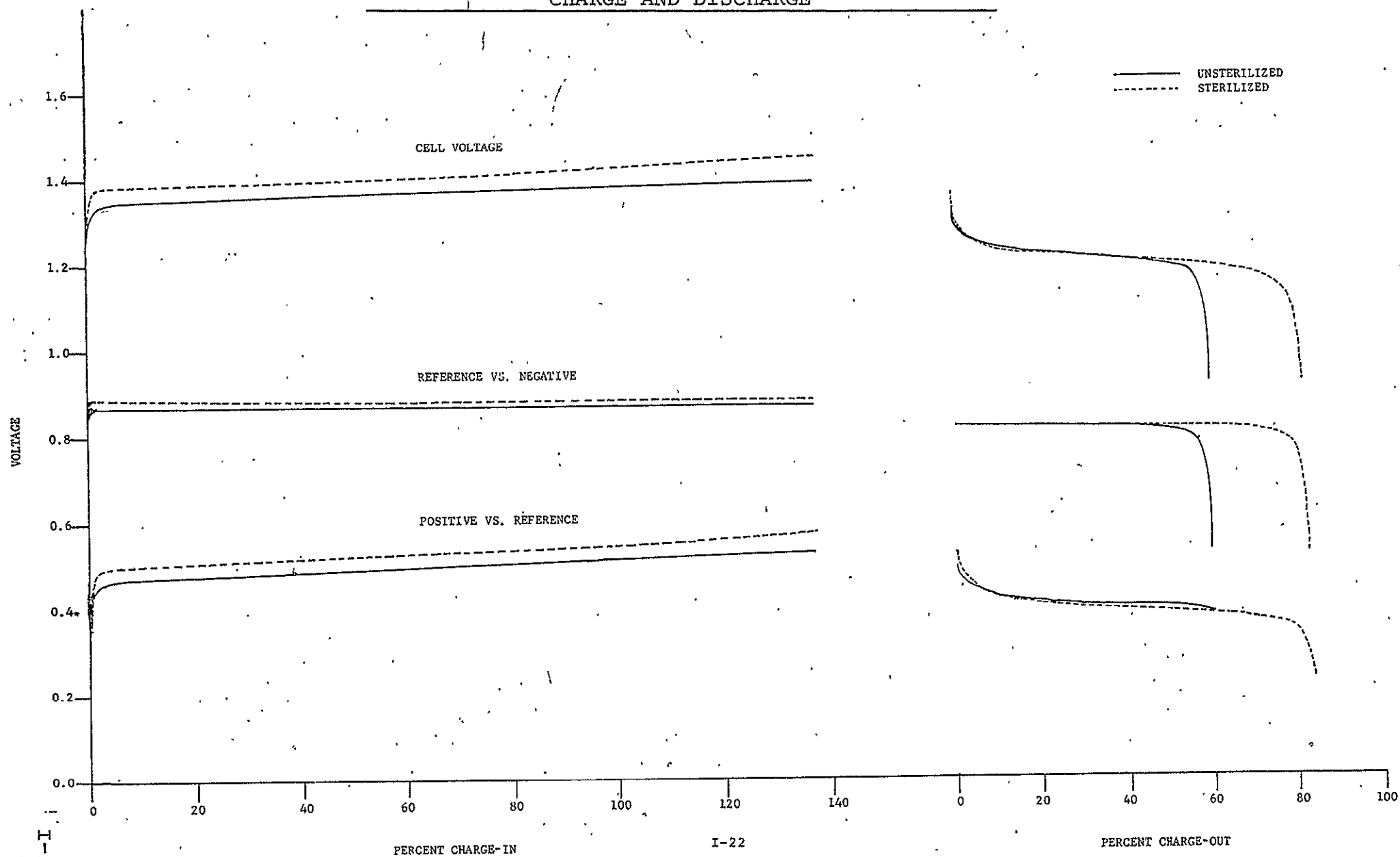
under test appears to be negative-limited on discharge.
Following sterilization, however, the negative electrode
exhibits greater capacity. In fact, both positive and
negative electrodes appear to have approximately the
same capacity. Further data using the previously
described reference electrode for fully charged cells
(C.L. 137%, C.R. C/12.5) and previously sterilized for
various lengths of time are given in Table I-44.

TABLE I-44

End of Charge Voltages as a Function of
Sterilization Time for Sealed Ni-Cd Cells

Cell	Sterili- zation Time	Cell Voltage	Positive to Reference	Negative to Reference
T-1	0. hrs.	1.428 V	.520 V	-.908 V
T-2	1 hr.	1.429 V	.568 V	-.861 V
T-5	8 hrs.	1.469 V	.568 V	-.901 V
T-6	16 hrs.	1.448 V	.546 V	-.902 V
T-7	32 hrs.	1.452 V	.565 V	-.887 V
T-8	64 hrs.	1.466 V	.592 V	-.874 V

It can be seen that a marked difference exists between
the end-of-charge, positive-to-reference voltage for
all sterilized cells and the one unsterilized cell.
The data in Table I-45 show that differences exist be-
tween sterilized and unsterilized positive with respect
to open circuit voltage as well as end-of-charge voltages.

metallurgical
materials division

Although oxygen potential decay on open circuit does contribute to observed OCV, it appears that differences exist between the sterilized and nonsterilized positives which go beyond that of mere oxygen overvoltage phenomenon and involve complex changes in the behavior of positive active material due to sterilization.

TABLE I-45

Open Circuit Stand Voltages vs. Time

Cell	Cell Voltage		Positive to Ref.		Negative to Ref.	
	6 min.	4½ hr.	6 min.	4½ hr.	6 min.	4½ hr.
T-1 (0)*	1.392V	1.344V	.500V	.459V	-.892V	-.885V
T-5 (8)	1.433V	1.365V	.540V	.472V	-.893V	-.893V
T-7 (32)	1.420V	1.344V	.548V	.484V	-.872V	-.860V
T-8 (64)	1.406V	1.344V	.568V	.508V	-.838V	-.834V

* Sterilization time in hours

The data also indicate the stability of the negative electrode potential during stand and the greater instability of sterilized positive as compared to the unsterilized positive. The unsterilized positive drops 41 mv during this stand (between 6 min. and 4½ hrs.) while the three other cells drop between 68 and 60 mv during that same stand time. The greatest drop in the negative was 12 mv. Open circuit decay data for the positive electrode were obtained for all six cells following the standard charge and plotted as voltage vs. log time.

metallurgical
materials division

These plots appear in Figures I-56 and I-57. Two separate decays were run for Cell T-1. The slopes of the E vs. log T plots are reasonably alike for all sterilized cells. The one unsterilized cell indicated a difference in the second slope b^1. The values of the slopes are given in the Table I-46.

TABLE I-46

Values of Slopes of the Plots in Figs. I-56 and I-57

Cell No.	b		b^1
T-1	Run 1:	26	35.
	Run 2:	23	30
T-2	Not Recorded		42
T-5		25	39
T-6		26	39
T-7		25	40
T-8		25	47

The initial slope represents the first hour of open circuit time, the second slope corresponds to decay beyond 1 hour. At present it is not possible to give a theoretical interpretation of these observations.

metallurgical
materials division

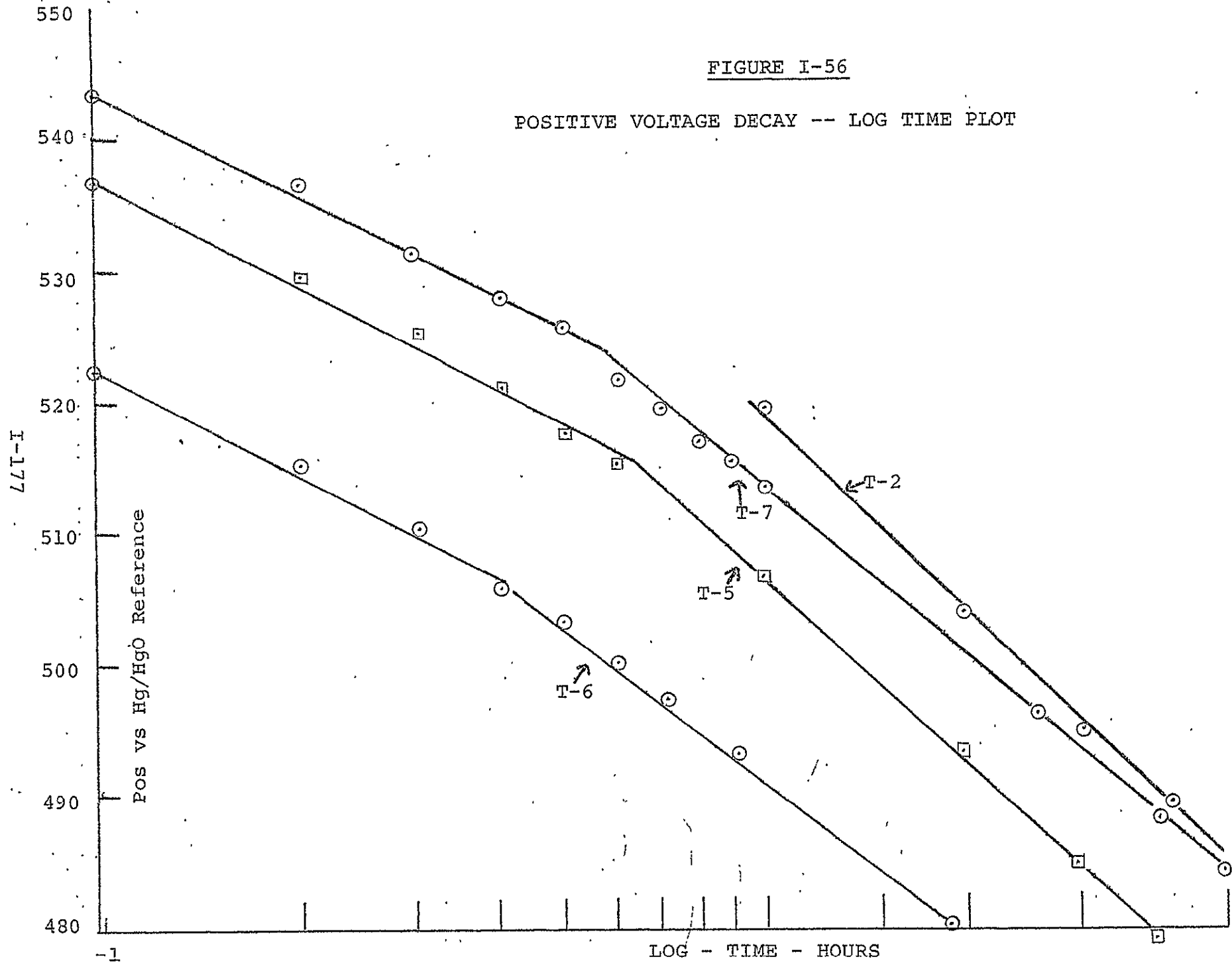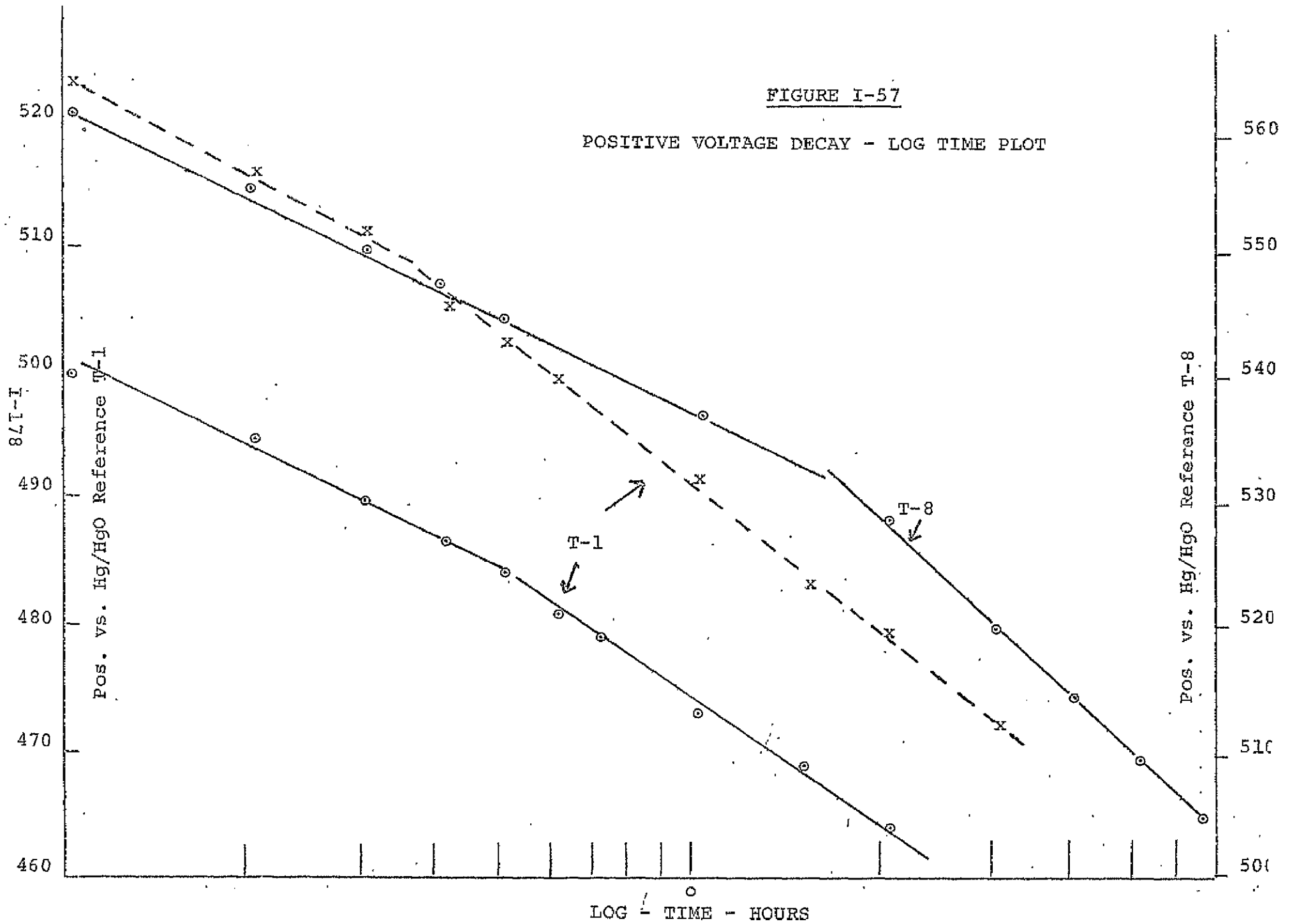FIGURE I-56

POSITIVE VOLTAGE DECAY -- LOG TIME PLOT

FIGURE I-57

POSITIVE VOLTAGE DECAY - LOG TIME PLOT

LOG - TIME - HOURS

3. Effect of Sterilization Time on the Capacity of Each Plate

All six cells mentioned above were discharged to reversal, following a standard charge, at the $C/12.5$ rate. Capacity data and each electrode potential appear in Table I-47.

TABLE I-47

Delivered Capacity of the Positive and Negative Plates
as a Function of Sterilization Time

Cell #	Ster. Time (Hrs)	Negative (AH)	Positive (AH)	Stand (Hrs)
T-1	0	3.53	4.07	64
T-2	1	3.63	4.20	64
T-5	8	4.07	4.40	5.25
T-6*	16	4.00	4.40	4.5
T-7*	32	4.00	4.33	4.5
T-8	64	3.70	4.65	5.25

* T-6 and T-7 = Third cycle after charge adjust by vented cycle. All the rest -- 2nd cycle after charge adjust.

In all cases the cells are negative limiting. They had been positive limiting on previous discharges following sterilization. This suggests a capacity change of the negative electrode during cycling.

L. Characterization of Sterilized Plates in Flooded Cells

The study of the end-of-charge voltage in sealed cells is complicated by possible interactions among plates, separator and electrolyte. It is useful to investigate this parameter separately at each electrode. Accordingly, it was

metallurgical
materials division

planned to remove electrodes from unsterilized and sterilized cells and observe their behavior in flooded cells containing fresh electrolyte, no separator and using a reference electrode.

The flooded cells containing a Hg/HgO reference electrode were prepared. Provision for measurement of electrode potentials during the complete charge-discharge cycle was made. Four cells were selected to supply the sample electrodes, two sterilized and two unsterilized. These cells were 18-plate, 30% KOH, 80% pore fill cells used in the initial evaluation of 18-plate cells. The unsterilized cells had undergone five cycles; the sterilized cells had undergone five presterilization cycles and five post-sterilization cycles.

The cells were cut open, the test plates removed from near the middle of the pack, placed immediately into 30% KOH in the flooded cells and charged. The charge rate and charge level were selected to correspond to the cycling condition of: $CR = C/12.5$, $CL = 137\%$, $DR = C/2.5$ where C is the formation capacity of the positive plate.

The first test consisted of three negative plates (1 plate for each flooded cell) removed from one unsterilized cell. Each counter electrode consisted of three as-received plates in each flooded cell. The second test consisted of three negatives from a sterilized cell. Since the results did not

differ significantly within each group of three plates, the third test was made utilizing two sterilized and one unsterilized positive plates from the remaining two cells.

The results (See Table I-48) show that the positive electrode after sterilization exhibits higher end-of-charge voltage (.031 volts greater) than prior to sterilization, while the potential of the negative at the same charge input remains unchanged. Sterilization also results in a slight decrease in flooded capacity (6-7% relative) for both the positive and negative plates. This confirms that the high end-of-charge voltage is associated with the positive plate and is caused by sterilization.

metallurgical
materials division

TABLE I-48

Behavior of Unsterilized & Sterilized Plates
in Flooded Cells

Electrode Material	E.C.V.[1] (137%)			Effcy.[2] (%)		
	Unster.	Ster.		Unster.	Ster.	
Neg. Plate	-0.903	-0.903		132	124	
Neg. Plate	-0.906	-0.909		135	126	
Neg. Plate	-0.909	-0.906		129	121	
Mean	-0.906	-0.906	0.000	132	124	8
Pos. Plate	0.512	0.544		91.	86	
		0.542			84	
Mean	0.512	0.543	0.031	91	85	6

[1] Voltage versus Hg/HgO Reference

[2] Charge Delivered/Formation Capacity of Positive

M. A Method for the Determination of Gas Composition in Sealed
   Ni-Cd Cells

It is well known that hydrogen gas does not recombine in a
sealed nickel cadmium cell unless special provision such as
the introduction of a third recombination electrode. In a
properly designed, sealed Ni-Cd cell, the evolution of
hydrogen does not occur. However, hydrogen can evolve during
charge or overcharge if for some reason the excess cadmium
hydroxide or oxygen is not available for reduction. It is
necessary to determine if any hydrogen evolution occurs in a
sterilized cell during charging and if so, under what condi-
tions.

It was therefore necessary to develop a method to determine
the gas composition in a sealed Ni-Cd cell. After reviewing
various methods, the gas chromatographic method was chosen
as the most suitable. The system was designed to determine
the amounts of O_2, H_2, N_2 and Ar gas mixtures. The range
and the sensitivity for each component are given in Table I-49.

TABLE I-49

Range and Sensitivity of the Gas Chromatographic Method

Gas	Analytical Range for 0.5 cc Sample @ 1 atm.		Relative Sensitivity $H_2 = 1$	Relative Standard Deviation	
	From V/O	To V/O		% @	O/U
H_2	1.0	80.	1	5.4	2.69
N_2	0.1	100.	41	1.8	94.60
O_2	0.1	100.	67	0.8	1.08
Ar	0.1	10.	69	0.9	1.63

The analyses for O_2, N_2 and Ar show excellent sensitivity and
precision. The results for hydrogen, while not as good, were
adequate for this investigation.

TABLE I-50

OPERATING CONDITIONS FOR ANALYSIS
OF BATTERY GASES BY GAS CHROMATOGRAPH

EQUIPMENT: Instrument: Aerograph 1720-1 column switching valve, recorder with disc integrator.

Columns: "A" before column switching valve – 6' x 1/8" SS – Poropak N.

"B" after column swithcing valve outside oven – 17' x 1/8" SS – Poropak Q

"C" after column switching valve inside oven – 1' x 1/8" SS – Poropak N

Temperatures: Injector – ambient
Detector – 135°C
Columns. – A and C ambient with temperature programming if analysis of other than fixed gases required – B – in dry ice (-78°C)

Detector: 150 milliamps

Gas: 30cc/min. – Helium

Syringes: Use only the 1.0 ml "Pressure-Lok" syringe made by Precision Sampling Co.

CALIBRATION: Calibration curves of integrator counts vs. moles of gas have been prepared for hydrogen, nitrogen, oxygen and argon.

metallurgical
materials division

TABLE I-51

Calibration Standards for Analysis of Battery Gases

Cylinder #	Vol. %				Wt. %			
	N_2	O_2	H_2	Ar	N_2	O_2	H_2	Ar
1	93.46	2.12	1.10	3.32	92.82	2.40	0.08	4.70
2	88.45	8.80	-	2.75	86.36	9.81	-	3.83
3	82.30	15.3	-	2.40	79.75	16.93	-	3.32
4	94.60	1.08	2.69	1.63	96.19	1.25	0.20	2.36
5	91.07	-	7.85	1.08	97.74	-	0.61	1.65
6	79.49	-	18.7	1.81	95.29	-	1.61	3.09
7	51.71	-	47.0	1.29	90.83	-	5.94	3.23
8	68.43	-	31.1	0.47	95.92	-	3.14	0.94
9								

The operating conditions are listed in Table I-50.

A column of Porapak Q in dry ice separates the components which are then detected by changes in thermal conductivity. The integrated response of the detector was found to be a linear function of the number of moles O_2, N_2 and Ar in the sample using the standards listed in Table I-51. The response to H_2, however, is nonlinear and the sample size must be reduced for high hydrogen concentrations.

Standard #4 was run three times in two weeks to establish the precision and sensitivity data presented above. Figure I-58, a tracing of a typical chromatographic recorder chart, shows that complete separation of the components is made in twelve minutes. Total time for analysis including sampling and calculations is approximately sixteen minutes.

Sampling of the cell gases is accomplished using a 0-1 cc pressure-lok gas syringe (Precision Sampling Corp. #306001-A). The needle of the syringe is inserted through the cap and rubber septum of the fitting shown in Figure I-59. This device can be screwed into the vent hole of our experimental cells or into a "T", also shown in Figure I-59, which in turn can be screwed into the cell. The "T" enables us to simultaneously measure pressure while sampling the gas. After introduction of the desired volume of gas into the syringe the valve on the syringe is closed and the needle withdrawn. Under

metallurgical
materials division

FIGURE I-58

GC Curve

Std. #4

DETECTOR RESPONSE

Inject

H₂

X1

X32

N₂

X1

Ar
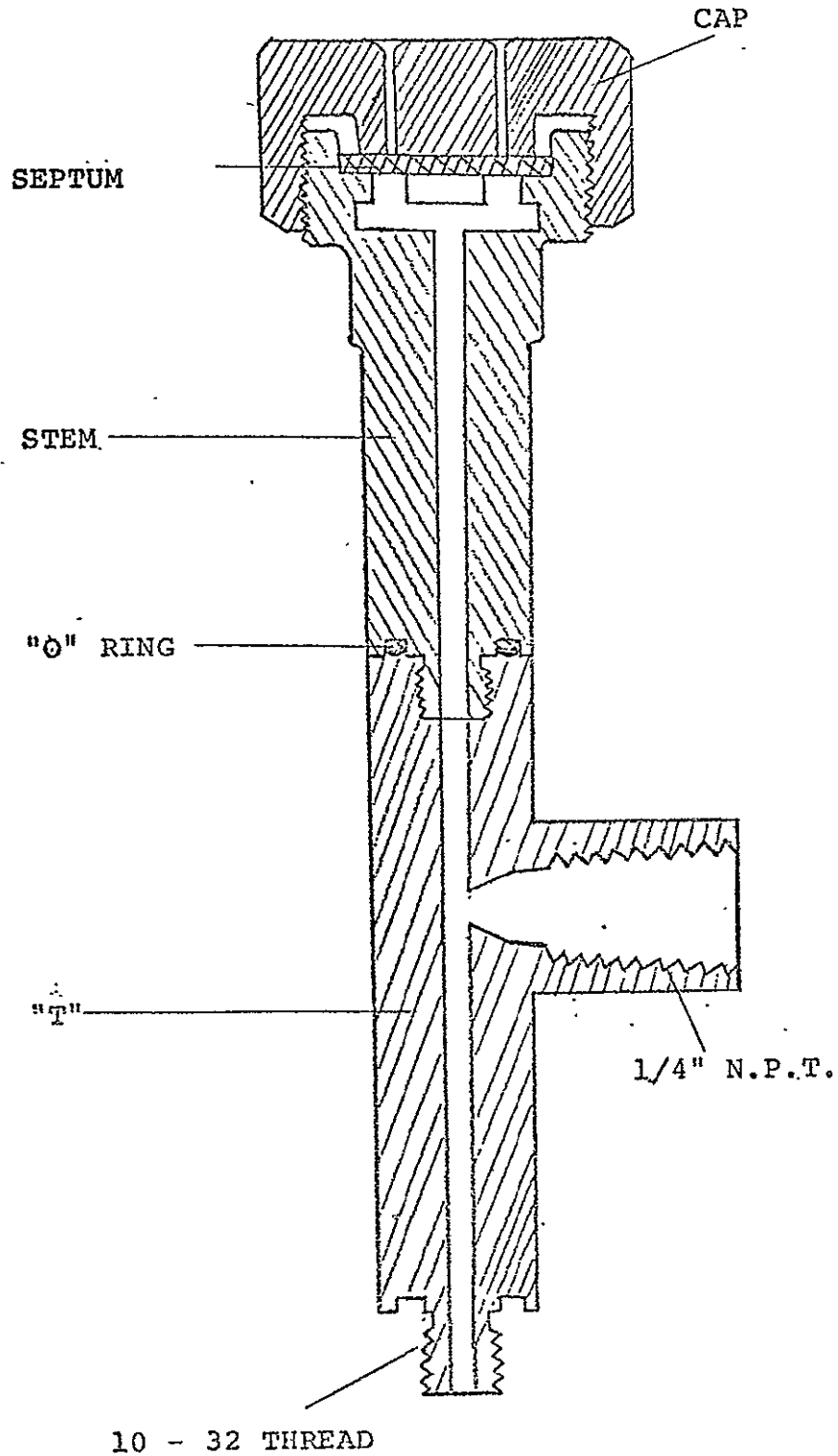
O₂

FIGURE I-59

DEVICE FOR GAS SAMPLING FROM "SEALED" CELLS

these conditions of sampling the number of moles of gas sample taken is a fixed fraction of the number of moles of the gas in the cell regardless of the cell pressure.

The sample is introduced into the gas chromatograph by inserting the needle through inlet septum of the chromatograph, opening the valve and injecting the sample.

metallurgical
materials division

N. Hydrogen Content in Sealed Ni-Cd Cells

Using the chromatographic method described in Section M,
samples of gas mixtures from four different cells (two 25 AH
cells and two 4 AH cells) were analyzed on two different days.
The results are shown in Table I-52. The two 25 AH cells had
developed pressures in excess of 200 psia at the end of charge.
The 4 AH.cell (RAI-1) made with Radiation Incorporated separator
treatment had developed 120 psia pressure at.the end of charge
while the 4 AH control cell (C-1) had developed only 70 psia at
the end of charge. As shown in Table I-52 all the four cells
contained 1.4 to. 3.7 volume percent of hydrogen. As expected,
the 25 AH cells contained approximately five times the amount
of hydrogen as the 4 AH cells, not significantly different
from the ratios of the capacities.

The sterilization treatment did not increase the amount of
hydrogen. This observation shows that the traces of hydrogen
generated are not associated with the sterilization treatment.
Also the amount of hydrogen does not build up to any signifi-
cant level during cycling of sterilized or unsterilized cells.
It is therefore encouraging that hydrogen gas does not present
a problem in sterilized or unsterilized cells during continued
charge-discharge cycling.

metallurgical
materials division

TABLE I-52

ANALYSIS OF GASES IN CELLS WITH HIGH END-OF-CHARGE PRESSURE

Cell	Size Nom.	Vol. cm³	Date	25°C Pressure Calcu'd psia	Meas'd psia	10⁻⁵ Moles H_2	N_2	O_2	Total	H_2 AH	O_2 AH	v/o H_2	v/o N_2	v/o O_2
P3	25 AH	57	4/15	11.1	<15	4.4	99.1	78.7	182.2	.0024	.084	2.4	55.0	42
P3	25 AH	57	4/17	12.2	<15	3.6	15.7	182.0	200.3	.0019	.195	1.8	7.8	90
P4	25 AH	57	4/15	12.2	<15	7.5	102.0	91.5	201.0	.0040	.098	3.7	51.0	46
P4	25 AH	57	4/17	28.8	30	4.9	171.0	294.0	469.9	.0026	.314	1.4	36.0	63
RAI-1	.4 AH	23	4/15	17.5	17	1.7	19.1	92.2	113.0	.00092	.099	1.5	17.0	82
RAI-1	4 AH	23	4/17	30.7	36	1.6	37.7	155.0	194.3	.00086	.165	0.83	19.0	80
C-1	4 AH	23	4/15	12.3	19	1.05	41.8	36.5	79.4	.00056	.039	1.3	53.0	46
C-1	4 AH	23	4/17	3.6	4	0.78	15.6	6.7	23.1	.00042	.007	3.4	67.0	29

O. Accomplishments. and Conclusions. :

1) Developed heat-sterilizable, chemically and electrochemically stable, polypropylene (Pellon FT2140) separator capable of long cycle life after heat-sterilization. Sealed Ni-Cd cells made with a single layer of this separator have undergone 248 post-sterilization deep discharge (100% depth-of-discharge) cycles without significant performance deterioration.

2) Developed inexpensive, heat-sterilizable, hermetic metal-to-nonmetal seal capable of long cycle life after sterilization.

3) Constructed 60 test stations for automatic charge-discharge cycling of 4 AH heat-sterilizable cells and 24 high-current stations for testing 25 AH cells.

4) Established technical and engineering capability of making 4 AH prismatic and 25 AH cylindrical and prismatic, sealed Ni-Cd cells capable of continued post-sterilization cycling without significant changes in performance.

5) Sterilized cells exhibit approximately 60 millivolts higher end-of-charge voltage than unsterilized cells. This is due to increased polarization at the positive (nickel) electrode and may be related to the changes in the pore structure, surface area and/or oxygen overvoltage

metallurgical
materials division

characteristics of the positive plate. This higher end-of-charge voltage, since it is not associated with the negative (cadmium) electrode is not indicative of hydrogen evolution in sterilized cells.

6) Heat-sterilization oxidizes some of the free cadmium metal (charge adjust) which can result in negative limited cells on discharge. This parameter needs further optimization.

7) Addition of cobalt to the positive plate and of indium or thallium to the negative plate did not show any improvement in the cell performance in flooded cell experiments. These additives are not considered essential in sterilized, sealed cells.

8) The optimum electrolyte amount (volume) is approximately 75% of the free pore volume of the cell for optimum performance. This is the most critical parameter having major effect on the cell performance.

9) Wetting and KOH absorption characteristics of the separator, the positive and the negative plates change during sterilization and cycling. Pre-treatments of the separator with (a) chromic acid, (b) surfactants or (c) RAI proprietary process show no permanent beneficial effect on the cell performance during post-sterilized cycling.

10) Studies concerning the effect of core-compression show that the prismatic 4 AH cells with 18 plates (higher compression) have better reproducibility than 17-plate cells.

11) Further physico-chemical characterization of the active components of the cell before and after sterilization was performed using x-ray diffraction, differential thermal analysis, thermo-gravimatic analysis, electron microscope and gas chromatographic techniques. The x-ray diffraction of plates did not indicate the formation of any new phases due to sterilization. The nickel hydroxide crystals in the positive became more orderly and of larger size due to the sterilization. However, the particle size of the positive nearly returned to its initial (pre-sterilization) state during post-sterilization cycling. The crystallite sizes of cadmium plates were too large to permit detection of any change. Electron-microscopic studies showed that the cadmium active material crystals become larger during sterilization, thus, resulting in reduced surface area. No definite conclusions could be made from TGA and DTA data.

12) The objective of Tasks I to VII to develop heat-sterilizable, sealed Ni-Cd cells of up to 25 AH capacity capable of long cycle life after heat sterilization has been achieved.

metallurgical
materials division

APPENDIX I

WORK STATEMENT FOR THE DEVELOPMENT
OF SEALED HEAT-STERILIZABLE NICKEL-CADMIUM CELLS
UNDER JPL CONTRACT 951972

The specific tasks under the above contract incorporating the latest modifications and/or extensions of the work statement are as follows;

Task I -- Electrochemistry

Use statistical factorial programs to perform studies to characterize electrodes, electrolyte solutions and separators of the nickel-cadmium system. This effort shall consist of, but not necessarily be limited to, the following studies:

1. Electrolyte Solution

    a) Effect of heat sterilization on cell performance at various concentrations of KOH.

    b) Effect of the addition of Lithium (Li^+), sodium (Na^+), and bismuth (Bi^{3+}) ions and of surfactants to the electrolyte solution.

2. Nickel Electrode

    a) Effect of heat sterilization on the structure and behavior of the nickel electrode.

    b) Efficacy of various formulation and fabrication methods to produce more efficient, heat sterilization-resistant electrodes.

    c) Effect of the addition of cobaltous ion (Co^{++}) to the electrode.

metallurgical
materials division

3. <u>Cadmium Electrode</u>

   a) Effect of heat sterilization on the structure and behavior
      of the cadmium electrode.

   b) Efficacy of various formulation and fabrication methods
      to produce more efficient heat sterilization-resistant
      electrodes.

   c) Effect of the addition of thallium (Tl^+) and indium (In^+)
      to the electrode.

4. <u>Separator</u>

   Behavior of various separators in cells comprised of selected
   electrodes and electrolyte solutions under conditions of heat
   sterilization and subsequent electrical cycling.

   Based upon the results of this Task, further work was defined
   in Task V.

Task II -- Cell Case

Develop, design, fabricate, and test cell-case materials, which
shall be sealed after activation, and which are intended to be,
capable of withstanding a storage life of twelve (12) months after
activation and sealing, and a minimum of twelve (12) months after
sterilization.

Task III -- Fabrication and Test

Fabricate and test cells of a prismatic configuration of about
four (4) AH capacity at the contractor's facilities in a parallel
effort to support a JPL in-house test program.

metallurgical
materials division

1. Develop a procedure for the characterization of nickel-cadmium cells which shall include, but not necessarily be limited to, the following:

    a) One or more sterilization cycles;

    b) Electrical cycling at various rates, depths-of-discharge, and temperature;

    c) Cell internal pressure measurements for various conditions;

    d) Cell voltage regulation with cycling;

    e) Cell voltage and/or capacity stability for a period of time at fifty degrees centigrade (50°C) on a charged stand test after sterilization and electrical cycling.

2. Perform the characterization in accordance with plan approved by Jet Propulsion Laboratory.

3. Test cells at the contractor's facility for the capability of withstanding the shock and vibration requirements stated in the applicable specifications.

4. Fabricate and characterize nickel-cadmium cells utilizing the electrochemical and mechanical design developed in Tasks I and II, and as approved by Jet Propulsion Laboratory, of a sealed cell capable of successfully surviving heat sterilization, shock and vibration environments as defined in Jet Propulsion Laboratory's specification GMP-50436-DSN-B.

metallurgical
materials division

a) Develop a test plan to prove the design;

b) Perform the tests in accordance with the test plan,

as approved by Jet Propulsion Laboratory.

This task was subsequently modified and incorporated in Task X

which included the Long-Range Testing Program for 25 AH cells.

Task IV -- Documentation

Submit the Monthly, Quarterly and Final Technical Progress

Reports as per JPL requirements.

Based upon the results of the above tasks, the following tasks

were subsequently added:

Task V -- Electrochemical Mechanisms Investigations

Determine the causes and mechanisms responsible for (a) capacity

degradation and (b) higher polarization of cells which have been

heat sterilized. The emphasis will be on model, analytical ap-

proaches; e.g., use of planar electrodes coated with the active

materials to avoid unnecessary complications of porous sinter

structure for mechanistic studies. The investigation shall in-

clude, but not be limited to, the following phenomena, which

have been observed to occur as a result of heat sterilization:

a) Oxidation of required excess cadmium metal to cadmium

oxide/hydroxide;

b) Carbonate formation;

c) Physical changes in the positive plate characteristics

during sterilization, including corrosion.

metallurgical
materials division

All the modern, pertinent·research and analytical tools, including
statistical methods and computer system as well as extensive .
library (literature review) facilities, shall be used in this
study.

Task VI -- Sealed Cell Design Optimization

An investigation to optimize a sealed cell design for delivered
capacity, cell resistance·, end-of-charge voltage, and oxygen
recombination rates shall be conducted and shall include, but
not be limited to, the. following parameters:

    a)   Electrochemical Parameters

        (1)   The ratio of total $Cd/Ni(OH)_2$;

        (2)   Level of negative plate charge adjustment;

        (3)   Electrolyte· composition and amount;.

        (4)   Types and layers of separators;

        (5)   Optimum charging method and procedure.

    b)   Packaging parameters for rectangular cells

        (1)   Number of positive and negative plates;

        (2)   Thickness of plates;

        (3)   Core compression

        (4)   Tab coating and· insulation.

Task VII -- Performance and Cycle Life Tests of Sealed Cells

Determine the performance and cycling capability of optimized
sealed cells at· various depths-of-discharge and temperatures of
interest before and after sterilization. Determine predominant
failure mode, if any, and provide feedback in Task VI for further

metallurgical
materials division

improvement. Use computerized test facilities for this task.
Demonstrate the capability of cells to achieve 400 charge-
discharge cycles at 60% depth-of-discharge after heat steriliza-
tion.

Task VIII -- Deliver Fifty (50) Improved Heat-Sterilizable Proto-Type Cells

This task was subsequently deleted and replaced by Task X.

Task IX -- Test Impact Resistant Capability of Ni-Cd Cells

1. Design and develop impact testing facility with the follow-
    ing capabilities:

    a) .Payload accommodation for various size cells weighing
       up to 5 lbs.;

    b) Impact velocity of 120 ft/sec.;

    c) Mechanical shock at 4000 g level;

    d) Square pulse shape of 1 msec duration.

2. Impact testing of Ni-Cd cells

    a) Testing of various existing designs of Ni-Cd cells;

    b) Testing of 25 AH prototype heat-sterilizable nonimpact-
       type cells.

3. Determine the mechanical properties of Ni-Cd electrodes for
    impact resistant cells:

    a) Static testing under several methods of loading to
       determine the prime mechanical properties and failure
       modes;

---

metallurgical
materials division

b) Dynamic testing under the same methods of loading to. establish the effect of high-rate loading on the prime mechanical properties;

c) Employ mechanical property data to predict theoretical dynamic response and establish impact-resistant design criteria.

Task X -- Develop 25 AH Prismatic and Cylindrical Heat-Sterilizable Batteries

Design, develop, fabricate and test Ni-Cd battery cells to meet the requirements of JPL Engineering Memorandum No. 342-68 entitled, "Design Requirements Heat Sterilizable, Impact Resistant, 400 Watt-Hour, Secondary Battery," dated September 16, 1968. The details of this task are as follows:

1. Fabricate one hundred sixty (160) Secondary Battery Cells consisting of the following quantities and mix:

   a) Twenty (20) cells of a development cylindrical design;

   b) Twenty (20) cells of a developmental design;

   c) Twenty (20) cells of either development cylindrical or prismatic design;

   d) One hundred (100) cells of a final design.

2. Provide quality control inspection in receiving and in-process (plaque, plate, separator and leak check) areas.

3. Provide a Long-Range Test Program (LRTP) for JPL approval which shall test the cells described in subparagraphs 1.a) and b) above, in accordance with the following requirements:

---

metallurgical
materials division

a) Cycling Test

   Twelve (12) cells shall be cycle tested and the cycling

   test variables shall be the following:

   (1) Temperatures equal to 30°F, 50°F, and 70°F;

   (2) Depth-of-discharge equal to seventy percent (70%)

       and eighty percent (80%);

   (3) Charge rate equal to C/10 and C/20;

   (4) Discharge rate equal to C/2.

b) Storage Tests

   The storage test period shall be of six (6) months

   duration and the parameters shall be the following:

   (1) Temperature equal to 70°F;

   (2) Periodically recharge two (2) cells which have

       been maintained in the charged state;

   (3) Fully recharge, at the end of six (6) months,

       two (2) cells which have been maintained in the

       discharged state;

   (4) Trickle charge, at constant current, two (2) cells

       which have been maintained in the charged state;

   (5) Float charge, at constant voltage, two (2) cells

       which have been maintained in the charged state.

Task X-3 (LRTP) after initiation of this task, was terminated

by Modification 14.

metallurgical
materials division

TEXAS INSTRUMENTS
INCORPORATED

METALLURGICAL MATERIALS DIVISION
ATTLEBORO, MASSACHUSETTS U.S.A.